PNNL-11652
UC-721

Pacific Northwest National Laboratory

Operated by Battelle for the
U.S. Department of Energy

Bench-Scale Crossflow Filtration of Hanford Tank C-106, C-107, B-110, and U-110 Sludge Slurries

J.G.H. Geeting
B. A. Reynolds

September 1997

Prepared for the U.S. Department of Energy
under Contract DE-AC06-76RLO 1830

PNNL-11652

DISCLAIMER

PACIFIC NORTHWEST NATIONAL LABORATORY
operated by
BATTELLE
for the
UNITED STATES DEPARTMENT OF ENERGY
under Contract DE-AC06-76RLO 1830

Printed in the United States of America

Available to DOE and DOE contractors from the Office of Scientific and Technical Information, P.O. Box 62, Oak Ridge, TN 37831; prices available from (615) 576-8401.

Available to the public from the National Technical Information Service, U.S. Department of Commerce, 5285 Port Royal Rd., Springfield, VA 22161

This document was printed on recycled paper.

PNNL-11652
UC-721

Bench-Scale Crossflow Filtration of Hanford Tank C-106, C-107, B-110, and U-110 Sludge Slurries

J.G.H. Geeting
B.A. Reynolds

MASTER

September 1997

DISTRIBUTION OF THIS DOCUMENT IS UNLIMITED

Prepared for
the U.S. Department of Energy
under Contract DE-AC06-76RLO 1830

Pacific Northwest National Laboratory
Richland, Washington 99352

Summary

Pacific Northwest National Laboratory[1] has a bench-scale crossflow filter installed in a shielded hot cell for testing radioactive feeds. During FY97 experiments were conducted on slurries from radioactive Hanford wastes from tanks C-106, C-107, B-110, and U-110. Each tank was tested at three slurry concentrations (8, 1.5, and 0.05 wt% solids). A two-parameter central composite design which tested transmembrane pressure from 5 to 40 psig and axial velocity from 3 to 9 ft/s was used for all feeds.

Crossflow filtration was found to remove solids effectively, as judged by filtrate clarity and radiochemical analysis. If the filtrates from these tests were immobilized in a glass matrix, the resulting transuranic and ^{90}Sr activity would not breach low activity waste glass limits of 100 nCi/g (TRU) and 20 µCi/ml (^{90}Sr). Two exceptions were the transuranic activity in filtrates from processing 1.5 and 8 wt% C-106 tank waste. Subsequent analyses indicated that the source of the TRU activity in the filtrate was most likely due to soluble plutonium caused by complexation with carbonate. Hence, filtration removed most of the insoluble activity, but obviously proved ineffective at removing the soluble plutonium species. Re-testing of the C-106 supported this hypothesis. These data suggest the need to control carbonate and pH when processing tank wastes for immobilization.

Processing data indicate that the filtrate flux rates generally declined during the course of an experiment at identical processing conditions. The flux degradation is attributed to two causes: filter fouling and feed deagglomeration (caused by shear and, in some instances, low ionic strength of the feed). The problem of filter fouling was largely corrected by filter media selection. Deagglomeration of the feed was confirmed by particle-size analysis, but this problem is not easily corrected with a bench-scale testing apparatus. It is not known if the observed deagglomeration is caused by the severe conditions under which the bench-scale apparatus operates, or if the deagglomeration will also be a problem at larger scale.

The nominal quasi steady-state filtrate flux was 0.05 gpm/ft^2 with extremes of 0.015 to 0.15 gpm/ft^2. Based on throughput of all soluble waste and wash solutions estimated in the Hanford flowsheet, the nominal rate corresponds to a 1140 ft^2 filter requirement. For comparison, Savannah River Site is currently operating a crossflow filter with 432 ft^2, indicating that the flux rates were more than adequate to make crossflow filtration a feasible candidate for solid/liquid separation of Hanford tank wastes.

---

[1] Pacific Northwest National Laboratory is operated by Battelle Memorial Institute for the U.S. Department of Energy under Contract DE-AC06-76RLO 1830.

Contents

Summary iii

1.0 Introduction 1.1
1.1 Background 1.1
1.2 Objectives 1.2
1.3 Theory 1.2
1.4 Feed Description 1.4
1.4.1 C-106 Feed 1.4
1.4.2 C-107 Feed 1.4
1.4.3 B-110 Feed 1.5
1.4.4 U-110 Feed 1.5
1.5 Definitions 1.5

2.0 Procedure 2.1
2.1 Procedural Changes 2.1
2.2 Radioactive Tests 2.2
2.3 Apparatus 2.2

3.0 Results and Discussion 3.1
3.1 C-106 .... 3.2
3.1.1 0.05 wt% Tank C-106 Slurry 3.2
3.1.2 1.5 wt% C-106 .... 3.6
3.1.3 8 wt% C-106 .... 3.9
3.2 C-107 .... 3.10
3.2.1 0.05 wt% Tank C-107 Slurry 3.14
3.2.2 1.5 wt% C-107 .... 3.17
3.2.3 8 wt% C-107 .... 3.17
3.3. B-110 .... 3.17
3.3.1 0.05 wt% B-110 .... 3.23
3.3.2 1.5 wt% B-110 .... 3.23
3.3.3 8 wt% B-110 .... 3.30
3.4 U-110 .... 3.30
3.4.1 0.05 wt% U-110 .... 3.30
3.4.2 1.5 wt% U-110 .... 3.32
3.4.3 7.5 wt% U-110 .... 3.32
3.5 Analytical Results 3.39
3.5.1 Radiochemical Results 3.39
3.5.2 Non-Radioactive Component Measurements 3.46
3.5.3 Particle-Size Distribution Measurements 3.46

4.0 Discussion 4.1
4.1 Comparison of the Graver and Mott Filters 4.1
4.2 Comparison of the Feeds 4.3

4.2.1 Filter-Cake Resistance 4.5
4.2.2 Deagglomeration Resistance 4.5
4.2.2.1 Estimate of Change in Mean Particle Diameter Based on Change in Filter-Cake Resistance 4.7
4.2.3 Fouling Resistance 4.9
4.2.4 Repeatability 4.10
4.4 Crossflow Filtration Feasibility for Use in Pretreatment of Hanford Tank Wastes 4.11

5.0 Conclusions and Recommendations 5.1
5.1 Conclusions 5.1
5.2 Recommendations 5.2

6.0 References 6.1

Appendix A A.1
Appendix B B.1

Figures

1.1 Simplified Hanford Tank Pretreatment Train Showing Major Solid/Liquid Separation Needs 1.2
1.2 Schematic Display of Fundamental Difference Between Crossflow Filtration and Conventional "Dead-End" Filtration 1.3
2.1 Statistically Designed Experimental Conditions Used in Testing 2.1
2.2 Cell Unit Filter Flow Diagram 2.4
3.1 0.05 wt% Tank C-106: Filtrate Flux as a Function of Time 3.2
3.2 0.05 wt% Tank C-106: Filtrate Flux as a Function of Axial Velocity 3.4
3.3 0.05 wt% Tank C-106: Filtrate Flux as a Function of Transmembrane Pressure 3.5
3.4 1.5 wt% Tank C-106: Filtrate Flux as a Function of Time 3.6
3.5 1.5 wt% Tank C-106: Filtrate Flux as a Function of Axial Velocity 3.7
3.6 1.5 wt% Tank C-106: Filtrate Flux as a Function of Transmembrane Pressure 3.8
3.7 8 wt% Tank C-106: Filtrate Flux as a Function of Time 3.9
3.8 8 wt% Tank C-106: Filtrate Flux as a Function of Axial Velocity 3.11
3.9 8 wt% Tank C-106: Filtrate Flux as a Function of Transmembrane Pressure 3.12
3.10 0.05 wt% Tank C-107: Filtrate Flux as a Function of Time 3.13
3.11 1.5 wt% Tank C-107: Filtrate Flux as a Function of Time 3.13
3.12 8 wt% Tank C-107: Filtrate Flux as a Function of Time 3.14
3.13 0.05 wt% Tank C-107: Filtrate Flux as a Function of Axial Velocity 3.15
3.14 0.05 wt% Tank C-107: Filtrate Flux as a Function of Transmembrane Pressure 3.16
3.15 1.5 wt% Tank C-107: Filtrate Flux as a Function of Axial Velocity 3.18
3.16 1.5 wt% Tank C-107: Filtrate Flux as a Function of Transmembrane Pressure 3.19
3.17 8 wt% Tank C-107: Filtrate Flux as a Function of Axial Velocity 3.20
3.18 8 wt% Tank C-107: Filtrate Flux as a Function of Transmembrane Pressure 3.21
3.19 0.05 wt% Tank B-110: Filtrate Flux as a Function of Time 3.22
3.20 1.5 wt% Tank B-110: Filtrate Flux as a Function of Time 3.22
3.21 8 wt% Tank B-110: Filtrate Flux as a Function of Time 3.23
3.22 0.05 wt% Tank B-110: Filtrate Flux as a Function of Axial Velocity 3.24
3.23 0.05 wt% Tank B-110: Filtrate Flux as a Function of Transmembrane Pressure 3.25
3.24 1.5 wt% Tank B-110: Filtrate Flux as a Function of Axial Velocity 3.26
3.25 1.5 wt% Tank B-110: Filtrate Flux as a Function of Transmembrane Pressure 3.27

3.26 8 wt% Tank B-110: Filtrate Flux as a Function of Axial Velocity 3.28
3.27 8 wt% Tank B-110: Filtrate Flux as a Function of Transmembrane Pressure 3.29
3.28 0.05 wt% Tank U-110: Filtrate Flux as a Function of Time 3.31
3.29 1.5 wt% Tank U-110: Filtrate Flux as a Function of Time 3.31
3.30 8 wt% Tank U-110: Filtrate Flux as a Function of Time 3.32
3.31 0.05 wt% Tank U-110: Filtrate Flux as a Function of Axial Velocity 3.33
3.32 0.05 wt% Tank U-110: Filtrate Flux as a Function of Transmembrane Pressure 3.34
3.33 1.5 wt% Tank U-110: Filtrate Flux as a Function of Axial Velocity 3.35
3.34 1.5 wt% Tank U-110: Filtrate Flux as a Function of Transmembrane Pressure 3.36
3.35 7.5 wt% Tank U-110: Filtrate Flux as a Function of Axial Velocity 3.37
3.36 7.5 wt% Tank U-110: Filtrate Flux as a Function of Transmembrane Pressure 3.38
3.37 Plutonium Concentration in C-106 Filtrate Compared with Equilibrium Solubility of Pu02*xH2O 3.45
4.1 Comparison of Feeds Tested with the 0.5-Micron Mott Filter 4.2
4.2 Comparison of Feeds Tested with the 0.1-Micron Graver Filter 4.2
4.3 Hydraulic Resistance for 8 wt% B-110 Feed 4.4

Tables

3.1 Experimental Conditions ... 3.1
3.2 Total Alpha Analysis ... 3.40
3.3 ^{90}Sr Analysis ... 3.41
3.4 Estimated Activity in LLW Glass Resulting from Immobilizing Filtrate ... 3.41
3.5 Total Alpha and ^{90}Sr Analysis for C-106 ... 3.42
3.6 Distribution of Measured Activity after 0.2 μm Millipore Filtration ... 3.43
3.7 Total Alpha Analysis from the 8 wt% C-106 Retest ... 3.43
3.8 ^{90}Sr Analysis from the 8 wt 8% C-106 Retest ... 3.44
3.9 Nonradioactive Components Measured in Filtrate Samples ... 3.47
3.10 Median Particle Size of Feeds Tested ... 3.48
4.1 Total Hydraulic Resistance Measured After each Run Indicated ... 4.3
4.2 Comparison of Hydraulic Resistance Measured for Feeds Tested ... 4.6
4.3 Calculated and Measured Mean Particle Diameters ... 4.8
4.4 Comparison of Graver Filter-Media Resistance ... 4.11
4.5 Comparison of Mott Filter-Media Resistance ... 4.11
4.6 Estimated Crossflow Filter Requirements for Various Hanford Pretreatment Needs ... 4.12

Acknowledgments

This work was prepared with the support of the following contributors:

- U.S. Department of Energy Headquarters: Office of Science and Technology, D.W. Geiser
- Focus Area/Program: Tank Focus Area, Phil McGinnis
- Operations Office: Richland Operations Office, Science and Technology Programs Division, Jeffrey A. Frey, Technical Program Officer
- Contractor: Pacific Northwest National Laboratory, Environmental Management Technology Development Program, Steven C. Slate, Manager

The authors gratefully acknowledge the help of Chuck Hymas (PNNL) in conducting this work. We also thank Dan McCabe (Savannah River Site [SRS]), Reid Peterson (SRS), and Charles Nash (SRS) for reviewing this document and providing insights and suggestions for the data analysis.

In Memoriam

Garry Richardson (PNNL), who contributed significantly to the timely completion of this work, suddenly and unexpectedly passed away shortly after the completion of the hot-cell experiments.

1.0 Introduction

Savannah River Site (SRS) and West Valley Nuclear Services (WVNS) both have crossflow filters which are used for the pretreatment of radioactive tank wastes. While there is considerable experience using crossflow filters around the U.S. Department of Energy (DOE) complex, gathering waste-specific data for each feed to be processed is crucial, as each waste type can behave differently and it is not possible to predict how filtering behavior may differ *a priori.*

The cell unit filter (CUF) is a bench-scale crossflow filter designed at SRS and set up in a Pacific Northwest National Laboratory (PNNL) hot cell to conduct filtration studies on Hanford tank wastes. Results from experiments on S-107 sludge and C-107 supernatant are reported in Geeting and Reynolds (1996). Results showed that crossflow filtration was effective in removing insoluble transuranic (TRU) and ^{90}Sr activity from the filtrate such that both were below Class A standards, yet the filter used in testing exhibited subsurface fouling, significantly reducing filtrate-flux rates. The subsurface fouling was reversible with 2 wt% oxalic acid cleaning; however, it is believed that a smaller pore-size filter may reduce or eliminate such fouling altogether.

This document reports on results of testing Hanford tank waste from tanks C-106, C-107, B-110, and U-110. The latter three waste types were tested with a smaller pore-size filter in an attempt to reduce the effects of subsurface filter fouling.

1.1 Background

A simplefied Hanford tank-waste pretreatment flowsheet with the major solid/liquid separations (SLS) needs identified is shown in Figure 1.1. Waste requiring sludge washing (leaching with 3 M NaOH) will be retrieved and the resulting leach and rinse liquors will be separated from the solids as identified in Need 1a. The solids will be immobilized in a high-level waste (HLW) form while the liquid will be sent to a low-level waste (LLW) form after additional pretreatment. Waste not requiring enhanced sludge washing will be retrieved and solids will be separated from liquids in Need 1b. Although feeds for Need 1a and 1b can be expected to have variable ionic strength and solids concentrations, these (Needs 1a and 1b) may be met physically by the same piece of equipment.

If required, the separated liquid may be evaporated, nominally to 5-7 M Na, before Cs removal. The evaporation would operate short of precipitation of any solids, although that possibility exists. Need 2 has been identified as a polishing step to prevent blinding or plugging of the Cs ion-exchange column. Post-ion-exchange filtration (Need 3) may be required to remove resin fines from the LAW stream, particularly if crystalline silico-titanates are used as the exchanger. The solids loading for this need should be low, as solids above 0.05 wt% are not expected during normal operations. Clearly, various SLS methods could be employed for each need identified, but crossflow filtration is one of the candidate technologies for all three of the SLS needs shown.

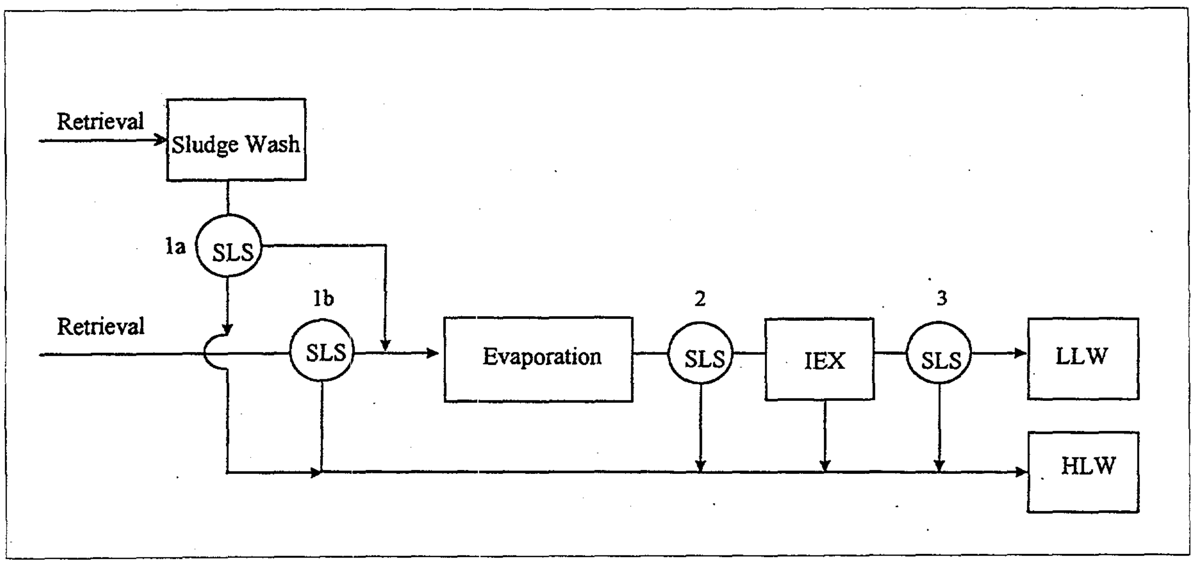

Figure 1.1. Simplified Hanford Tank Pretreatment Train Showing Major Solid/Liquid Separation Needs

1.2 Objectives

The objective of this work was to determine the crossflow filtration solids-removal efficiency for Hanford tank wastes tested, and thereby provide a preliminary assessment of whether crossflow filtration may be implemented in Hanford tank-waste pretreatment. Other objectives were to obtain data on filtrate flux as a function of axial velocity and pressure for scale-up use, and to identify issues relating to the filtration of such wastes.

1.3 Theory

The difference between crossflow filtration and conventional dead-end filtration is displayed schematically in Figure 1.2. Crossflow filtration uses velocity of the feed suspension to sweep away particles deposited on the filter media, thereby limiting the thickness of the filter cake.

The filtrate flux rate may be limited either by the viscous resistance of the fluid passing through the porous media or by the capability of the fluid to transport solids away from the filter cake. Back-transport of solids away from the membrane and into the bulk stream is required to prevent the cake thickness from continually increasing.

If the limiting resistance to filtrate flux is caused by the back-transport of solids away from the membrane, then the filtrate flux may be described as follows.

$$J_{mt}=k \ln(C_w/C_b) \quad (1)$$

where J_{mt} is the mass transfer limited steady-state flux; k is the back mass-transfer coefficient; and C_w and C_b are the concentration at the wall and in the bulk, respectively. In this instance, an increase in pressure results in a corresponding increase in the thickness of the filter cake and no increase in the steady-state filtrate flux.

Porter (1972) observed that experimental flux values were often one to two orders of magnitude higher than those indicated by the mass transfer evaluated for laminar and turbulent flow and the Stokes-Einstein relationship for Brownian motion diffusivity. Nevertheless, Equation 1 is thought to be valid with the correct mass-transfer coefficient. Investigators (e.g., Zydney and Colton 1986) have suggested various particle-transport augmentations to account for the difference in predicted vs. experimental fluxes.

If mass transport of solids away from the accumulated bed does not limit filtrate flow, then filtrate flux at steady-state should vary in accordance with Darcy's Law for pressure filtration.

$$J_f = P/\mu(L/K + R_m) \qquad (2)$$

where

J_f = pressure filtration limited flux (m^3/m^2*S)
P = filtration pressure (Pa)
μ = liquid viscosity (Pa*S)
R_m = filter-media resistance (1/m)
L/K = filter-cake resistance (R_L), where L= cake thickness (m) and K= cake permeability (m^2).

Equation 2 indicates the filtration rate J_f increases when P increases or K increases. The filtration rate J_f decreases when L increases, and R_m increases, or μ increases.

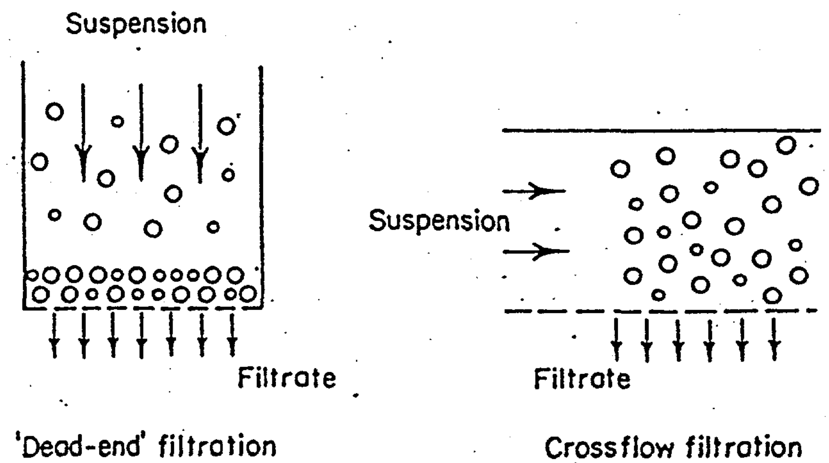

Figure 1.2. Schematic Display of Fundamental Difference between Crossflow Filtration and Conventional "Dead-End" Filtration (Murkes and Carlsson 1988)

There are two operating regimes for crossflow filtration, depending on which equation (1 or 2) governs the filtrate flux rate. These two regimes are described as follows.

- **Regime I** - If Darcy's Equation (Equation 2) governs the filtrate flux rate, (i.e., $J_f < J_{mt}$), then the filtrate flux will vary linearly with pressure. In this regime, little filter cake has built up on the filter media and the current axial velocity effectively prevents accumulation of the filter cake. Consequently, increasing the axial velocity further will result in little or no flux increase.

- **Regime II** - If Equation 1 governs the filtrate flux rate, then the flux will vary with axial velocity. In this regime, a significant filter cake has built up on the media and the current axial velocity is ineffective at preventing the accumulation of filter cake. Consequently, increasing the axial velocity will cause higher flux rates because it decreases the cake thickness. Increased pressure will bring about an increase in cake resistance, R_L, by means of growth in cake thickness or decrease in the cake permeability (or both). While an increase in pressure may cause a temporary increase in flux, the cake resistance will increase and result in no flux increase. In this second regime, velocity alone effectively increases the filtrate flux.

From a practical standpoint, we find that at low transmembrane pressures the filtrate flux varies linearly with pressure, indicating that the hydraulic resistance limits the flux. While at high transmembrane pressures the filtrate flux is pressure-independent, indicating back-transport limits the filtrate flux, and J_{mt} approximately equals J_f. From Equation 1 we see that increased solids loading in the feed, C_b, causes J_{mt} to decrease. Therefore, increasing solids loading decreases the pressure at which the transition from Regime I to Regime II occurs, and a given system can transition from Regime I to Regime II merely by increasing the solids loading in the feed.

1.4 Feed Description

1.4.1 C-106 Feed

The main waste types stored in tank C-106 are strontium sludge and waste from the tributyl phosphate (TBP) uranium-extraction process at U plant. Strontium sludge was generated from the plutonium-uranium extraction (PUREX) process during the 1970s and contains high concentrations of Al, Fe, Na, and Si. C-106 is a member of sort on radioactive waste type (SORWT) group XXIII which makes up 3 vol% of the sludge in the single-shell tanks (SSTs) (Hill and Simpson 1994). There is some organic matter in the C-106 sludge and relatively high levels of ^{137}Cs and ^{90}Sr. The C-106 sludge used in testing was obtained from a grab sample. The sludge had appreciable quantities of ~½" spherical particles resembling amorphous rocks which would not go into solution. These particles were not put into the cell unit filter (CUF). The C-106 feed plugged a 1/4" drain line which had to be replaced. The C-106 feed was generally more difficult to process than the S-107 that was tested.

1.4.2 C-107 Feed

The C-107 sludge used in testing was a mixture of Core 68, 69, and 71. The C-107 sludge tested underwent enhanced sludge washing (ESW) before testing in the CUF. ESW consists of leaching the sludge with 3 M NaOH to dissolve aluminum, phosphorus, chromium, and any other amphoteric components. A description of the ESW of the C-107 sludge is contained in Brooks et al. (1996).

The main waste types stored in tank C-107 are strontium sludge and first-cycle decontamination waste from the $BiPO_4$ process at B and T plants. The latter waste type consists of by-products co-precipitated from a plutonium-containing solution. Coating waste from the removal of aluminum fuel-element cladding makes up about 24% of this waste stream. C-107 is in the solitary SORWT group which is comprised of tanks of dissimilar composition. The sludge in tank C-107 comprises 3 vol% of the sludge in all the SSTs (Hill and Simpson 1994). A brief description of the former waste type, strontium sludge, is provided in the description of the C-106 feed, above.

1.4.3 B-110 Feed

The sludge used in testing was a composite from cores 1, 2, 3, 4, 9, 10, and 16 from the 1989 and 1990 sampling of tank B-110. The primary waste type stored in SST B-110 is the second-cycle decontamination waste from the bismuth-phosphate process. Other wastes added to this tank include waste from tank 5-6 at B Plant, and fission-products waste produced at B Plant. B-110 is a member of SORWT group XV which makes up 4 vol% of the sludge in the SSTs (Hill and Simpson 1994).

1.4.4 U-110 Feed

The U-110 sludge used in testing was a composite sample from core 14 which had dried under ambient conditions in the hot cell where it was stored. The primary waste type stored in tank U-110 is the neutralized first-cycle decontamination waste from the bismuth-phosphate process. Other wastes added to this tank include reduction-oxidation (REDOX) process HLW, cladding waste, and laboratory waste from the 222-S building. U-110 is a member of SORWT group XVII which makes up 2 vol% of the sludge in the SSTs (Hill and Simpson 1994).

1.5 Definitions

Throughout the text fouling is discussed; to avoid confusion, the following definitions are made.

- Fouling: A general term which encompasses any combination of surface and subsurface fouling.
- Subsurface fouling: The deposition and capture of fine particles within the filter membrane pores resulting in a reduction in permeate flux. Such fouling requires chemical cleaning to remove it.
- Surface fouling: The deposition of fine particles on the filter membrane surface resulting in a reduction in permeate flux. The difference between surface fouling and filter cake is that the latter is removable by back-pulsing, while the former is defined to require a system rinse for removal.
- Transmembrane pressure drop: The total pressure drop between the feed and the filtrate.

2.0 Procedure

2.1 Procedural Changes

A few procedural changes were made based on lessons learned from previous testing (Geeting and Reynolds 1996).

(1) Each feed tested herein was made separately by diluting the feed stock with inhibited water (0.01 M NaOH, 0.01 M $NaNO_2$); however, feeds were not diluted further or reconstituted for additional filtration studies. In contrast, previous testing of S-107 began with the 8 wt% feed, which was subsequently diluted to 1.5 wt% and 0.05 wt% for further testing. It was observed that the 8 wt% feed deagglomerated; consequently, flux rates were lower than expected for the 1.5 wt% and 0.05 wt% feed tests.

(2) The decision about whether to acid-clean the filter underwent a few changes during the testing. Because the Mott filter required acid cleaning after the S-107 testing, the filter was cleaned before each C-106 feed test so that filter fouling could be more easily attributed to the feed and conditions at which fouling occurred. Subsequent feeds (i.e., C-107, B-110, and U-110) were tested with the Graver filter which was acid-cleaned only if there was a significant increase in filter fouling as measured by the clean water flux. As it turns out, the Graver filter required acid cleaning only after the 1.5 wt% B-110 feed.

(3) For the C-107, B-110, and U-110 feeds, the CUF was run for two hours after the second back-pulse during condition 11, instead of 30 minutes. This was done to see if there were any significant filtrate flux changes between 30 minutes and 120 minutes after back-pulsing.

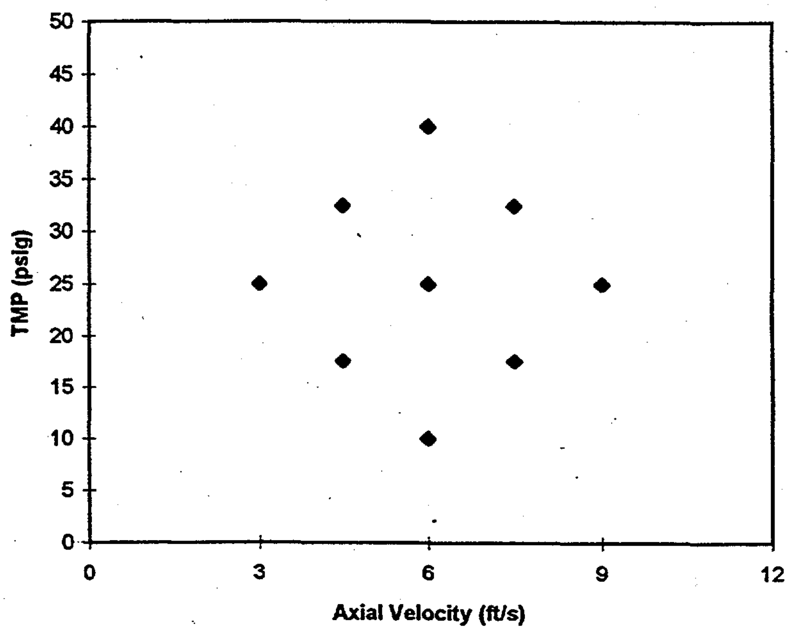

Figure 2.1. Statistically Designed Experimental Conditions Used in Testing

2.2 Radioactive Tests

A sample test procedure is contained in Geeting and Reynolds (1996). Below is a brief description of how the tests were conducted.

Radioactive filtration tests were conducted in the 325 Building C-cell with nominally 0.05 wt%, 1.5 wt%, and 8 wt% insoluble tank-sludge solids prepared by adding inhibited water (0.01 M NaOH, 0.01 M $NaNO_2$) to the sludge.

Approximately 800 ml feed volume was required to fill the cell unit filter (CUF). Each of eleven conditions were established by setting the desired axial velocity and transmembrane pressure (TMP). The experimental conditions were chosen based on a central composite response surface design. The conditions and run order used in the experimental design for the 0.05 wt% and 1.5 wt% slurries are shown in Figure 2.1. The center condition is tested three times: first, middle, and last.

The design for the 8 wt% slurry was similar, but shifted down 5 psig such that the design center was 20 psig instead of 25 psig because the CUF was unable to meet the latter condition at high solids loading.

After establishing each condition, an initial back-pulse was conducted and a clock was started. Each condition was run for at least 60 minutes, measuring and recording TMP, axial velocity, temperature, and filtrate-flux data. Data were recorded every 10 minutes, except for the center point which was recorded every 5 minutes. Slurry temperature was maintained by adjusting the cell-supplied heat exchanger as required. A back-pulse was conducted after 30 minutes for each condition. Filtrate samples were taken at the four corners and center of the central composite design for a total of five samples/feed.

After completion of the testing, the CUF was drained and rinsed at least 3 times with deionized water. A feed sample of each feed was taken from a well mixed sample of the drained slurry. The test procedure was repeated for each feed.

2.3 Apparatus

The CUF, shown schematically in Figure 2.2, was designed at the Savannah River Site (SRS) and used for all testing. The slurry feed was introduced into the CUF through the slurry reservoir. A Moyno progressive-cavity pump, powered by an air motor, pumped the slurry from the reservoir though the magnetic flowmeter and a 0.5" diameter x 6"-long sintered-metal filter. Two filter elements were used in the testing: a 0.5-micron Mott filter was used for the C-106 feed while a 0.1-micron Graver filter was used for the C-107, B-110, and the U-110 feeds. The axial velocity and TMP were controlled by adjusting the pump speed and the throttle valve (V1). A back-pressure (check) valve was installed to prevent over-pressurization of the system. Filtrate passed through the filter and was reconstituted with the slurry in the slurry reservoir. The filtrate flow rate was measured by means of a fill-and-drain graduated cylinder. Filtrate samples could be taken at the sampling valve (V6). The slurry temperature was measured by a type J thermocouple installed in a temperature well in the slurry reservoir.

Filter back-pulsing was conducted by opening the toggle valve (V3) and allowing the back-pulse chamber to fill with filtrate. The toggle valve was closed and the back-pulse chamber was pressurized with air through a three-way valve (V7). Once charged, the toggle valve was then opened, allowing the pressurized filtrate to back-pulse the filter element. After completing a run, the system was drained through valves V2, V6, X1, and X2.

Upon receipt of the CUF from SRS, minor modifications were made by PNNL as follows:

- a cooling jacket was added to the outside of the slurry reservoir to control the slurry temperature because during simulant-testing temperatures in excess of 80°C were observed;

- a single baffle was added to the slurry reservoir to prevent vortex formations observed in simulant testing;

- a larger Moyno pump (model SP-33304) with a nominal capacity of 7 gpm at 25 psig replaced the Moyno SP-23203, which had a nominal capacity of 4 gpm at 20 psig, to permit testing at higher flowrates and TMPs;

- a 50 psig check valve replaced the 30 psig check valve to permit testing at higher TMPs; and

- two drain valves (X1 and X2) were added to aid in draining between runs and thus minimize rinse volumes.

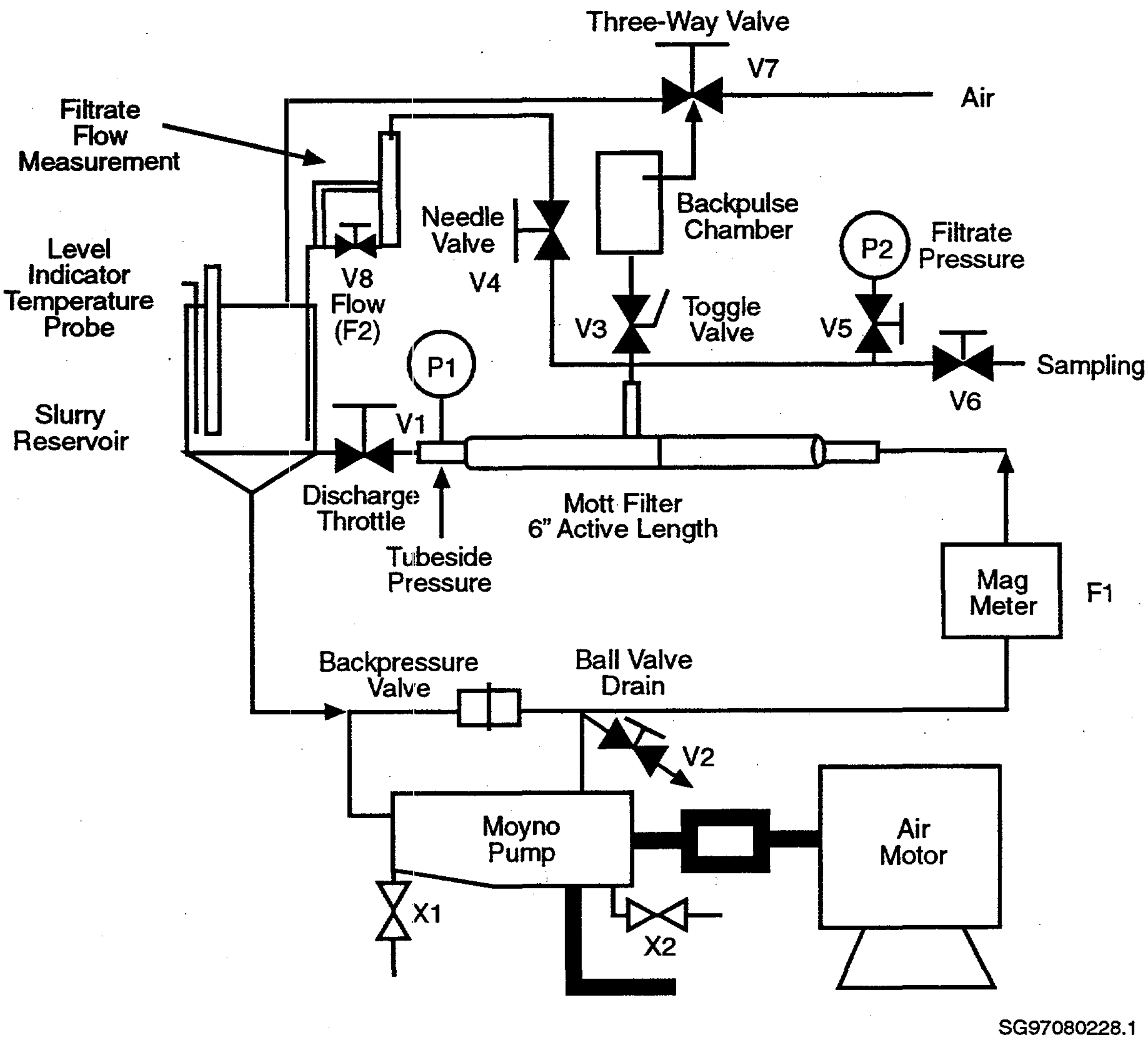

Figure 2.2 Cell Unit Filter Flow Diagram

3.0 Results and Discussion

The conditions and run order used in the experimental design for the 0.05 wt% and 1.5 wt% slurries are shown in Table 3.1. Note that condition 1, 6, and 11 had identical processing conditions and served as a control point. The design for the 8 wt% slurry was similar, but shifted down 5 psig such that the design center was 20 psig instead of 25 psig because the CUF was unable to meet the latter condition at the higher solids loading.

We found that there was a dependence on run order, possibly caused by filter fouling and feed deagglomeration, which caused a decline in the filtrate-flux rate as the experiment progressed. For each feed, a partial least-squares regression model was used to estimate the effect of run order and normalize all data to condition 6, thus eliminating the effect of run order and leaving only the influence of changes in transmembrane pressure (TMP) and axial velocity on the filtrate flux. For plots with time as the independent variable, the data normalization was not performed. Data from each test are provided in Appendix A.

The presentation in this section is organized on a tank-by-tank basis. For consistency, all values of filtrate flux plotted were measured 30 minutes after back-pulsing (unless the independent variable in the plot was time).

Table 3.1. Experimental Conditions

Condition	Axial Velocity (ft/s)	Transmembrane Pressure (psig)
Condition 1	6.0	25.0
Condition 2	7.5	32.5
Condition 3	3.0	25.0
Condition 4	6.0	10.0
Condition 5	7.5	17.5
Condition 6	6.0	25.0
Condition 7	4.5	32.5
Condition 8	6.0	40.0
Condition 9	4.5	17.5
Condition 10	9.0	25.0
Condition 11	6.0	25.0

3.1 C-106

3.1.1 0.05 wt% Tank C-106 Slurry

The mean (average of 2 data points) filtrate flux (gpm/ft^2) for conditions 1, 6, and 11 as a function of time (minutes) since back-pulse is displayed in Figure 3.1. These three conditions all had the same processing parameters of 25 psig TMP and 6 ft/s axial velocity. The flux at condition 1 declined as a function of time, but the flux at condition 6 and 11 effectively did not vary significantly with time, and back-pulsing had little effect on restoring the flux for these two latter conditions. Such behavior is expected when feed particles are deposited irreversibly within the filter membrane (subsurface fouling) and therefore back-pulsing becomes ineffective. If the particles were deposited reversibly on the membrane, then one would expect flux-rate recovery after a back-pulse. Analysis in Section 4.1 demonstrates that although the C-106 feed fouled the Mott filter, no feed deagglomeration was measured during the run. We conclude that most of the flux-rate reduction between condition 1 and conditions 6 and 11 was attributed to subsurface fouling.

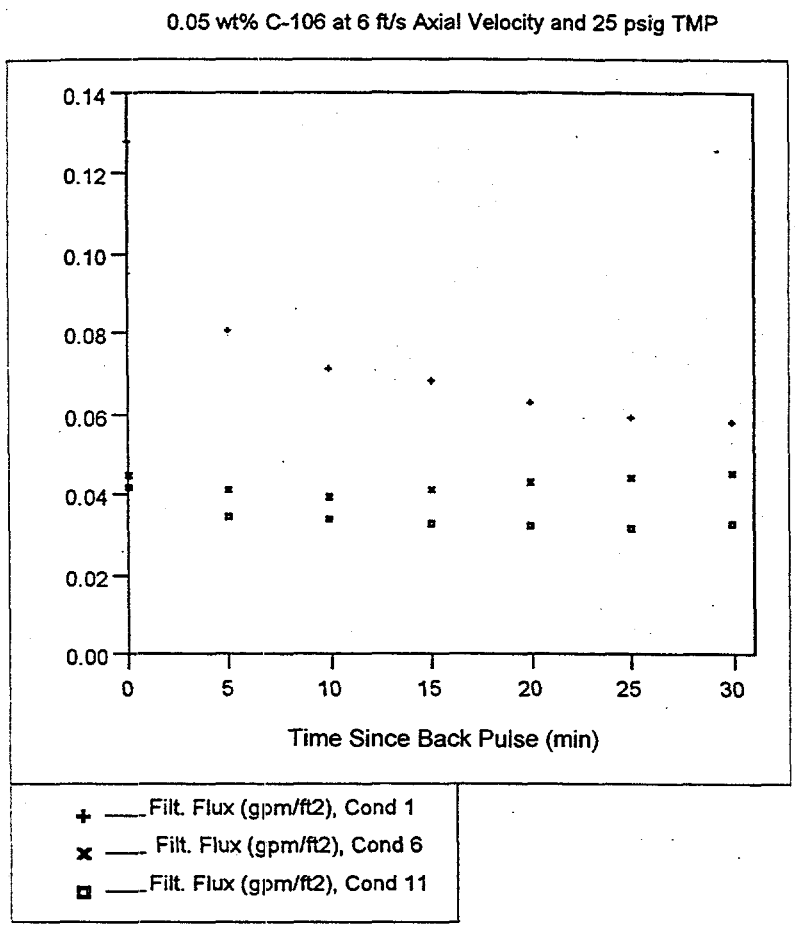

Figure 3.1. 0.05 wt% Tank C-106: Filtrate Flux as a Function of Time (6 ft/s, 25 psig)

An interesting result is that the filtrate flux is a negative function of the axial velocity, clearly observed in Figure 3.2 which displays a plot of mean filtrate flux (gpm/ft^2) as a function of axial velocity. The negative relationship evident between filtrate flux and axial velocity is not the norm; however, such phenomena have been reported in the literature (Tartleton and Wakeman 1993) and attributed to an increase in hydraulic resistance of the filter cake at higher axial velocities. The cake hydraulic resistance, R_L, is:

$$R_L = 180(1-\epsilon)^2 \delta_L / d_p^2 \epsilon^3$$

Thus we see an increase in cake resistance may be caused by a decrease in particle diameter, d_p; a decrease in cake porosity, ϵ; or an increase in the cake thickness, δ_L. Because of the increased shear at higher velocities, it is unlikely that an increased cake thickness caused the observed decline in filtrate flux with velocity. The decrease may have been caused by smaller diameter particles in the filter cake, which would have the added impact of decreasing porosity, as filter cakes with smaller particles have lower porosities. Tartleton and Wakeman (1993) suggest the phenomena is caused by preferential deposition of finer particle species at the septum surfaces as the crossflow velocity is raised, forming higher resistance deposits leading to lower filtration rates.

A plot of filtrate flux (gpm/ft^2) as a function of TMP is displayed in Figure 3.3. The filtrate-flux data shown in the figure is approximately linear with pressure indicating that the data was taken below the critical pressure, at which the filtrate flux is pressure-independent. If the flux rate were velocity- independent, then we would conclude that under these conditions the filtrate flux was controlled primarily by Darcy's equation rather than being limited by back-transport. This may be true; however, the fact that the filtrate flux is a negative function of axial velocity complicates matters. If the cause of the negative axial velocity dependence is, as Tartleton and Wakeman (1993) suggest, a change in the resistance of the filter cake, then the flux nevertheless may be limited by Darcy's equation.

Filt Flux (gpm/ft2) By Flowrate (ft/s)

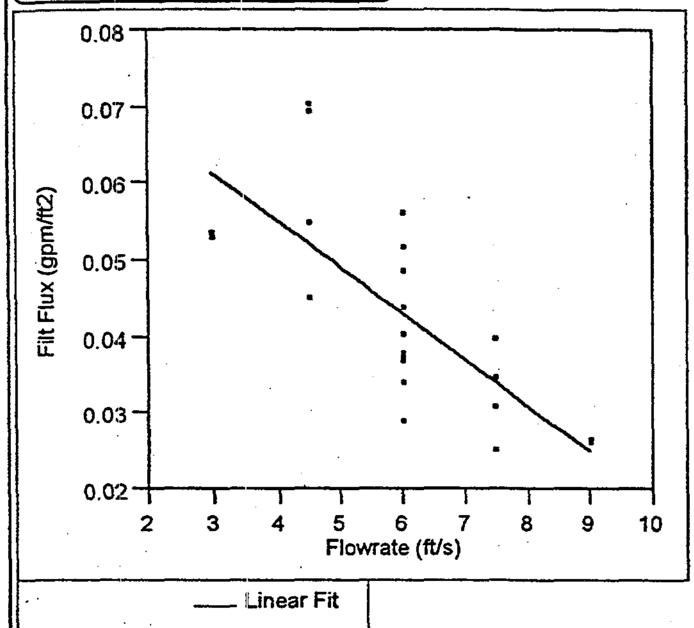

Linear Fit

Filt Flux (gpm/ft2) = 0.07957 – 0.00605 Flowrate (ft/s)

Summary of Fit

RSquare	0.55284
RSquare Adj	0.530482
Root Mean Square Error	0.008937
Mean of Response	0.043291
Observations (or Sum Wgts)	22

Analysis of Variance

Source	DF	Sum of Squares	Mean Square	F Ratio
Model	1	0.00197479	0.001975	24.7267
Error	20	0.00159730	0.000080	Prob>F
C Total	21	0.00357209		<.0001

Parameter Estimates

Term	Estimate	Std Error	t Ratio	Prob>|t|
Intercept	0.0795749	0.007541	10.55	<.0001
Flowrate (ft/s)	-0.006047	0.001216	-4.97	<.0001

Figure 3.2. 0.05 wt% Tank C-106: Filtrate Flux as a Function of Axial Velocity

Filt. Flux (gpm/ft2) By Pressure (psig)

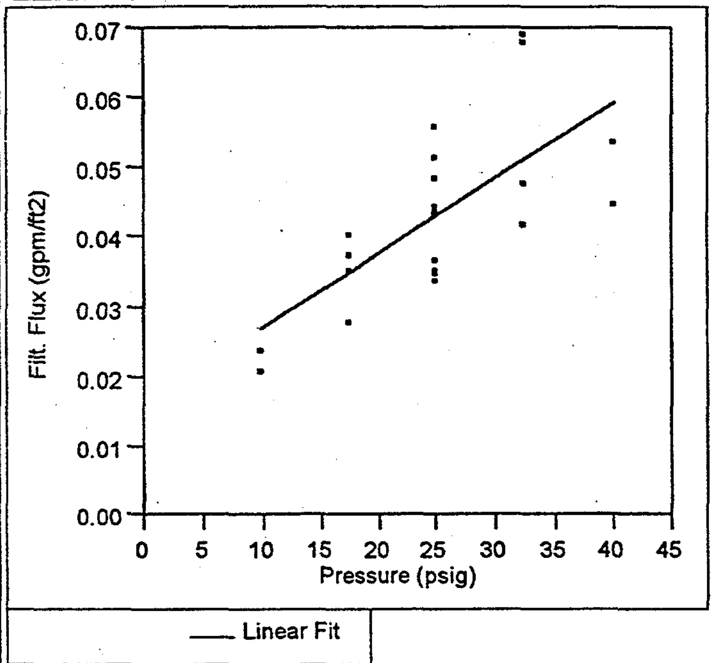

Linear Fit

Filt. Flux (gpm/ft2) = 0.01633 + 0.00108 Pressure (psig)

Summary of Fit

RSquare	0.495646
RSquare Adj	0.470428
Root Mean Square Error	0.008937
Mean of Response	0.043291
Observations (or Sum Wgts)	22

Analysis of Variance

Source	DF	Sum of Squares	Mean Square	F Ratio
Model	1	0.00156972	0.001570	19.6547
Error	20	0.00159730	0.000080	Prob>F
C Total	21	0.00316702		0.0003

Parameter Estimates

Term	Estimate	Std Error	t Ratio	Prob>|t|
Intercept	0.0163331	0.006372	2.56	0.0185
Pressure (psig)	0.0010783	0.000243	4.43	0.0003

Figure 3.3. 0.05 wt% Tank C-106: Filtrate Flux as a Function of Transmembrane Pressure

3.1.2 1.5 wt% C-106

The 1.5 wt% C-106 feed was the most difficult feed to test because it foamed excessively and dripped out of the reservoir and into the drip pan. The most likely explanation is that air was drawn from the feed reservoir into the pump. Enough feed was lost during testing that conditions 10 and 11 and the run could not be completed because insufficient feed was available to maintain the desired flowrate and pressure. The analysis that follows is for results from testing conditions 1 through 9.

The mean filtrate flux (gpm/ft^2) for conditions 1 and 6 as a function of time (minutes) since back- pulse is displayed in Figure 3.4. These conditions had the same processing parameters of 25 psig TMP and 6 ft/s axial velocity. Some filtrate-flux decline with time and between conditions is evident. Some of the decline was reversible, as seen by the increase in the filtrate flux from condition 1 at 30 minutes to condition 6 immediately after back-pulse (0 minutes). The remaining decline could not be recovered by back-pulsing alone, indicating subsurface-filter fouling.

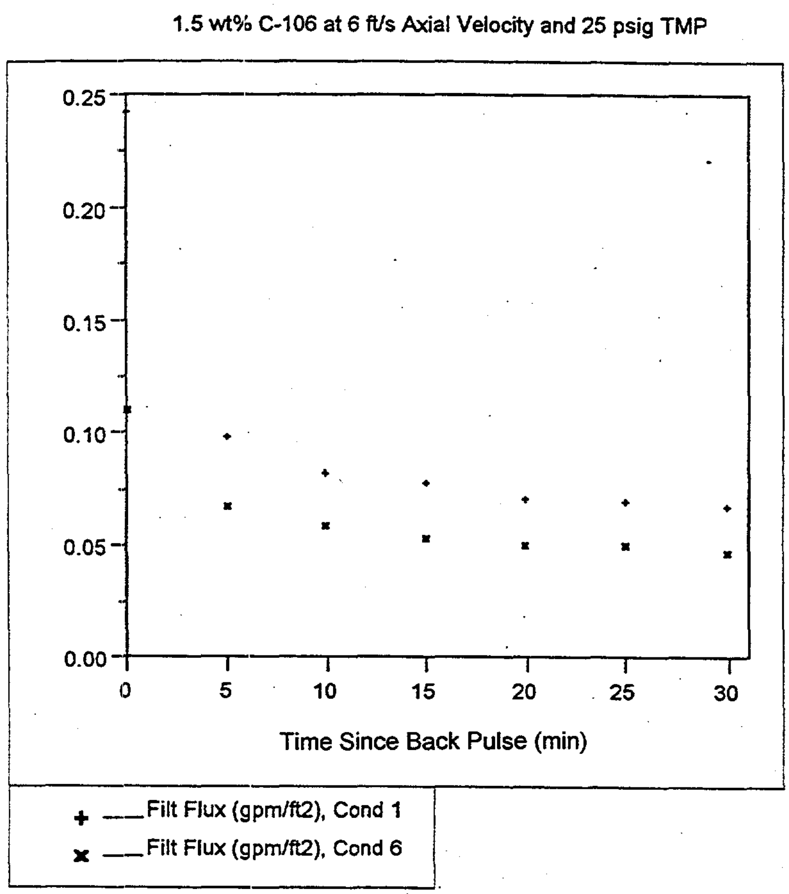

Figure 3.4. 1.5 wt% Tank C-106: Filtrate Flux as a Function of Time (6 ft/s, 25 psig)

Filt. Flux (gpm/ft2) By Flowrate (ft/s)

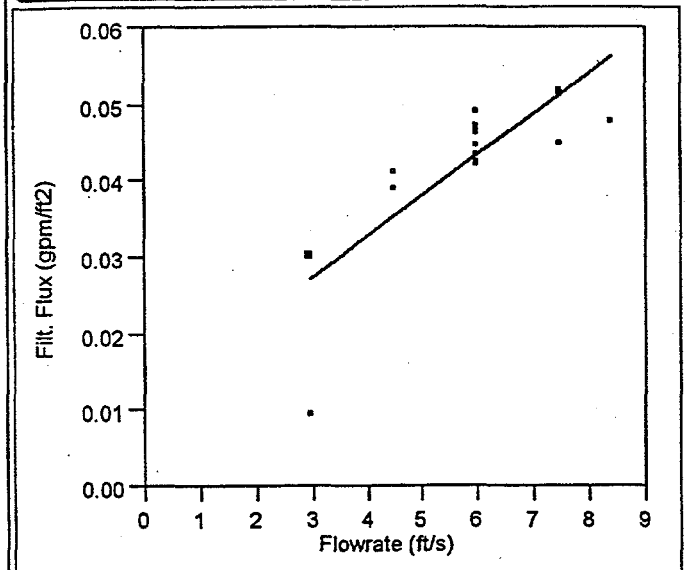

—— Linear Fit

Linear Fit

Filt. Flux (gpm/ft2) = 0.01094 + 0.00542 Flowrate (ft/s)

Summary of Fit

RSquare	0.663763
RSquare Adj	0.641347
Root Mean Square Error	0.006081
Mean of Response	0.043282
Observations (or Sum Wgts)	17

Analysis of Variance

Source	DF	Sum of Squares	Mean Square	F Ratio
Model	1	0.00109490	0.001095	29.6114
Error	15	0.00055464	0.000037	Prob>F
C Total	16	0.00164954		<.0001

Parameter Estimates

Term	Estimate	Std Error	t Ratio	Prob>|t|
Intercept	0.0109392	0.006124	1.79	0.0943
Flowrate (ft/s)	0.0054224	0.000996	5.44	<.0001

Figure 3.5. 1.5 wt% Tank C-106: Filtrate Flux as a Function of Axial Velocity

Filt Flux (gpm/ft2) By Pressure (psig)

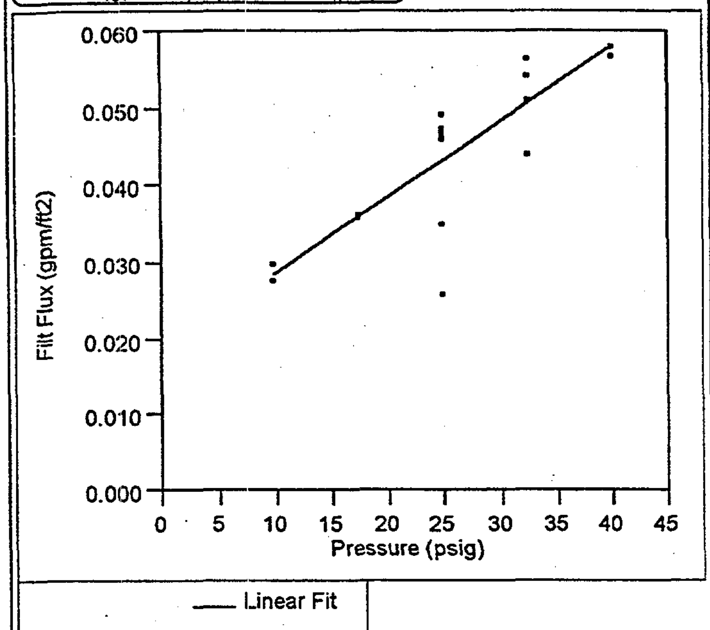

Linear Fit

Filt Flux (gpm/ft2) = 0.01878 + 0.00099 Pressure (psig)

Summary of Fit

RSquare	0.682915
RSquare Adj	0.661776
Root Mean Square Error	0.006081
Mean of Response	0.044345
Observations (or Sum Wgts)	17

Analysis of Variance

Source	DF	Sum of Squares	Mean Square	F Ratio
Model	1	0.00119454	0.001195	32.3059
Error	15	0.00055464	0.000037	Prob>F
C Total	16	0.00174918		<.0001

Parameter Estimates

Term	Estimate	Std Error	t Ratio	Prob>|t|
Intercept	0.0187789	0.004734	3.97	0.0012
Pressure (psig)	0.0009878	0.000174	5.68	<.0001

Figure 3.6. 1.5 wt% Tank C-106: Filtrate Flux as a Function of Transmembrane Pressure

Oddly, the filtrate-flux dependence at the 1.5 wt% solids loading changed from being a negative function of axial velocity (as was seen for the 0.05 wt% slurry) to a positive function. This is more clearly observed in Figure 3.5, which displays a plot of mean filtrate flux (gpm/ft^2) as a function of velocity. A positive functionality is predicted by crossflow-filtration theory. Evidently for the 1.5 wt% slurry, the decrease in hydraulic resistance caused by increased shear, and consequently thinner filter cake, overcame the disadvantage of decreased porosity observed for the 0.05 wt% slurry at higher shear rates.

A plot of filtrate flux (gpm/ft^2) as a function of TMP is displayed in Figure 3.6. The filtrate-flux data shown in the figure are approximately linear with pressure, indicating that the data were taken below the critical pressure at which the filtrate flux is pressure-independent. Because the flux rate is also velocity-dependent, we conclude that under these conditions the filtrate flux is in the transition region where flux rate is controlled partially from Darcy's equation and partially by back-transport.

3.1.3 8 wt% C-106

This feed also foamed during testing, but not as severely as the 1.5 wt% C-106 test. The mean filtrate flux (gpm/ft^2) for conditions 1, 6, and 11 as a function of time (minutes) since back-pulse is displayed in Figure 3.7. These three conditions all had the same processing parameters of 25 psig TMP and 6 ft/s axial velocity. What is unusual about this data, compared with the 0.05 wt% feed data, is that very little subsurface fouling was evident. There was an initial flux-rate decline and leveling out for condition 1. Flux rates at conditions 6 and 11 were nearly identical with time, indicating that fouling was not a continuing problem. The decrease evident when comparing conditions 1 with conditions 6 and 11 (especially at time 0) should be expected, because the filter was chemically cleaned before running the 8 wt% slurry.

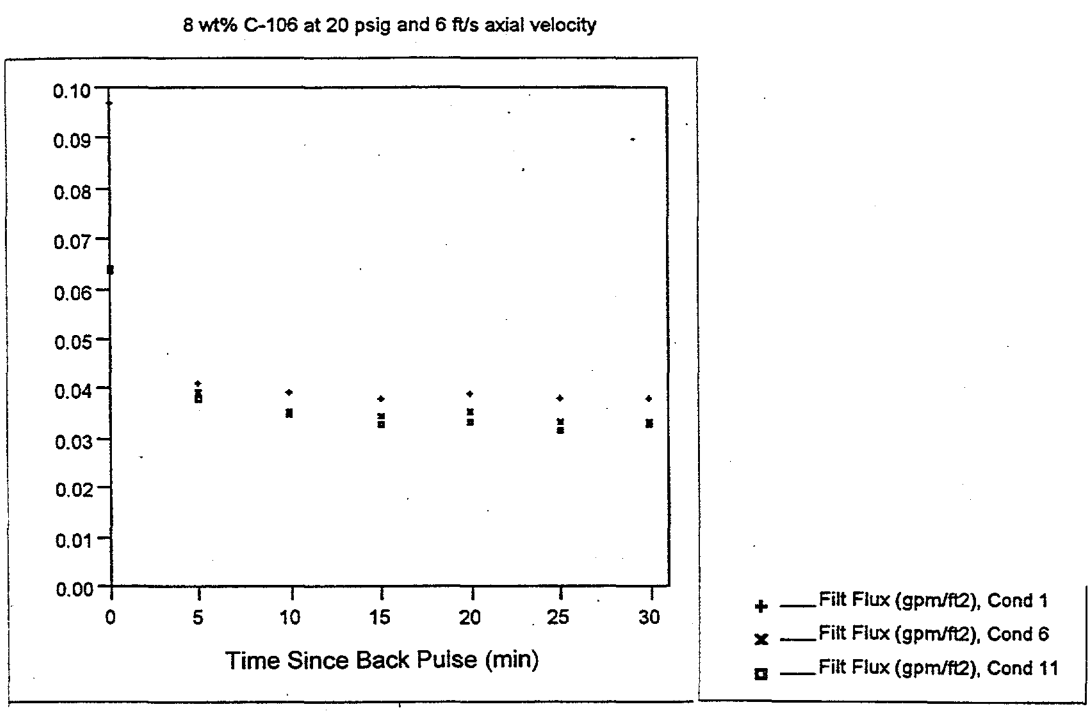

Figure 3.7. 8 wt% Tank C-106: Filtrate Flux as a Function of Time (6 ft/s, 20 psig)

Based on reviewing the fouling of the three different wt% slurries (i.e., 0.05, 1.5, and 8 wt%), the conclusion is that, at least for the C-106 feed, filter fouling is less a problem at higher solids loading. There are at least three possible explanations for this observation. First, at higher solids loading (e.g., 8 wt%) a filter cake may form immediately on the filter membrane, serving to augment the filtration process and prevent many small particles from reaching the sintered-metal membrane; thus, fouling is reduced. At lower solids loading (e.g., 0.05 wt%) the filter cake which forms is too thin to prevent small particles from reaching the sintered-metal filter effectively; therefore, more fouling is evident. The second possible explanation is that at lower solids loading (i.e., 0.05 wt%) the ionic strength, as measured by Na^+, is 1/40th that at 8 wt% solids loading (674 vs. 25600 µg/ml). The low ionic strength may have caused the 0.05 wt% feed to peptize before filtering. Because smaller particles were being filtered in the 0.05 wt% feed than the 8 wt% feed, the filter fouled more. A third explanation is that solids (e.g., aluminum hydroxide) may have precipitated when diluting during the feed preparation. Evidence for this explanation may result through comparing the soluble Al concentration in the 0.05 wt% filtrate with that in the 8 wt% filtrate. If the Al concentration in the 0.05 wt% filtrate is less than calculated based on simple dilution, then it may imply precipitation. This explanation was not supported by evaluation of data provided in Table 3.6.

Analysis in Section 4.1 concludes that the C-106 feed did not appreciably deagglomerate with shear. This does not, however, rule out the second possibility presented because the feed may have peptized before testing, and as a result the filter-cake resistance did not increase during the run. Comparison of the particle-size distribution (PSD) of the 8 wt% feed and 0.05 wt% feed would help to determine the cause; unfortunately, the PSD of the 0.05 wt% feed is not available because the 0.05 wt% C-106 feed sample was spilled in the hot cell during sample preparation.

An increase in axial velocity causes a significant increase in filtrate flux at 8 wt% solids loading, as shown in Figure 3.8. The filtrate flux (shown in Figure 3.9) basically is independent of pressure above 15 psig, indicating that the data were generally taken above the critical pressure. We conclude that the 8 wt% feed was controlled primarily by back-transport in the region tested.

3.2 C-107

The C-107, B-110, and U-110 feed stocks were tested using the 0.1-micron Graver filter. Section 4.1 provides a comparison of the two filters.

The filtrate flux (gpm/ft^2) as a function of time (minutes) since back-pulse for the 0.05 wt%, 1.5 wt%, and 8 wt% feeds, respectively, are shown in Figures 3.10, 3.11, and 3.12. The conditions within each individual figure were measured at the same TMP and axial velocity.[1] For the 1.5 and 8 wt% feeds, there is a significant decline between the flux measured at condition 1 with that measured at condition 6, with less decline between the flux measure at condition 6 with that measured at condition 11. For the 0.05 wt% feed, the filtrate flux declined more steadily between runs. In all instances, back-pulsing was effective at improving, albeit for a short while, the flux rates. The clean-water flux was restored between

[1] All of the data shown for the 0.05 and 1.5 wt% feed were measured at 6 ft/s axial velocity and 25 psig TMP. All of the data for the 8 wt% feed were measured at 6 ft/s axial velocity and 20 psig TMP.

Filt. Flux (gpm/ft2) By Flowrate (ft/s)

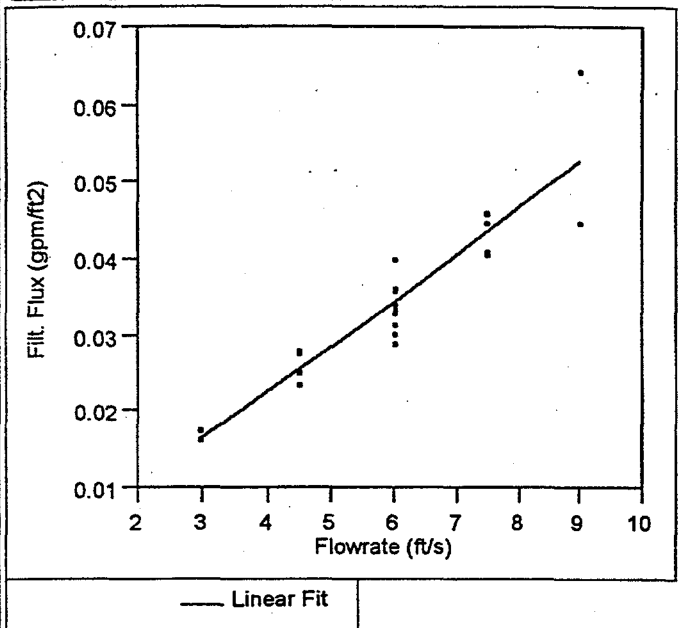

Linear Fit

Filt. Flux (gpm/ft2) = -0.0016 + 0.00604 Flowrate (ft/s)

Summary of Fit

RSquare	0.855229
RSquare Adj	0.84761
Root Mean Square Error	0.004191
Mean of Response	0.034608
Observations (or Sum Wgts)	21

Analysis of Variance

Source	DF	Sum of Squares	Mean Square	F Ratio
Model	1	0.00197109	0.001971	112.2421
Error	19	0.00033366	0.000018	Prob>F
C Total	20	0.00230475		<.0001

Parameter Estimates

Term	Estimate	Std Error	t Ratio	Prob>|t|
Intercept	-0.001642	0.003542	-0.46	0.6481
Flowrate (ft/s)	0.0060417	0.00057	10.59	<.0001

Figure 3.8. 8 wt% Tank C-106: Filtrate Flux as a Function of Axial Velocity

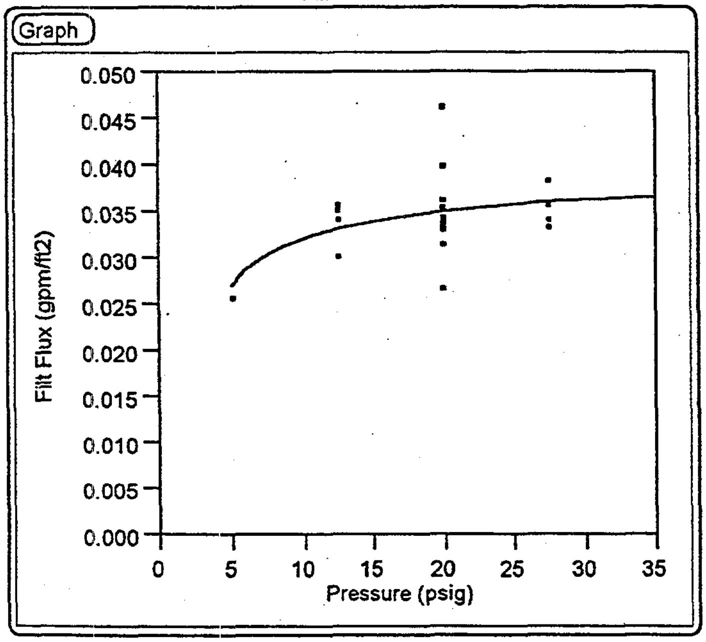

Figure 3.9. 8 wt% Tank C-106: Filtrate Flux as a Function of Transmembrane Pressure

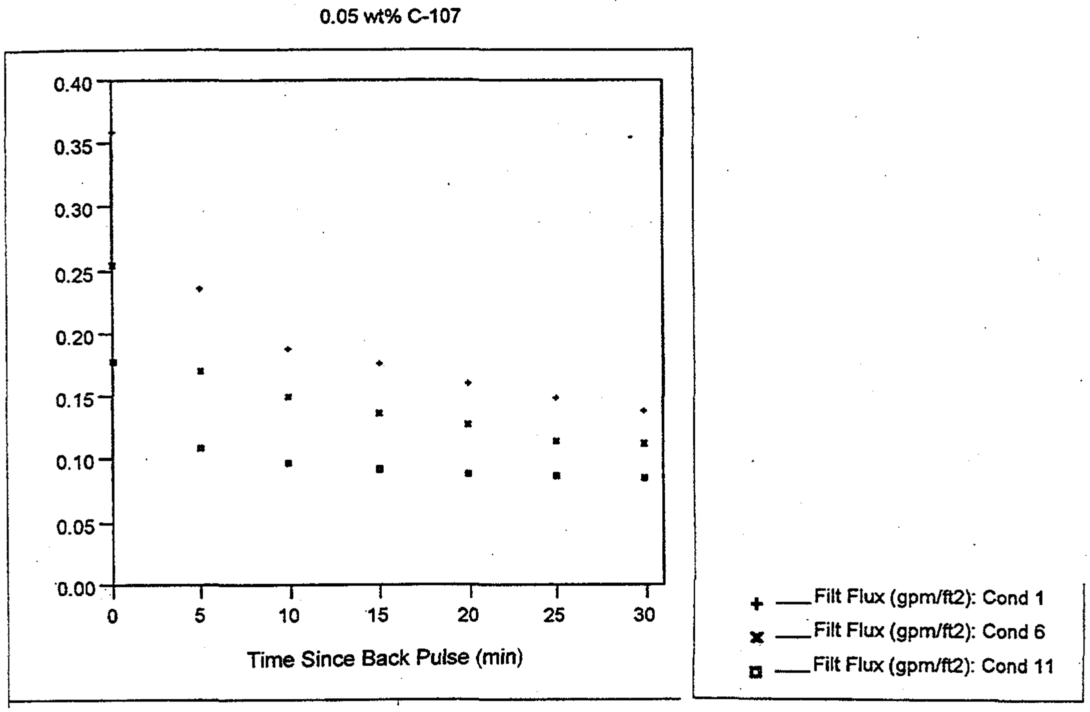

Figure 3.10. 0.05 wt% Tank C-107: Filtrate Flux as a Function of Time (6 ft/s, 25 psig)

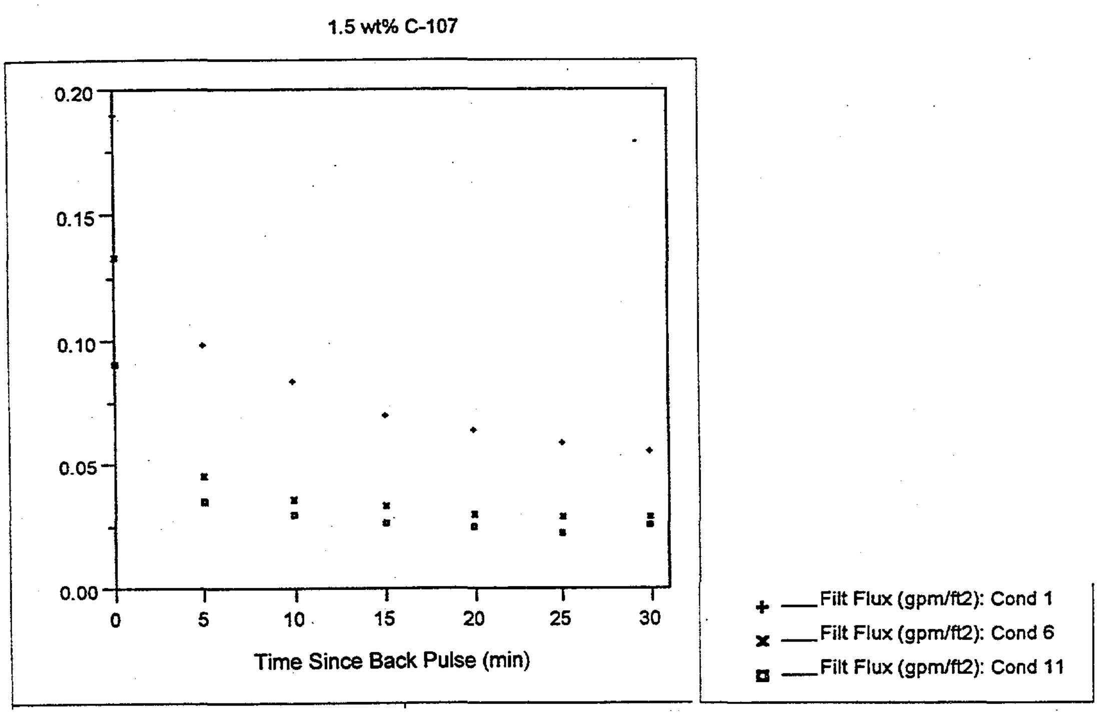

Figure 3.11. 1.5 wt% Tank C-107: Filtrate Flux as a Function of Time (6 ft/s, 25 psig)

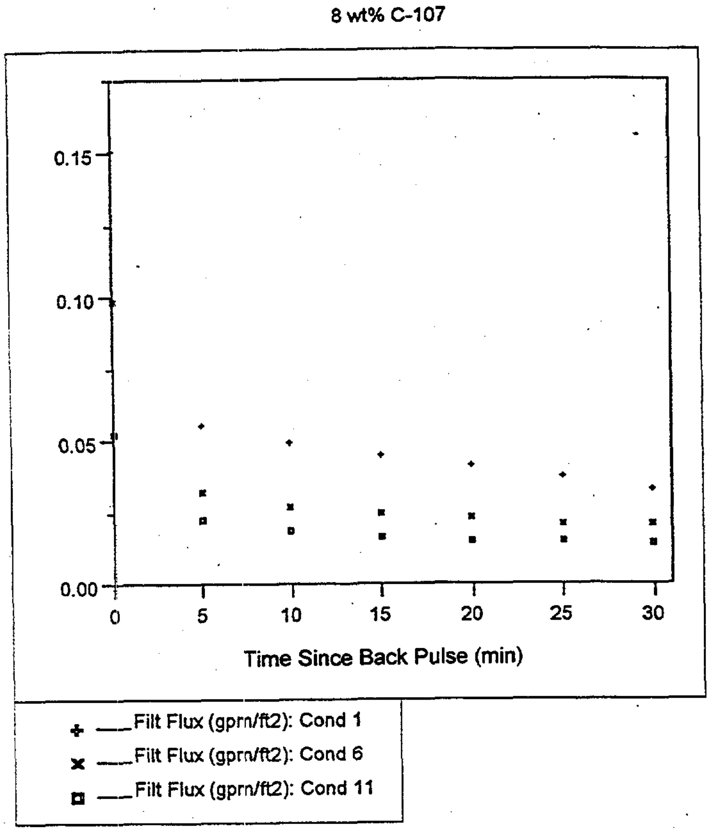

Figure 3.12. 8 wt% Tank C-107: Filtrate Flux as a Function of Time (6 ft/s, 20 psig)

runs by rinsing the system, indicating that subsurface filter fouling was not evident. Consistent with crossflow-filtration theory, the filtrate flux of the 0.05 wt% feed generally was higher than that of the 1.5 wt% feed, which in turn was higher than the 8 wt% feed. Analysis in Section 4.1 indicates that the cause of the flux decline with time for the C-107 feed was feed deagglomerating during testing and surface fouling of the filter.

3.2.1 0.05 wt% Tank C-107 Slurry

A plot of mean filtrate flux (gpm/ft2) as a function of velocity, displayed in Figure 3.13, clearly indicates very little if any dependence on axial velocity in the region tested, indicating that the velocity was sufficient in removing the filter cake. A mean fit line and the best linear fit are included in the figure to illustrate that the filtrate flux is virtually independent of axial velocity; therefore, higher filtrate flux is not achievable without increasing TMP.

A plot of filtrate flux (gpm/ft^2) as a function of TMP is displayed in Figure 3.14. The filtrate-flux data shown in the figure are approximately linear with pressure, indicating that the data were taken below the critical pressure at which the filtrate flux is pressure-independent. Under these conditions, the filtrate flux is controlled primarily by Darcy's equation rather than being limited by back-transport.

Filt Flux (gpm/ft2) By Flowrate (ft/s)

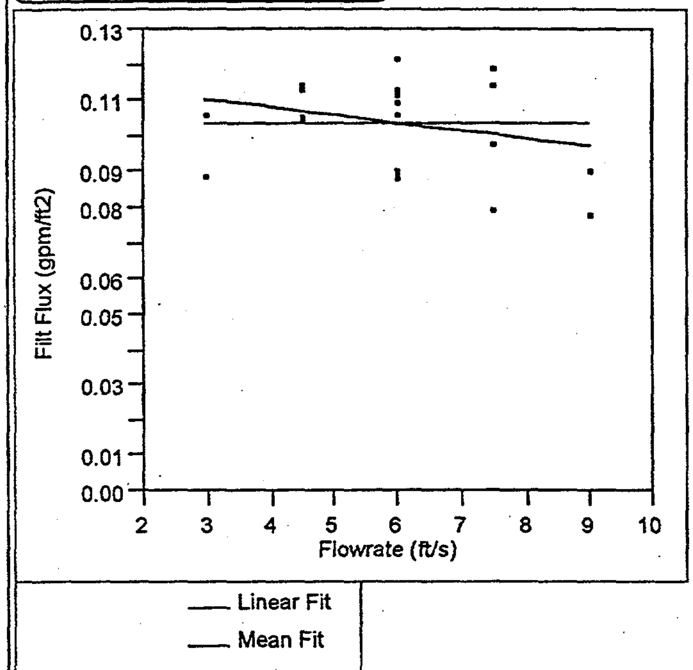

Linear Fit

Filt Flux (gpm/ft2) = 0.11717 – 0.00221 Flowrate (ft/s)

Summary of Fit

RSquare	0.074957
RSquare Adj	0.028704
Root Mean Square Error	0.012758
Mean of Response	0.103909
Observations (or Sum Wgts)	22

Analysis of Variance

Source	DF	Sum of Squares	Mean Square	F Ratio
Model	1	0.00026379	0.000264	1.6206
Error	20	0.00325550	0.000163	Prob>F
C Total	21	0.00351929		0.2176

Parameter Estimates

Term	Estimate	Std Error	t Ratio	Prob>|t|
Intercept	0.1171704	0.010766	10.88	<.0001
Flowrate (ft/s)	-0.00221	0.001736	-1.27	0.2176

Mean Fit

Figure 3.13. 0.05 wt% Tank C-107: Filtrate Flux as a Function of Axial Velocity

Filt. Flux (gpm/ft2) By Pressure (psig)

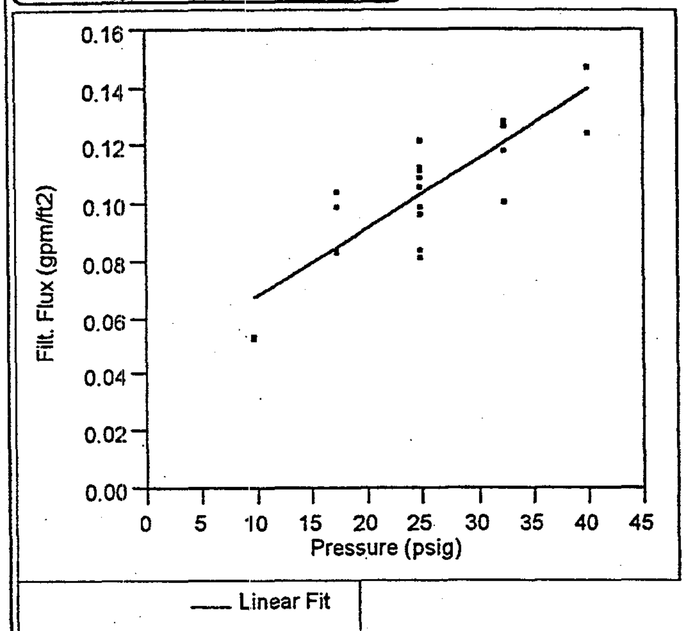

Linear Fit

Filt. Flux (gpm/ft2) = 0.04335 + 0.00242 Pressure (psig)

Summary of Fit

RSquare	0.708741
RSquare Adj	0.694178
Root Mean Square Error	0.012758
Mean of Response	0.103909
Observations (or Sum Wgts)	22

Analysis of Variance

Source	DF	Sum of Squares	Mean Square	F Ratio
Model	1	0.00792183	0.007922	48.6674
Error	20	0.00325550	0.000163	Prob>F
C Total	21	0.01117733		<.0001

Parameter Estimates

Term	Estimate	Std Error	t Ratio	Prob>|t|
Intercept	0.0433491	0.009097	4.77	0.0001
Pressure (psig)	0.0024224	0.000347	6.98	<.0001

Figure 3.14. 0.05 wt% Tank C-107: Filtrate Flux as a Function of Transmembrane Pressure

3.2.2 1.5 wt% C-107

A plot of filtrate flux (gpm/ft^2) as a function of velocity is displayed in Figure 3.15. The filtrate flux is dependent on axial velocity, indicating that this solids loading is sufficient to produce a filter cake. The filtrate flux is also linearly dependent on TMP, as shown in Figure 3.16, indicating that these data were taken in a transition region where back-transport and Darcy's equation are both important.

3.2.3 8 wt% C-107

A plot of filtrate flux (gpm/ft^2) as a function of velocity is displayed in Figure 3.17. The filtrate- flux dependency on axial velocity is about the same as that measured for the 1.5 wt% slurry and is linear over the range tested. Some data scatter is evident but not unexpected, based on the flux decline observed in Figure 3.12.

Likewise, Figure 3.18 displays a plot of filtrate flux (gpm/ft^2) as a function of TMP. The data shown in the figure correspond to that reported by other researchers (e.g., Porter 1972) and to past testing of 8 wt% tank-waste feed, where the filtrate flux loses pressure-dependency as the pressure increases above a certain critical value. In this figure, the filtrate flux seems to be insensitive to TMP above the range of 15-20 psig, indicating that the data were taken above the critical pressure. We conclude that under these conditions the filtrate flux is controlled by back-transport.

3.3. B-110

Filtrate flux (gpm/ft^2) as a function of time (minutes) since back-pulse for the 0.05 wt%, 1.5 wt% and 8 wt% feeds, respectively, is shown in Figures 3.19, 3.20, and 3.21. The conditions within each figure were measured at the same TMP and axial velocity.[2] In each instance, there was a significant decline between the flux measured at condition 1 with that measured at condition 6, with comparatively little, if any, decline between the flux measured at condition 6 with that measured at condition 11. Also, back-pulsing was effective at improving the flux rates. Except after the 1.5 wt% feed, the clean- water flux was restored between runs by rinsing the system, indicating that filter subsurface fouling was not evident. The 1.5 wt% feed was the only feed tested with the Graver filter that required acid cleaning (2 wt% oxalic acid) to restore the clean-water-flux rate. It is not known why this feed concentration caused the filter to foul. During condition 1, the filtrate flux of the 0.05 wt% feed generally was higher than that of the 1.5 or 8 wt% feeds. By condition 6, however, contrary to crossflow-filtration theory, the filtrate flux of the 8 wt% feed generally was higher than that measured for the 1.5 or 0.5 wt% feeds. If one excludes the unlikely possibility that the filter cake was thinner while running the 8 wt% feed, then one must conclude that the 8 wt% feed filter cake was more permeable at the latter conditions. This makes sense if the lower feed concentrations are composed of smaller particles, suggesting that the B-110 was more susceptible to deagglomeration at low salt content. This conclusion is supported by the analysis conducted in Section 4.

---

[2] All of the data shown for the 0.05 and 1.5 wt% feed were measured at 6 ft/s axial velocity and 25 psig TMP. All of the data for the 8 wt% feed were measured at 6 ft/s axial velocity and 20 psig TMP.

Filt Flux (gpm/ft2) By Flowrate (ft/s)

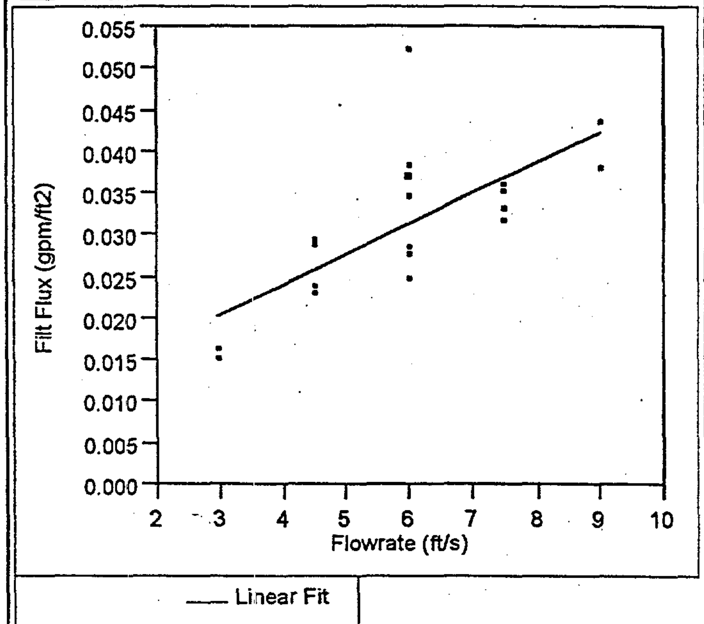

Linear Fit

Filt Flux (gpm/ft2) = 0.00957 + 0.00364 Flowrate (ft/s)

Summary of Fit

RSquare	0.47378
RSquare Adj	0.447469
Root Mean Square Error	0.006301
Mean of Response	0.031405
Observations (or Sum Wgts)	22

Analysis of Variance

Source	DF	Sum of Squares	Mean Square	F Ratio
Model	1	0.00071495	0.000715	18.0069
Error	20	0.00079409	0.000040	Prob>F
C Total	21	0.00150904		0.0004

Parameter Estimates

Term	Estimate	Std Error	t Ratio	Prob>|t|
Intercept	0.0095725	0.005317	1.80	0.0869
Flowrate (ft/s)	0.0036387	0.000857	4.24	0.0004

Figure 3.15. 1.5 wt% Tank C-107: Filtrate Flux as a Function of Axial Velocity

Filt. Flux (gpm/ft2) By Pressure (psig)

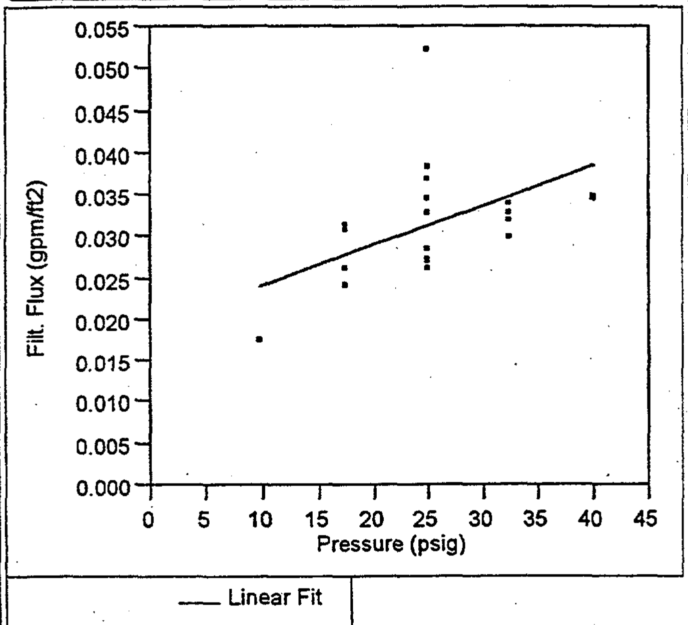

Linear Fit

Filt. Flux (gpm/ft2) = 0.01954 + 0.00047 Pressure (psig)

Summary of Fit

RSquare	0.276729
RSquare Adj	0.240566
Root Mean Square Error	0.006301
Mean of Response	0.031405
Observations (or Sum Wgts)	22

Analysis of Variance

Source	DF	Sum of Squares	Mean Square	F Ratio
Model	1	0.00030382	0.000304	7.6522
Error	20	0.00079409	0.000040	Prob>F
C Total	21	0.00109791		0.0119

Parameter Estimates

Term	Estimate	Std Error	t Ratio	Prob>|t|
Intercept	0.0195445	0.004493	4.35	0.0003
Pressure (psig)	0.0004744	0.000171	2.77	0.0119

Figure 3.16. 1.5 wt% Tank C-107: Filtrate Flux as a Function of Transmembrane Pressure

Filt Flux (gpm/ft2) By Flowrate (ft/s)

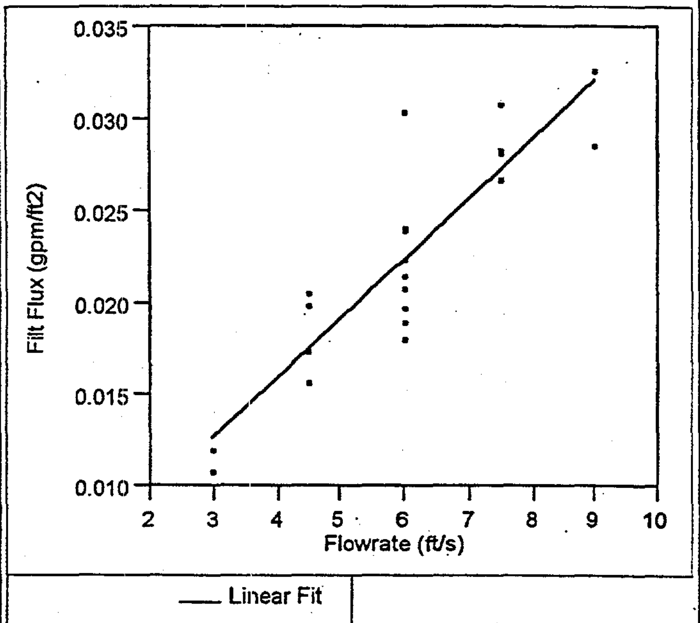

Linear Fit

Filt Flux (gpm/ft2) = 0.00286 + 0.00326 Flowrate (ft/s)

Summary of Fit

RSquare	0.780502
RSquare Adj	0.769527
Root Mean Square Error	0.002842
Mean of Response	0.022427
Observations (or Sum Wgts)	22

Analysis of Variance

Source	DF	Sum of Squares	Mean Square	F Ratio
Model	1	0.00057424	0.000574	71.1169
Error	20	0.00016149	0.000008	Prob>F
C Total	21	0.00073574		<.0001

Parameter Estimates

Term	Estimate	Std Error	t Ratio	Prob>|t|
Intercept	0.0028613	0.002398	1.19	0.2467
Flowrate (ft/s)	0.003261	0.000387	8.43	<.0001

Figure 3.17. 8 wt% Tank C-107: Filtrate Flux as a Function of Axial Velocity

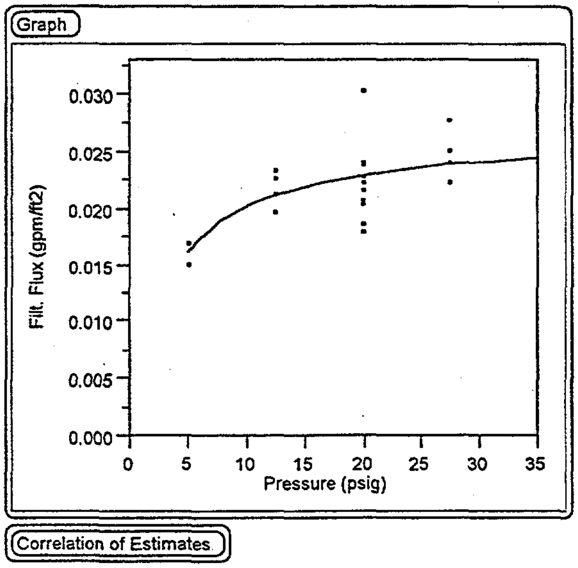

Figure 3.18. 8 wt% Tank C-107: Filtrate Flux as a Function of Transmembrane Pressure

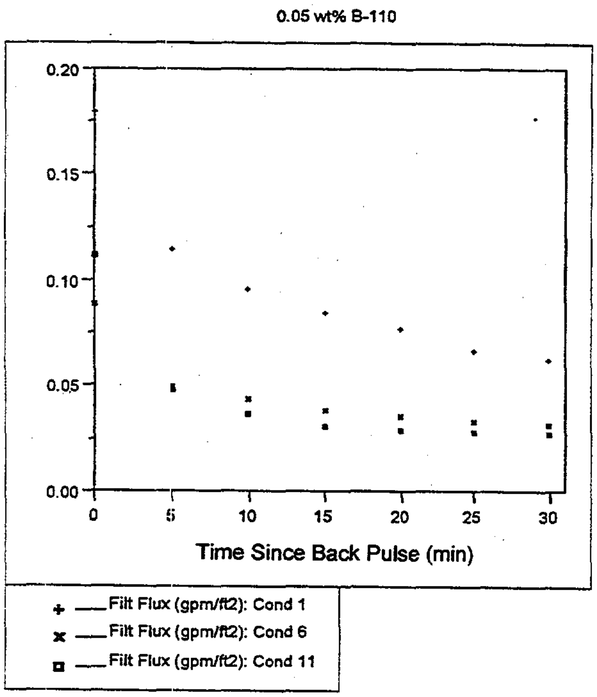

Figure 3.19. 0.05 wt% Tank B-110: Filtrate Flux as a Function of Time (6 ft/s, 25 psig)

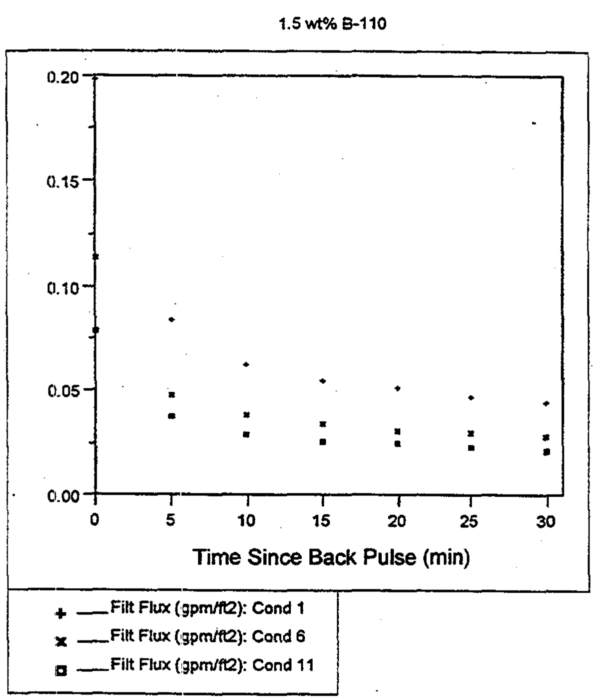

Figure 3.20. 1.5 wt% Tank B-110: Filtrate Flux as a Function of Time (6 ft/s, 25 psig)

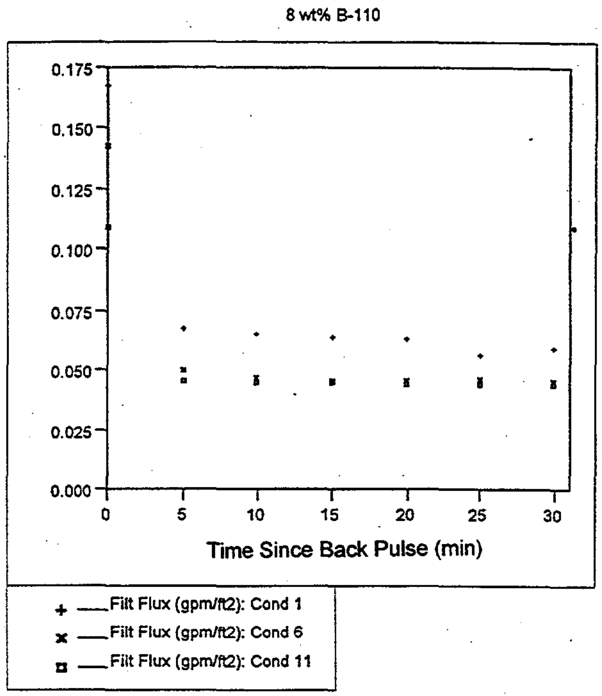

Figure 3.21. 8 wt% Tank B-110: Filtrate Flux as a Function of Time (6 ft/s, 20 psig)

3.3.1 0.05 wt% B-110

A plot of filtrate flux (gpm/ft^2) from the 0.05 wt% feed as a function of velocity is displayed in Figure 3.22. The filtrate flux shows some dependency on axial velocity, indicating that a filter cake formed at this low solids loading. A stronger filtrate-flux dependency with TMP is observed as shown in Figure 3.23, indicating that these data were taken below the critical pressure at which the filtrate flux is pressure-independent. Because the flux is dependent on both TMP and axial velocity, under these conditions the filtrate flux is in the transition region controlled by Darcy's equation and back mass transport.

3.3.2 1.5 wt% B-110

A plot of filtrate flux (gpm/ft^2) as a function of velocity is displayed in Figure 3.24. The filtrate flux shows approximately the same dependency with axial velocity that was seen for the 0.05 wt% feed (shown in Figure 3.22). The filtrate flux also appears to be in a transition state and the data could be fit to a line or a curve (appearing to plateau at 40 psig); however, Figure 3.25 has the data plotted linearly. It is thought that these data were taken in a transition region where both back-transport and Darcy's equation both exhibit some control over the filtrate-flux rate.

Filt Flux (gpm/ft2) By Flowrate (ft/s)

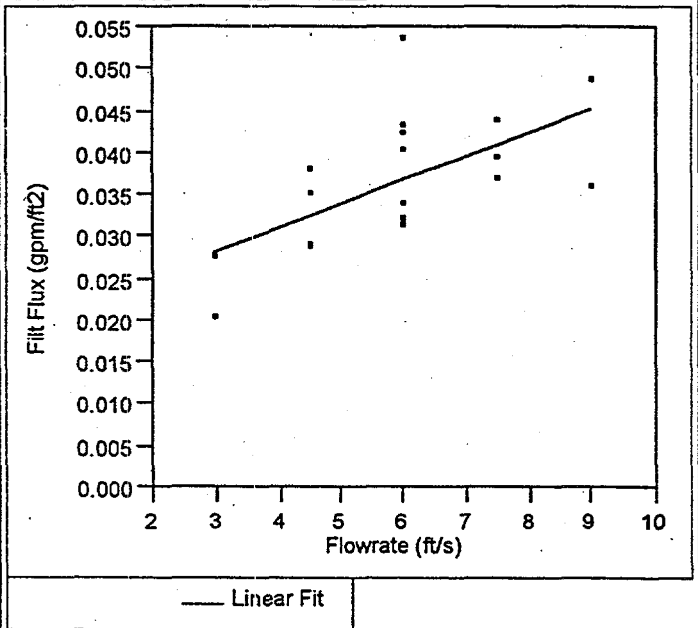

Linear Fit

Filt Flux (gpm/ft2) = 0.01966 + 0.00285 Flowrate (ft/s)

Summary of Fit

RSquare	0.370189
RSquare Adj	0.338699
Root Mean Square Error	0.006119
Mean of Response	0.036786
Observations (or Sum Wgts)	22

Analysis of Variance

Source	DF	Sum of Squares	Mean Square	F Ratio
Model	1	0.00044012	0.000440	11.7556
Error	20	0.00074879	0.000037	Prob>F
C Total	21	0.00118891		0.0027

Parameter Estimates

Term	Estimate	Std Error	t Ratio	Prob>|t|
Intercept	0.019657	0.005163	3.81	0.0011
Flowrate (ft/s)	0.0028549	0.000833	3.43	0.0027

Figure 3.22. 0.05 wt% Tank B-110: Filtrate Flux as a Function of Axial Velocity

Filt. Flux (gpm/ft2) By Pressure (psig)

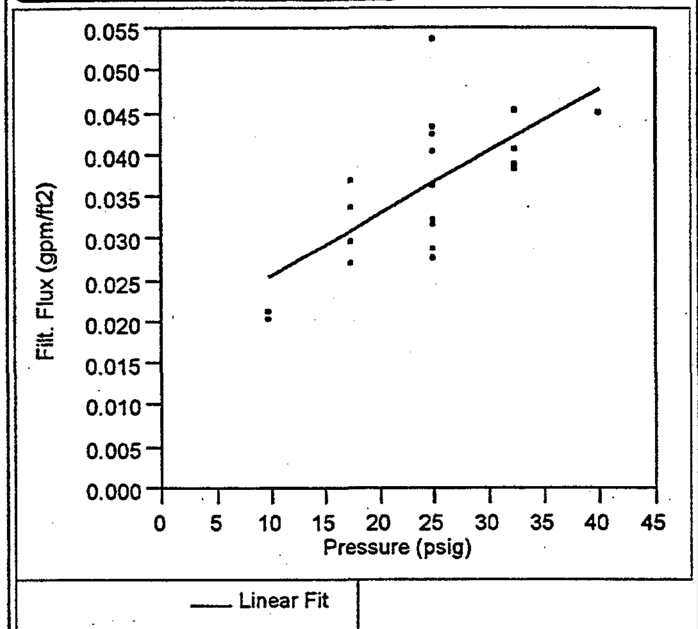

Linear Fit

Filt. Flux (gpm/ft2) = 0.01826 + 0.00074 Pressure (psig)

Summary of Fit

RSquare	0.497459
RSquare Adj	0.472332
Root Mean Square Error	0.006119
Mean of Response	0.036786
Observations (or Sum Wgts)	22

Analysis of Variance

Source	DF	Sum of Squares	Mean Square	F Ratio
Model	1	0.00074121	0.000741	19.7978
Error	20	0.00074879	0.000037	Prob>F
C Total	21	0.00149000		0.0002

Parameter Estimates

Term	Estimate	Std Error	t Ratio	Prob>|t|
Intercept	0.0182619	0.004363	4.19	0.0005
Pressure (psig)	0.000741	0.000167	4.45	0.0002

Figure 3.23. 0.05 wt% Tank B-110: Filtrate Flux as a Function of Transmembrane Pressure

Filt Flux (gpm/ft2) By Flowrate (ft/s)

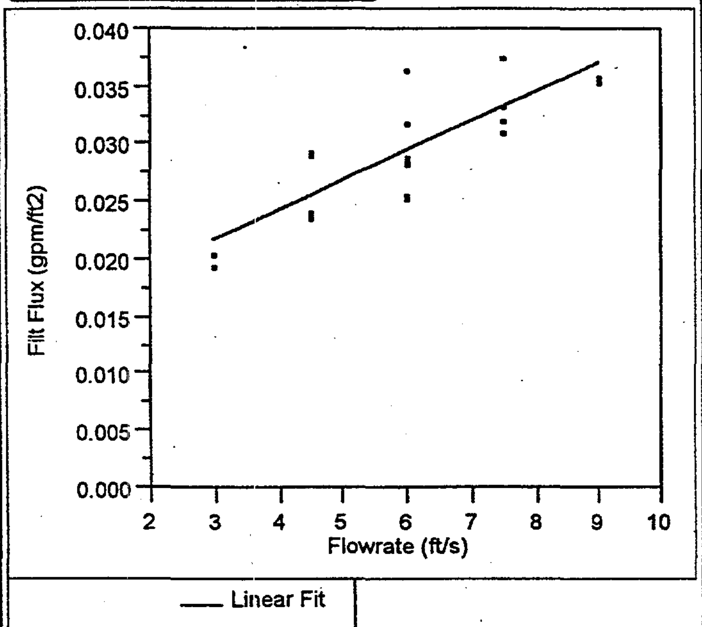

Linear Fit

Filt Flux (gpm/ft2) = 0.01426 + 0.00254 Flowrate (ft/s)

Summary of Fit

RSquare	0.643318
RSquare Adj	0.625484
Root Mean Square Error	0.003103
Mean of Response	0.029482
Observations (or Sum Wgts)	22

Analysis of Variance

Source	DF	Sum of Squares	Mean Square	F Ratio
Model	1	0.00034741	0.000347	36.0724
Error	20	0.00019262	0.000010	Prob>F
C Total	21	0.00054003		<.0001

Parameter Estimates

Term	Estimate	Std Error	t Ratio	Prob>|t|
Intercept	0.0142632	0.002619	5.45	<.0001
Flowrate (ft/s)	0.0025364	0.000422	6.01	<.0001

Figure 3.24. 1.5 wt% Tank B-110: Filtrate Flux as a Function of Axial Velocity

Filt. Flux (gpm/ft2) By Pressure (psig)

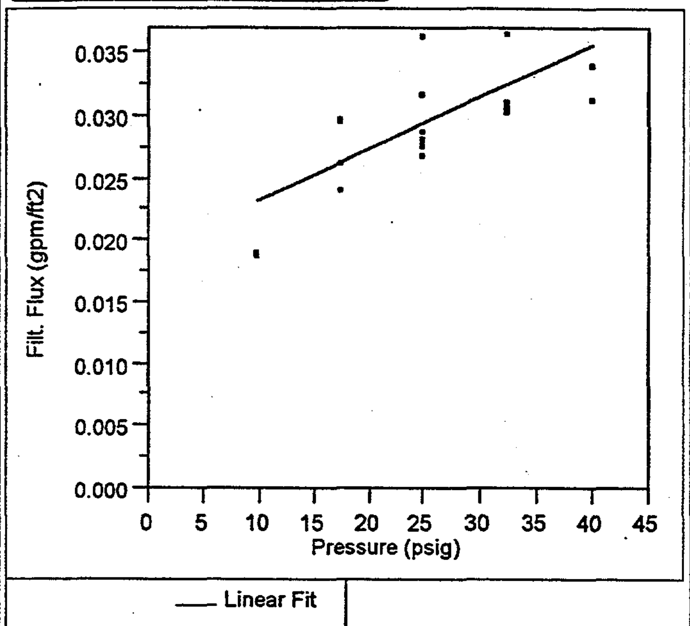

Linear Fit

Filt. Flux (gpm/ft2) = 0.01911 + 0.00042 Pressure (psig)

Summary of Fit

RSquare	0.546989
RSquare Adj	0.524339
Root Mean Square Error	0.003103
Mean of Response	0.029482
Observations (or Sum Wgts)	22

Analysis of Variance

Source	DF	Sum of Squares	Mean Square	F Ratio
Model	1	0.00023258	0.000233	24.1491
Error	20	0.00019262	0.000010	Prob>F
C Total	21	0.00042520		<.0001

Parameter Estimates

Term	Estimate	Std Error	t Ratio	Prob>|t|
Intercept	0.0191052	0.002213	8.63	<.0001
Pressure (psig)	0.0004151	0.000084	4.91	<.0001

Figure 3.25. 1.5 wt% Tank B-110: Filtrate Flux as a Function of Transmembrane Pressure

Filt Flux (gpm/ft2) By Flowrate (ft/s)

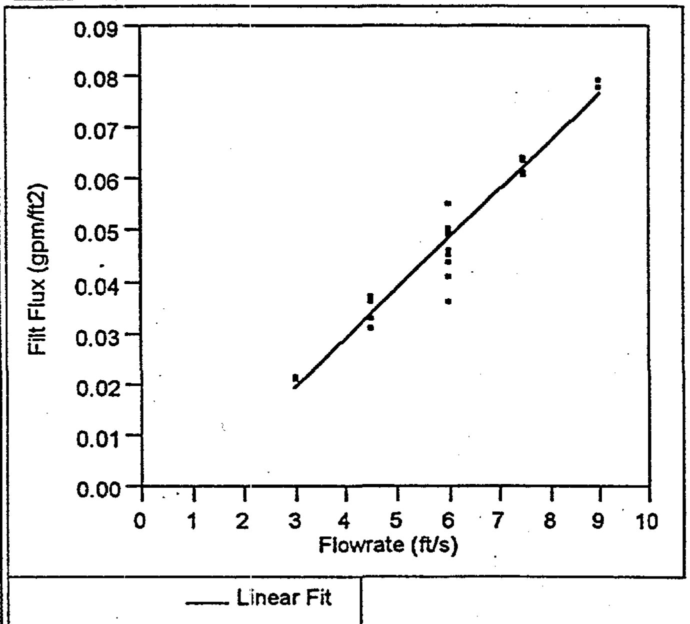

Linear Fit

Filt Flux (gpm/ft2) = -0.0091 + 0.00958 Flowrate (ft/s)

Summary of Fit

RSquare	0.934626
RSquare Adj	0.931357
Root Mean Square Error	0.004163
Mean of Response	0.048359
Observations (or Sum Wgts)	22

Analysis of Variance

Source	DF	Sum of Squares	Mean Square	F Ratio
Model	1	0.00495650	0.004957	285.9328
Error	20	0.00034669	0.000017	Prob>F
C Total	21	0.00530319		<.0001

Parameter Estimates

Term	Estimate	Std Error	t Ratio	Prob>|t|
Intercept	-0.009124	0.003513	-2.60	0.0172
Flowrate (ft/s)	0.0095806	0.000567	16.91	<.0001

Figure 3.26. 8 wt% Tank B-110: Filtrate Flux as a Function of Axial Velocity

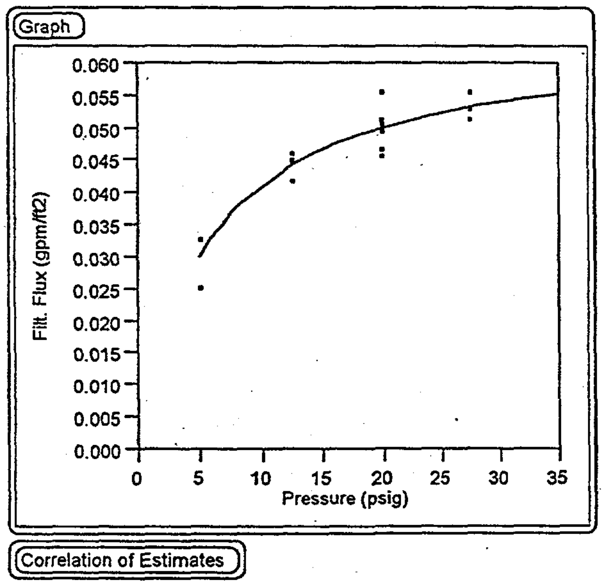

Figure 3.27. 8 wt% Tank B-110: Filtrate Flux as a Function of Transmembrane Pressure

3.3.3 8 wt% B-110

As the feed is increased to 8 wt%, the strongest filtrate-flux dependence on axial velocity was observed, as seen in Figure 3.26. Figure 3.27 indicates that the filtrate flux still appears to be in a transition state and the data could be fit to a line or a curve; however, Figure 3.27 has the data fit to a curve. It is thought that both back-transport and Darcy's equation exhibit some control over the filtrate- flux rate, and Figure 3.27 shows that the filtrate-flux pressure dependency wanes at 20 psig and may be pressure-independent above 30 psig, at which point back-mass transport controls the filtrate flux. Data taken at a higher pressure would be necessary to confirm if the flux is independent above 30 psig.

3.4 U-110

The filtrate flux (gpm/ft^2) as a function of time (minutes) since back-pulse for the 0.05 wt%, 1.5 wt%, and 8 wt% feeds, respectively, is displayed in Figures 3.28, 3.29, and 3.30. The conditions in each figure were measured at the same TMP and axial velocity.[3] As was seen for the B-110 feed, in each instance there is a significant decline between the flux measured at condition 1 with that measured at condition 6, with little decline between the flux measure at condition 6 with that measured at condition 11. Also back pulsing was effective at improving the flux rates. The clean-water flux was restored between runs by rinsing the system, indicating that subsurface filter fouling was not evident. The filtrate flux of the 0.05 wt% feed generally was lower than that of the 1.5 or 8 wt% feeds for all conditions. This result is similar to that obtained for the B-110 feed. It was established that filter fouling was not evident; therefore, if one excludes the unlikely possibility that the filter cake was thicker while running the 0.05 wt% feed, then one must conclude that the filter cake was less permeable for the 0.05 wt% feed during the latter conditions. This observation suggests that the U-110 feed, like the B-110 feed, is more susceptible to deagglomeration in a shear field at low salt content. Such a phenomenon explains the low flux rate measured at the 0.05 wt% loading as well as the low cake permeability. This conclusion is supported by the analysis conducted in Section 4.

3.4.1 0.05 wt% U-110

A plot of filtrate flux (gpm/ft^2) from the 0.05 wt% feed as a function of velocity is displayed in Figure 3.31. The filtrate flux shows a greater dependency on axial velocity than is normally seen for such a dilute slurry. Conversely, there is also a weaker filtrate-flux dependency with TMP, as shown in Figure 3.32. The pressure dependency is less than that observed for the 1.5 wt% slurry (refer to section 3.3.2, Figure 3.34), indicating that the feeds 0.05 wt% feed and the 1.5 wt% feed were fundamentally different. The 0.05 wt% feed behaves as though the feed were more concentrated or the particles were smaller than those in the 1.5 wt% feed. Because the former was measured and known to be correct, the particles of the 0.05 wt% feed must be smaller. Based on these results, we hypothesized that the U-110 feed is more susceptible to deagglomeration at the low salt content of the 0.05 wt% feed. If this hypothesis is true, then it accounts for the results.

---

[3] All of the data shown for the 0.05 and 1.5 wt% feed were measured at 6 ft/s axial velocity and 25 psig TMP. All of the data for the 8 wt% feed were all measured at 6 ft/s axial velocity and 20 psig TMP.

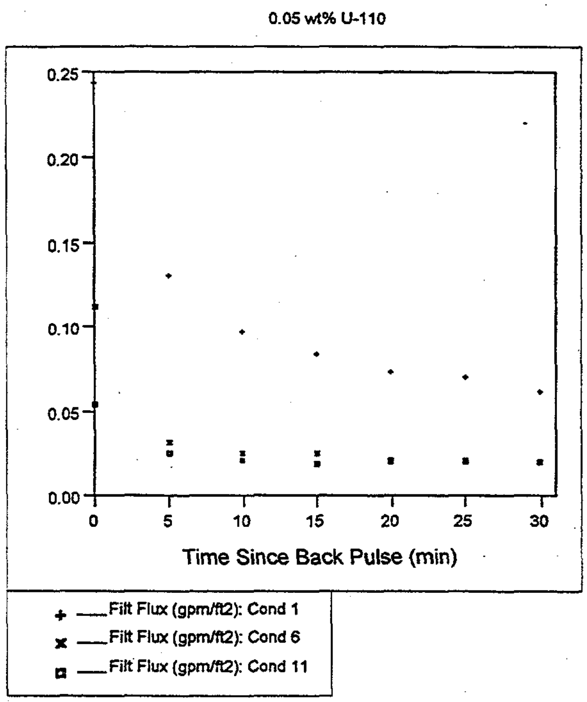

Figure 3.28. 0.05 wt% Tank U-110: Filtrate Flux as a Function of Time (6 ft/s, 25 psig)

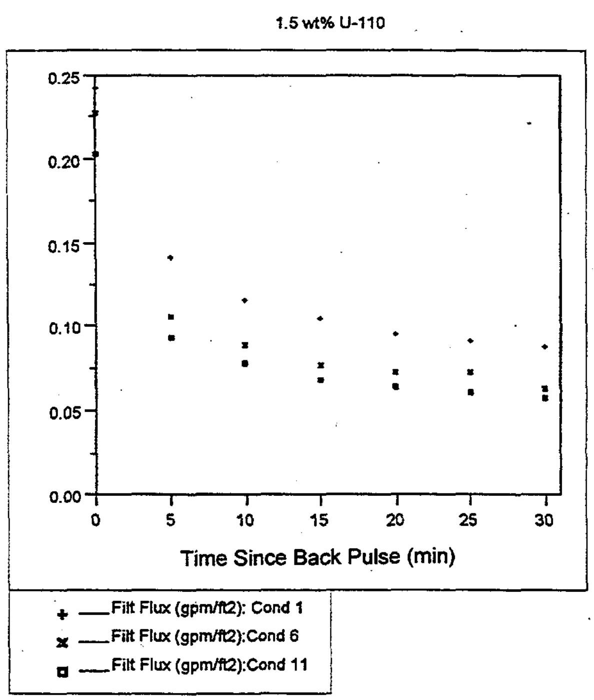

Figure 3.29. 1.5 wt% Tank U-110: Filtrate Flux as a Function of Time (6 ft/s, 25 psig)

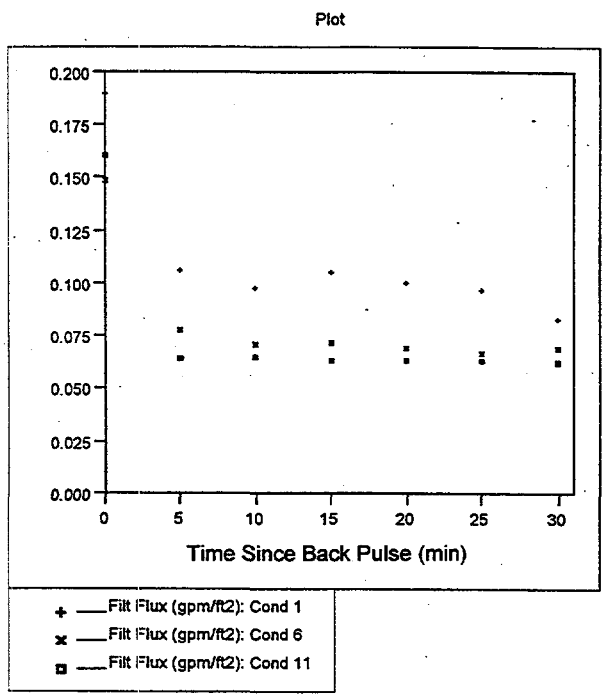

Figure 3.30. 8 wt% Tank U-110: Filtrate Flux as a Function of Time (6 ft/s, 20 psig)

3.4.2 1.5 wt% U-110

A plot of filtrate flux (gpm/ft^2) as a function of velocity is displayed in Figure 3.33. The filtrate flux shows a greater dependency with axial velocity than was seen for the 0.05 wt% feed. As previously mentioned, the filtrate-flux dependency with TMP, shown in Figure 3.34, also was greater than that seen for the 0.05 wt% feed. These data indicate that the measurements were taken in a transition region where both back-transport and Darcy's equation both exhibit some control over the filtrate-flux rate.

3.4.3 7.5 wt% U-110

A 7.5 wt% slurry was tested in lieu of the standard 8 wt%, because there weren't enough solids available for testing to reach the targeted solids concentration.

For the feed containing 7.5 wt% solids, Figure 3.35 displays the strongest filtrate-flux dependence on axial velocity, indicating that increased axial velocity reduces the filter cake built up on the membrane, resulting in improved flux rates. At the same time, as seen in Figure 3.36, the pressure dependency is still evident; this indicates that these data, too, were taken in the transition region where both back-transport and Darcy's equation exhibit some control over the filtrate-flux rate.

Filt Flux (gpm/ft2) By Flowrate (ft/s)

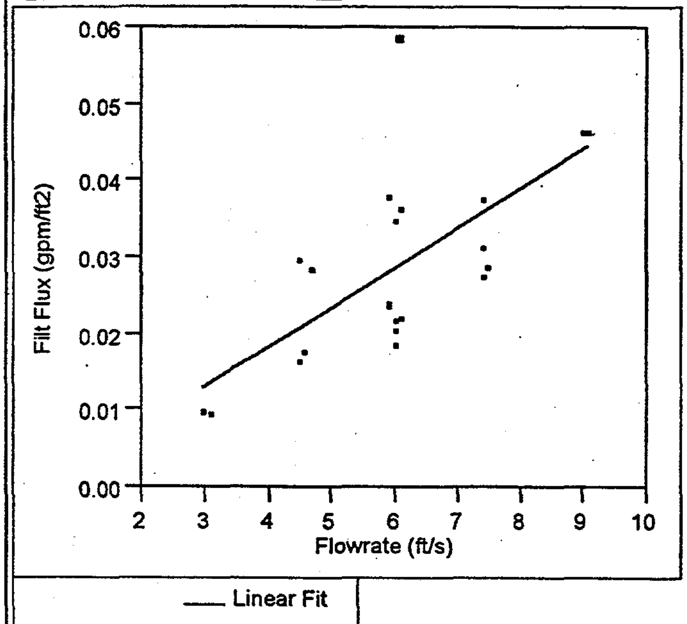

Linear Fit

Filt Flux (gpm/ft2) = -0.0024 + 0.00517 Flowrate (ft/s)

Summary of Fit

RSquare	0.453136
RSquare Adj	0.425793
Root Mean Square Error	0.009189
Mean of Response	0.02868
Observations (or Sum Wgts)	22

Analysis of Variance

Source	DF	Sum of Squares	Mean Square	F Ratio
Model	1	0.00139921	0.001399	16.5722
Error	20	0.00168863	0.000084	Prob>F
C Total	21	0.00308785		0.0006

Parameter Estimates

Term	Estimate	Std Error	t Ratio	Prob>|t|
Intercept	-0.002384	0.007878	-0.30	0.7653
Flowrate (ft/s)	0.0051695	0.00127	4.07	0.0006

Figure 3.31. 0.05 wt% Tank U-110: Filtrate Flux as a Function of Axial Velocity

Filt. Flux (gpm/ft2) By Pressure (psig)

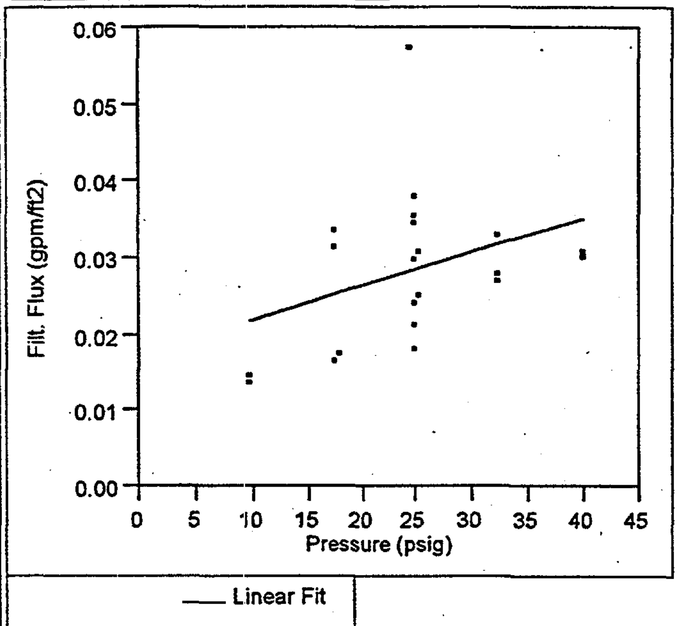

Linear Fit

Filt. Flux (gpm/ft2) = 0.01771 + 0.00044 Pressure (psig)

Summary of Fit

RSquare	0.131892
RSquare Adj	0.088487
Root Mean Square Error	0.009189
Mean of Response	0.028653
Observations (or Sum Wgts)	22

Analysis of Variance

Source	DF	Sum of Squares	Mean Square	F Ratio
Model	1	0.00025655	0.000257	3.0386
Error	20	0.00168863	0.000084	Prob>F
C Total	21	0.00194519		0.0967

Parameter Estimates

Term	Estimate	Std Error	t Ratio	Prob>|t|
Intercept	0.0177082	0.006577	2.69	0.0140
Pressure (psig)	0.000437	0.000251	1.74	0.0967

Figure 3.32. 0.05 wt% Tank U-110: Filtrate Flux as a Function of Transmembrane Pressure

Filt Flux (gpm/ft2) By Flowrate (ft/s)

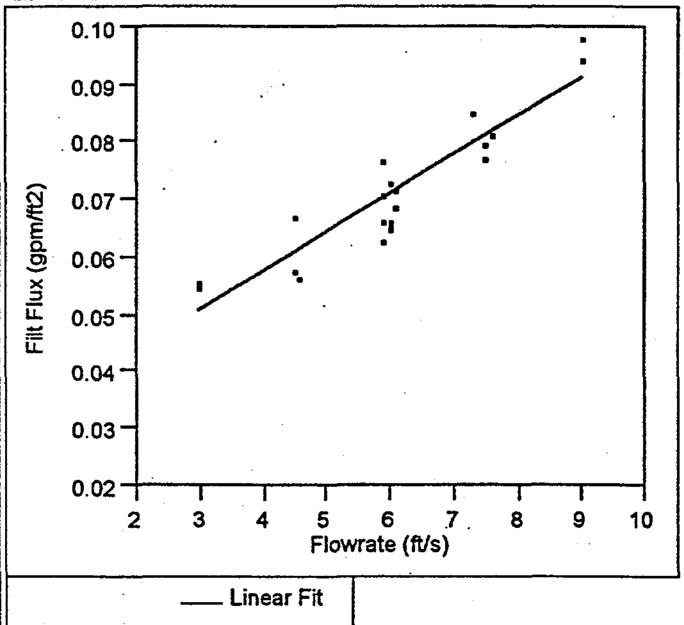

Linear Fit

Filt Flux (gpm/ft2) = 0.03092 + 0.00672 Flowrate (ft/s)

Summary of Fit

RSquare	0.833019
RSquare Adj	0.82467
Root Mean Square Error	0.004919
Mean of Response	0.071159
Observations (or Sum Wgts)	22

Analysis of Variance

Source	DF	Sum of Squares	Mean Square	F Ratio
Model	1	0.00241421	0.002414	99.7739
Error	20	0.00048394	0.000024	Prob>F
C Total	21	0.00289815		<.0001

Parameter Estimates

Term	Estimate	Std Error	t Ratio	Prob>|t|
Intercept	0.0309217	0.004163	7.43	<.0001
Flowrate (ft/s)	0.0067164	0.000672	9.99	<.0001

Figure 3.33. 1.5 wt% Tank U-110: Filtrate Flux as a Function of Axial Velocity

Filt. Flux (gpm/ft2) By Pressure (psig)

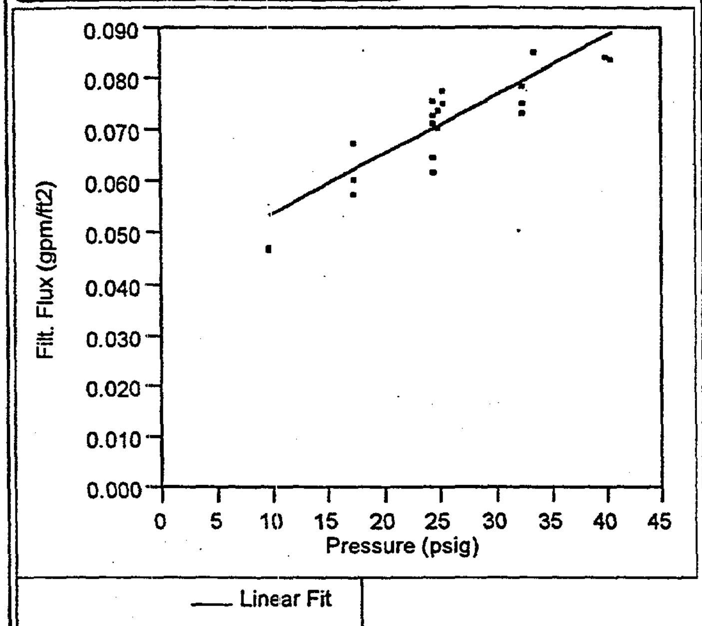

Linear Fit

Filt. Flux (gpm/ft2) = 0.04239 + 0.00115 Pressure (psig)

Summary of Fit

RSquare	0.791748
RSquare Adj	0.781336
Root Mean Square Error	0.004919
Mean of Response	0.07122
Observations (or Sum Wgts)	22

Analysis of Variance

Source	DF	Sum of Squares	Mean Square	F Ratio
Model	1	0.00183987	0.001840	76.0375
Error	20	0.00048394	0.000024	Prob>F
C Total	21	0.00232380		<.0001

Parameter Estimates

Term	Estimate	Std Error	t Ratio	Prob>|t|
Intercept	0.042385	0.003469	12.22	<.0001
Pressure (psig)	0.0011534	0.000132	8.72	<.0001

Figure 3.34. 1.5 wt% Tank U-110: Filtrate Flux as a Function of Transmembrane Pressure

Filt Flux (gpm/ft2) By Flowrate (ft/s)

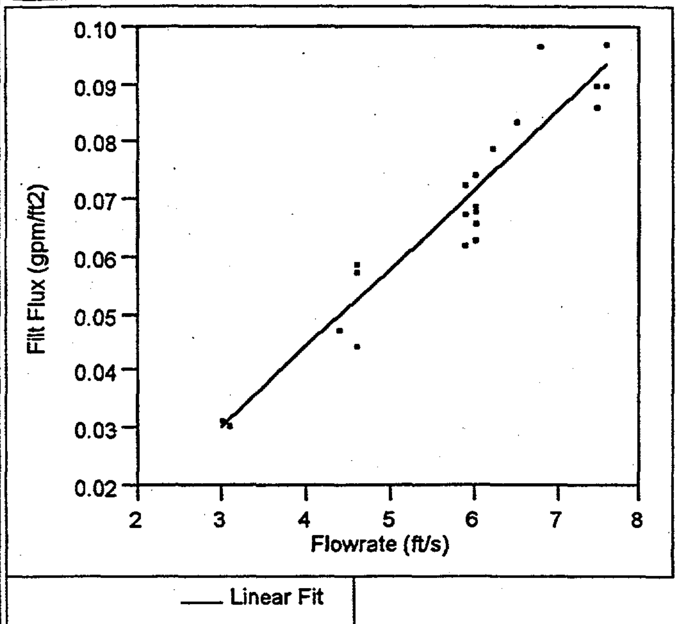

Linear Fit

Filt Flux (gpm/ft2) = -0.0109 + 0.01376 Flowrate (ft/s)

Summary of Fit

RSquare	0.908811
RSquare Adj	0.904252
Root Mean Square Error	0.005813
Mean of Response	0.068956
Observations (or Sum Wgts)	22

Analysis of Variance

Source	DF	Sum of Squares	Mean Square	F Ratio
Model	1	0.00673461	0.006735	199.3248
Error	20	0.00067574	0.000034	Prob>F
C Total	21	0.00741035		<.0001

Parameter Estimates

Term	Estimate	Std Error	t Ratio	Prob>|t|
Intercept	-0.010892	0.00579	-1.88	0.0746
Flowrate (ft/s)	0.0137561	0.000974	14.12	<.0001

Figure 3.35. 7.5 wt% Tank U-110: Filtrate Flux as a Function of Axial Velocity

Filt. Flux (gpm/ft2) By Pressure (psig)

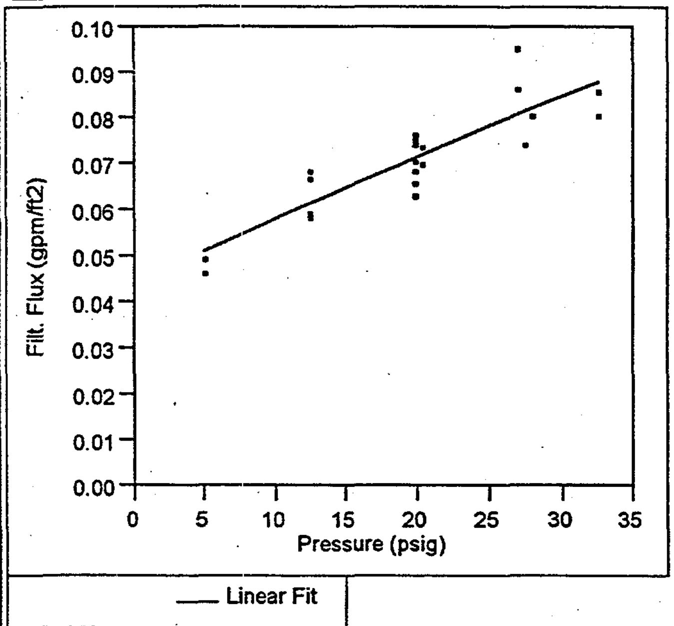

Linear Fit

Filt. Flux (gpm/ft2) = 0.04482 + 0.00134 Pressure (psig)

Summary of Fit

RSquare	0.762344
RSquare Adj	0.750462
Root Mean Square Error	0.005813
Mean of Response	0.071371
Observations (or Sum Wgts)	22

Analysis of Variance

Source	DF	Sum of Squares	Mean Square	F Ratio
Model	1	0.00216763	0.002168	64.1554
Error	20	0.00067574	0.000034	Prob>F
C Total	21	0.00284337		<.0001

Parameter Estimates

Term	Estimate	Std Error	t Ratio	Prob>|t|
Intercept	0.0448242	0.003538	12.67	<.0001
Pressure (psig)	0.001341	0.000167	8.01	<.0001

Figure 3.36. 7.5 wt% Tank U-110: Filtrate Flux as a Function of Transmembrane Pressure

3.5 Analytical Results

Radionuclide analyses focused on insoluble radionuclide species. Results of the total alpha analysis, which was used for measuring TRU elements, and ^{90}Sr analyses are presented. Additional analyses, including ^{99}Tc and gamma energy analysis to measure the gamma-emitting isotopes are provided in Appendix B. PNNL Analytical Chemistry Laboratory procedures were used for all analysis performed.

Radionuclide analyses of the C-106 waste feeds were measured and compared with measurements of the five filtrate samples (which were taken at different processing conditions) to confirm whether TMP and axial velocity had an effect on the filtrate quality. Analysis of all subsequent waste types (C-107, B-110 and U-110) also included radionuclide measurements of the feed, but filtrate analysis was limited to one sample taken from the center of the experimental test matrix. In addition, the gamma energy analysis was omitted. Fewer analytical tests were motivated by significant cost savings and the conclusion that these additional analyses were of marginal benefit.

The major metallic elements were determined in the filtrate by inductively coupled plasma/atomic emission spectroscopy (ICP-AES). Particle-size-distribution analyses were performed on the initial and final feed samples.

3.5.1 Radiochemical Results

Summary results of the total alpha/TRU and ^{90}Sr in the feed and filtrate are provided in Tables 3.2 and 3.3. In general the activity in the filtrate show significant decontamination through the filtration of solids. For comparison, Class A standards for TRU and ^{90}Sr are 10 nCi/g and 0.04 µCi/ml, respectively. Decontamination factors (DF) are also provided in the tables in order to compare the activity in the original feed to that in the corresponding filtrate. In a few instances (0.05 wt% B-110, 0.05 wt% U-110, and 1.5 wt% C-107), the activities in the feeds were greater than expected based on dilution calculations. Knowledge of how the samples were prepared and subsequent observation of the quantity of solids in these feed samples clearly indicated that the high activities were not caused by having an order of magnitude more of the solids than expected. The high readings most likely are the result of difficulties in obtaining a representative subsample for analysis.

The total alpha activity in the 1.5 and 8 wt% C-106 filtrate are between two and three orders of magnitude higher than the concentration found in any other tank waste filtrate. The ^{90}Sr activities for these two filtrates are also high but not by orders of magnitude. For example, the ^{90}Sr activity in 8 wt% B-110 is 0.013 µCi/ml, which is the same order of magnitude as 0.079 µCi/ml, which was measured in the 8 wt% C-106.

Estimates of the activity resulting from a glass matrix used to immobilize the filtrates are provided in Table 3.4. The estimates were based on a typical glass density of 2.6 g/cm^3 and 20 wt% Na_2O as the limiting oxide in the glass. All of the ^{90}Sr activity in this hypothetical glass is an order of magnitude below the low activity waste (LAW) glass limit of 20 µCi/ml. The TRU activity is also lower than the glass limit of 100 nCi/g, with the exception of the 1.5 and 8 wt% C-106. Re-analysis of total alpha in the 1.5 and 8 wt% C-106 filtrate provided similar results, leading to the conclusion that the measured results were actual and not caused by instrument error.

Table 3.2. Total Alpha Analysis

Feed Sample	Feed (nCi/g)	Filtrate (nCi/ml)	Decontamination Factor [a]
C-106, 0.05 wt%	1.9 [b]	0.06	32
C-106, 1.5 wt%	58 [b]	10	6
C-106, 8 wt%	310	68	5
C-107, 0.05 wt%	5.3	0.13	41
C-107, 1.5 wt%	210	0.0087	24,000
C-107, 8 wt%	1700	0.023	74,000
B-110, 0.05 wt%	9 [c]	0.0041	2200
B-110, 1.5 wt%	11	<0.003	>3700
B-110, 8 wt%	63	<0.03	>2100
U-110, 0.05 wt%	6 [c]	0.017	350
U-110, 1.5 wt%	9	<0.003	>3000
U-110, 7.5 wt%	<20	0.0094	<2100

[a] Decontamination factors were calculated by converting filtrate values from volumetric basis (nCi/ml) to mass basis (nCi/g) by applying specific gravity of 1.0.

[b] Sample lost during transfer or analytical preparation. Value reported was calculated based on dilution.

[c] Measured value is an order of magnitude higher than expected, based on dilution.

Table 3.3. ^{90}Sr Analysis

Feed Sample	Feed (μCi/g)	Filtrate (μCi/ml)	Decontamination Factor [a]
C-106, 0.05 wt%	0.2 [b]	0.0004	500
C-106, 1.5 wt%	6.1 [b]	0.019	320
C-106, 8 wt%	32	0.079	400
C-107, 0.05 wt%	2.2	0.0028	790
C-107, 1.5 wt%	79 [c]	0.0011	72,000
C-107, 8 wt%	70	0.00049	140,000
B-110, 0.05 wt%	5.1 [c]	0.00078	6500
B-110, 1.5 wt%	4.9	0.011	450
B-110, 8 wt%	15	0.013	1200
U-110, 0.05 wt%	2.8 [c]	0.00074	3800
U-110, 1.5 wt%	5.1	0.000093	55,000
U-110, 7.5 wt%	28	0.0034	8200

[a] Decontamination factors were calculated by converting filtrate values from volumetric basis (μCi/ml) to mass basis (μCi/g) by applying specific gravity of 1.0.
[b] Sample lost during transfer or analytical preparation. Value reported was calculated based on dilution.
[c] Measured value is an order of magnitude higher than expected, based on dilution.

Table 3.4. Estimated Activity in LAW Glass Resulting from Immobilizing Filtrate

Feed Sample	EstimatedTRU Activity in LAW Glass Resulting from Immobilizing Filtrate (nCi/g glass)	Is TRU activity less than LAW glass limit of 100 nCi/g?	Estimated 90Sr Activity in LAW Glass Resulting from Immobilizing Filtrate (uCi/ml glass)	Is 90Sr activity less than LAW glass limit of 20 uCi/ml?
C-106, 0.05 wt%	13	Yes	0.23	Yes
C-106, 1.5 wt%	181	No	0.89	Yes
C-106, 8 wt%	391	No	1.18	Yes
C-107, 0.05wt%	37	Yes	2.09	Yes
C-107, 1.5 wt%	2.0	Yes	0.65	Yes
C-107, 8 wt%	2.0	Yes	0.11	Yes
B-110, 0.05 wt%	0.9	Yes	0.47	Yes
B-110, 1.5 wt%	0.10	Yes	0.98	Yes
B-110, 8 wt%	0.19	Yes	0.22	Yes
U-110, 0.05 wt%	4	Yes	0.43	Yes
U-110, 1.5 wt%	0.27	Yes	0.02	Yes
U-110, 7.5 wt%	0.24	Yes	0.23	Yes

Activity estimate was based on a typical glass density of 2.6 g/cm3 and 20 wt% Na2O as the limiting oxide in the LLW glass.

For the C-106 feeds, there were five measurements of alpha and ^{90}Sr from the five filtrate samples taken during testing. The individual sample analysis and the conditions under which the sample was taken for alpha and ^{90}Sr are shown in Table 3.5. The measurements of the 0.05 wt% filtrate are low relative to the Class A limits for TRU and ^{90}Sr, and consistent, with one exception. The five measurements of the filtrate from the 8 wt% feed were also consistent. There was a sharp increase in concentration in the latter two samples from the 1.5 wt% feed.

Table 3.5. Total Alpha and ^{90}Sr Analysis for C-106

Feed Sample Identification	Total Alpha Measured in Filtrate (nCi/ml)	^{90}Sr Measured in Filtrate (μCi/ml)	Process Condition [a]
C-106, 0.05 wt%	0.0073	0.0006	1
	0.0086	<0.0006	3
	0.24	0.00018	4
	0.0084	0.0002	8
	0.044	0.00032	9
C-106, 1.5 wt%	2.1	<0.02	1
	1.6	0.01	3
	1.4	0.014	4
	13	<0.02	8
	32	0.033	9
C-106, 8 wt%	60	0.067	1
	70	0.089	3
	72	<0.07	4
	62	0.073	8
	77	0.096	9

(a) Processing condition sample was taken. For corresponding TMP and axial velocity, refer to Table 3.1.

Table 3.6. Distribution of Measured Activity after 0.2 μm Millipore Filtration

	Alpha Activity Measured (% of total)	^{90}Sr Activity Measured (% of total)
Filter 1	4.7	2.8
Filter 2	3.1	2.7
Final Filtrate	92.2	94.5

The following plan of action was carried out to provide more information. The filtrate samples from the 8 wt% C-106 were composited. The composited volume (20 ml) was passed sequentially through two 0.2-micron millipore filters, with the expectation that particulates larger than 0.2 microns would be captured on the filter. The final filtrate and the two filters were each analyzed for total alpha and ^{90}Sr. A small percentage of the total measured activity was captured by the filter, indicating colloidal or soluble activity as the cause for the high alpha and ^{90}Sr measurements in the filtrate from the 8 wt% C-106 feed, as shown in Table 3.6. Comparison of the sum of the activities of the filters and final filtrates with the activity in the initial sample indicates that the activity balance did not close well. For both the total alpha and ^{90}Sr, only approximately 30% of the activity of the initial feed was measured in the filters or final filtrate.

Particle size distribution analysis of the 8 wt% C-106 filtrate using the photon correlation spectrometer indicate that there were colloidal particles between 0.004 and 0.01 microns. Clearly the filters tested would be generally ineffective at removing such particulate.

Retesting of the 8 wt% C-106 using the same feed resulted in total alpha activities in the filtrate which were an order of magnitude lower than the original test, but similar or higher ^{90}Sr activities in the filtrate, as shown in Tables 3.7 and 3.8. Two filters were used in the retest, the 0.1μm Graver filter and the 0.5μm Mott filter. Recall that the original test with C-106 was performed using the Mott filter. The ^{90}Sr activities in the filtrate are effectively the same in the original test and the retest using the same Mott filter (0.079 and 0.049 μCi/ml, respectively). That the ^{90}Sr activities were higher in the retest using the Graver filter (0.11 μCi/ml) may indicate that the Graver filter retains less particulate.

Table 3.7 Total Alpha Analysis from the 8 wt% C-106 Retest

Feed Sample	Feed (nCi/g)	Filtrate (nCi/ml)	Decontamination Factor[a]
8 wt% C-106 (0.1μm Graver Filter)	540	8.2	66
8 wt% C-106 (0.5μm Mott Filter)	420	1.5	280

Table 3.8 ^{90}Sr Analysis from the 8 wt% C-106 Retest

Feed Sample	Feed (μCi/g)	Filtrate (μCi/ml)	Decontamination Factor[a]
8 wt% C-106 (0.1μm Graver Filter)	58	0.11	530
8 wt% C-106 (0.5μm Mott Filter)	52	0.049	1100

Three possibilities for the high total alpha activity in the filtrate are presented in increasing likelyhood.

1) Contamination--Because of their high activity, the C-106 samples were prepared for analysis in a hot cell rather than a hood. Sample contamination may have occurred during repackaging or preparation. In addition, filtrate samples with high alpha activity, i.e. all the 8 wt% C-106 filtrates and the latter two filtrate samples from the 1.5 wt% C-106 (processing condition 8 and 9 in Table 3.5) were packaged together during transfer to the analytical chemistry laboratory. During transfer one of the C-106 feed samples leaked causing external contamination. Because of the consistency in the alpha activities in the 8wt% C-106 filtrate samples, there is considerable doubt as to whether this was the explanation. Adding more doubt, only submicron particulate were measured in the filtrate. If contamination from a spilled feed sample were the cause, large particulate would be expected. Therefore, while this explanation hasn't been ruled out, it is also believed to be unlikely.

2) Colloidal solids-- The high readings may have been caused by the small colloidal particles which went through the filter. While colloidal solids were measured in the filtrate this explanation is believed to be unlikely for the total alpha activity because if colloidal particles were the cause we would expect to see similarly high activities in the C-106 retest. However, we did see similar ^{90}Sr activities in the retest, suggesting the cause of this activity in the filtrate may have resulted from the sub-micron solids measured in the filtrate.

3) Soluble TRU-- Although this explanation contradicts results by Lumetta et al. (1996) which measured <32 nCi/ml total alpha in the decanted wash solution, there are some interesting data which support this possibility. Plotted in Figure 3.37 is the equilibrium solubility of PuO2*xH2O with carbonate at pH 10 and pH 12-13. Also plotted are the plutonium concentration in the C-106 filtrate assuming all the total alpha activity is derived from ^{239}Pu. Carbonate concentrations were not measured in the C-106 filtrate, but were calculated based on measurement in the initial feed. The slope of plutonium concentration as a function of carbonate concentration in the first C-106 test at 0.05, 1.5 and 8 wt% corresponds well with the slope in the solubility curve.

The C-106 retests, also plotted, have lower alpha activity, but are still in the region of Pu/carbonate equilibrium solubility. Carbonate concentrations in the filtrates from the C-106 retest were measured. Note that in the retest, the plutonium concentration (as measured by alpha activity) decreased with decreasing carbonate concentration.

Because there was significant foaming during the original C-106 testing, it is suspected that entrained air caused elevated carbonate concentrations (greater than that plotted which is based on the concentration in the original feed) and reduced pH. High carbonate and low pH increase the solubility of plutonium. No foaming was observed during the retest and the resulting plutonium concentration may have been lower as a result. These data clearly suggest that carbonate and pH will need to be controlled during tank waste processing.

While an absolute answer may never be obtained because the original C-106 samples have been consumed with the analysis, the hypothesis of soluble plutonium causing the elevated alpha activity and submicron particulate causing the elevated 90Sr activity seems to match the data the best.

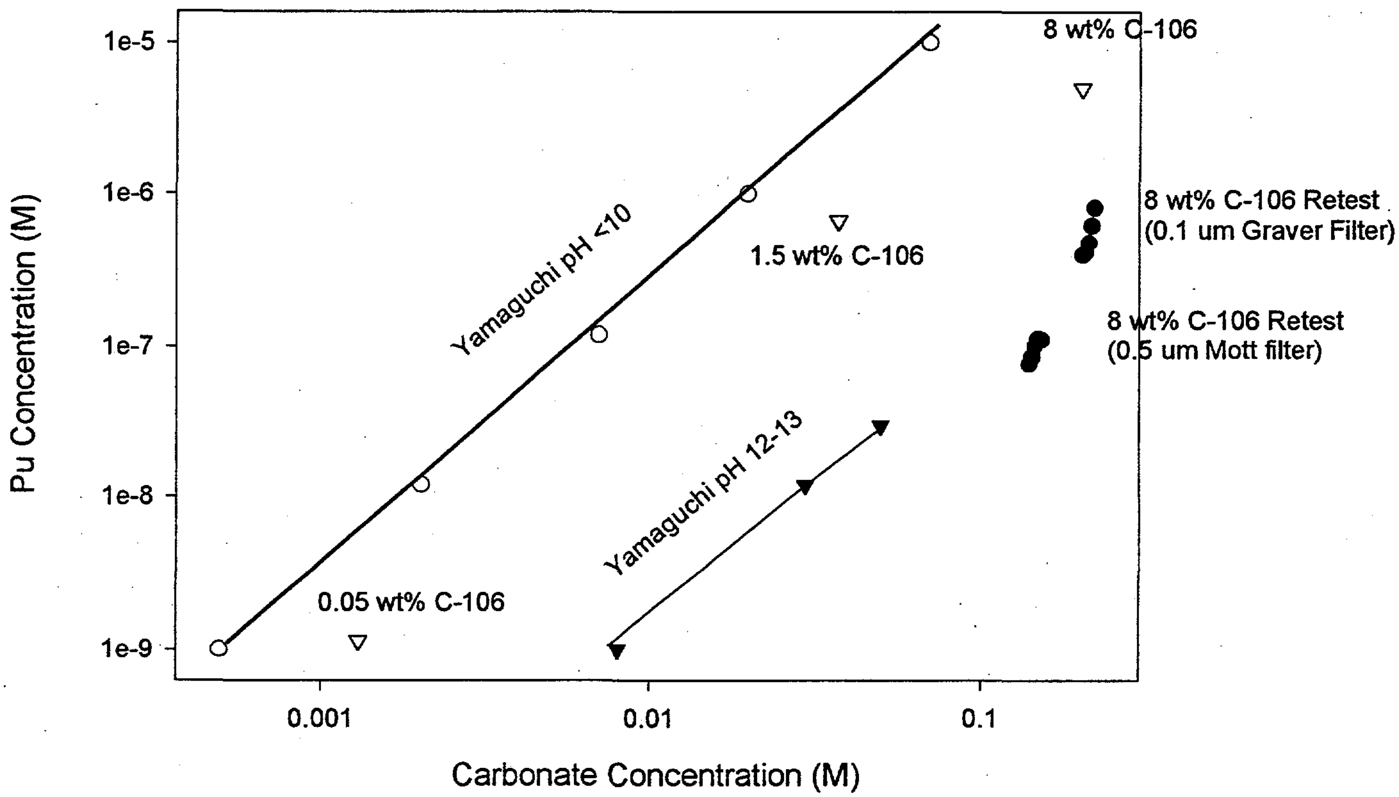

Figure 3.37. Plutonium Concentration in C-106 Filtrate Compared with Equilibrium Solubility of PuO2*xH2O

3.5.2 Non-Radioactive Component Measurements

The concentrations of nonradioactive components measured in the filtrate samples indicated are provided in Table 3.9.

3.5.3 Particle-Size Distribution Measurements

Portions of the slurry feeds were analyzed before introduction into the CUF crossflow filter. Because the tests with differing wt% solids used the same feed stock, one sample was used from each tank waste as the "prior to testing" sample. After testing was completed a sample of each feed was taken for analysis. These samples constitute the "after testing" samples. Particle-size measurements were made using a Brinkmann 2010 particle-size analyzer. A summary of the median particle diameter (number distribution) of the feeds is provided in Table 3.10.

The trends in Table 3.10 are discussed in Section 4.2.2.1 and support the analysis conducted in Section 4.2.

Table 3.9. Nonradioactive Components Measured in Filtrate Samples

	C-106 Filtrate Samples			C-107 Filtrate Samples			B-110 Filtrate Samples			U-110 Filtrate Samples		
	0.05 wt%	1.5 wt%	8 wt%	0.05 wt%	1.5 wt%	8 wt%	0.05 wt%	1.5 wt%	8 wt%	0.05 wt%	1.5 wt%	7.5 wt%
Component	Conc., µg/ml	Conc., µg/ml	Conc., µg/ml	Conc., µg/ml	Conc., µg/ml	Conc., µg/ml	Conc., µg/ml	Conc., µg/ml	Conc., µg/ml	Conc., µg/ml	Conc., µg/g	Conc., µg/ml
Ag	[0.04]	[0.10]						[0.24]	1.96			
Al	5.96	8.3	15.5	5.7	17.6	76.5	6.21	[0.14]		1.14	12.3	71.8
B	7.69	4.41	10.5	6.01	6.67	7.34	5.89	7.05	8.43	6.81	7.52	8.42
Bi										[0.87]		[0.13]
Ca									[9.7]			[0.37]
Cr	0.84	1.25	[1]	1.61	0.46	2.24	0.82	2.63	17.5	0.58	7.85	32.8
Cu		[0.17]	[0.6]									
Fe	[0.09]	[0.29]	[0.6]	1.07	[0.05]	[0.08]	[0.07]	[0.03]	[0.34]	1.24	[0.04]	[0.09]
K		[17]	[62]					[11]	[66]		[2.3]	[5.0]
Li	[0.04]				[0.23]	0.66	[0.03]	[0.03]				
Mo	[0.23]	1.24	[4]	[0.20]	[0.06]	[0.13]	[0.10]	[0.23]	[1.4]			
Na	674	8130	25600	512	650	1680	640	4300	23000	652	1640	5690
Ni	[0.04]	1.18	[3]	[0.08]					[0.24]			
P	3.95	59.2	114	1.24	4.62	22.3	22.5	366	1830	66.8	214	793
Si	19.9	[3.4]		18.5	35.4	57.3	35.2	41.3	64.5	45.2	25.2	21
Tl				[0.03]								
U		60	[230]			[2.5]						[4.3]
Zn						[0.06]				[0.11]		[0.08]
Zr		11.7	48.1	[0.12]								

Note: Values in brackets [] are within 10-times detection limit with errors likely to exceed 15%. Overall error for other values estimated to be within +/- 15%.

Table 3.10. Median Particle Size (Number Distribution) of Feeds Tested

Feed	Median Particle Size Prior to Testing (µm)	Median Particle Size After Testing (µm)
C-106, 0.05 wt%	0.71	na
C-106, 1.5 wt%	0.71	na
C-106, 8 wt%	0.71	0.71
C-107, 0.05 wt%	0.74	0.87
C-107, 1.5 wt%	0.74	0.73
C-107, 8 wt%	0.74	0.74
B-110, 0.05 wt%	0.87	0.72
B-110, 1.5 wt%	0.87	0.73
B-110, 8 wt%	0.87	0.87
U-110, 0.05 wt%	0.93	0.76
U-110, 1.5 wt%	0.93	0.74
U-110, 7.5 wt%	0.93	0.82

na: not available.

4.0 Discussion

When available, the following discussion includes data measured during the testing of simulants and Hanford tank S-107 to include these feeds in the comparison. The source data and analysis for these feeds is provided in Geeting and Reynolds (1996).

4.1 Comparison of the Graver and Mott Filters

Two filter elements were used in the testing: a 0.5-micron Mott filter for the C-106 feed (and previously for the S-107 feed and S-3 and S-103 simulants reported in Geeting and Reynolds [1996]), and a 0.1-micron Graver filter for the C-107, B-110, and the U-110 feeds. The 0.1-micron Graver filter is believed to be superior to the 0.5-micron Mott filter to filter Hanford tank wastes because, unlike the latter, the Graver filter did not exhibit significant subsurface fouling which degrades the filtrate flux and requires acid cleaning to remove. It should be noted, however, that this conclusion and following discussion are based on a comparison of filtering different wastes, and fouling was found to be waste- dependent. To state that one filter is definitively better than another, a comparison should be made using the same feed.

The Graver filter is an anisotropic filter with a TiO_2 coating on a 2-micron sintered stainless-steel substrate. This fabrication method brings the effective pore rating down to 0.1 micron at the filtration surface; all of the filtering should occur on the filter surface rather than in the 2-micron substrate. Particles smaller than 0.1 microns which make it past the TiO_2 coating should likely make it through the filter. In contrast, the Mott filter is isotropic, composed of a 0.5-micron pore diameter sintered stainless- steel throughout. Particles which make it past the surface of this filter are more likely to get caught in the tortuous fluid path within the filter, making the Mott filter effectively an "in-depth" filter. It is this "in-depth" filtration process which makes the Mott more susceptible to subsurface fouling than the Graver filter. Although not tested, Mott makes a 0.2-micron pore diameter filter which would likely exhibit less subsurface fouling for the wastes tested than the 0.5-micron Mott filter.

The filtrate flux of each waste tested using the 0.5-micron Mott filter is shown in Figure 4.1. For the simulants tested, there was virtually no decline in filtrate flux between condition 1 and 11, indicating that the simulants did not deagglomerate and the filter was correctly sized for the simulants tested. The S-107 and C-106 wastes tested, however, exhibited significant flux declines caused by filter fouling and feed deagglomeration as the run progressed, as discussed in Section 4.2.

The filtrate flux of each waste tested using the 0.1-micron Graver filter is shown in Figure 4.2. These tank wastes, too, exhibited a filtrate-flux decline as the run progressed. Analysis in Section 4.2 indicates that the flux decline observed was largely caused by feed deagglomeration.

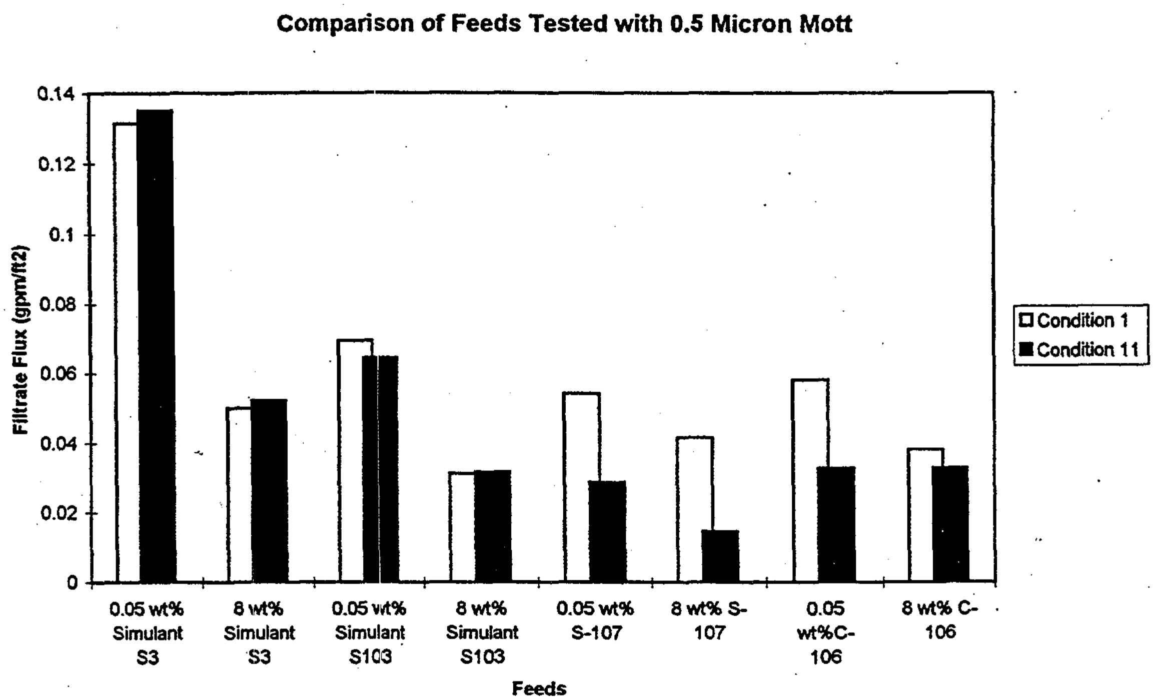

Figure 4.1. Comparison of Feeds Tested with the 0.5-Micron Mott Filter

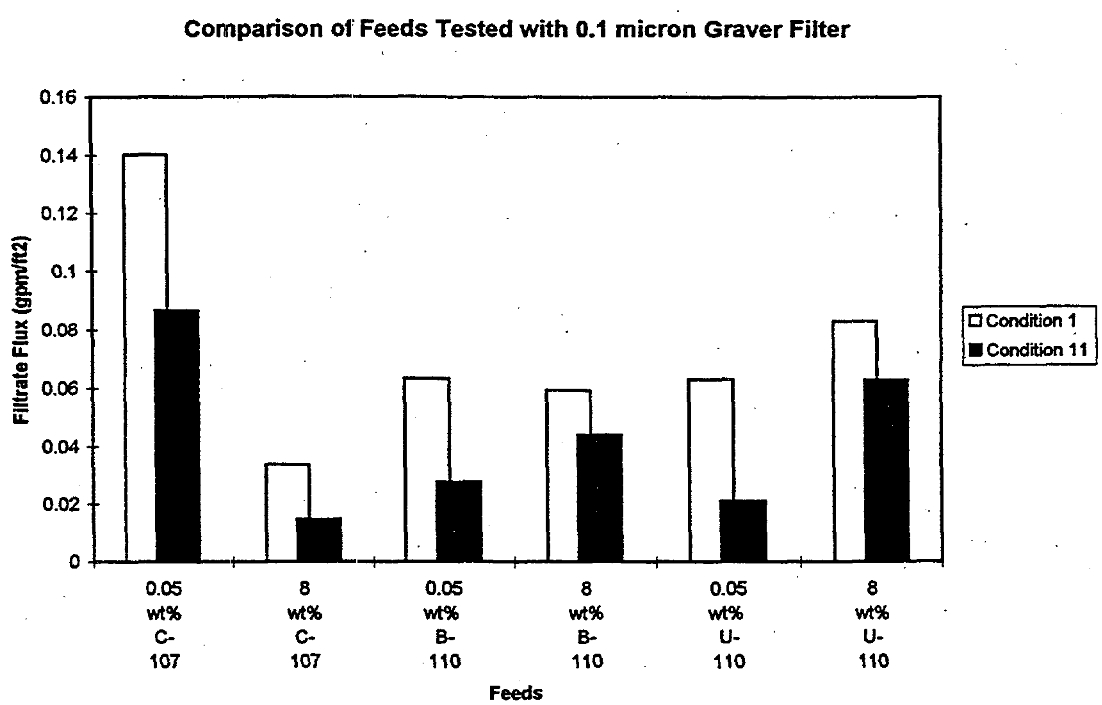

Figure 4.2. Comparison of Feeds Tested with the 0.1-Micron Graver Filter

Table 4.1. Total Hydraulic Resistance Measured After each Run Indicated ($10^{11} * m^{-1}$)

Solids Content	C-106 (Mott)	C-107 (Graver)	B-110 (Graver)	U-110 (Graver)
0.05 wt%	21	12	11	11
1.5 wt%	27	11	20	10
8 wt%	NM	12	10	9

NM-Not Measured

The total hydraulic resistance to clean water at the conclusion of each run indicated is shown in Table 4.1. [1] The measurement includes media resistance plus any fouling resistance resulting from the run. During testing the total hydraulic resistance of the Graver filter was approximately $10*10^{11} * m^{-1}$ and was relatively constant for each feed tested, indicating that after the initial filter "break in" the filter did not foul. The one exception to this was the 1.5 wt% B-110, which did foul and required acid cleaning to restore the flux. Despite the fact that the Mott filter was acid-cleaned between running the C-106 feeds, the hydraulic resistance was about twice that of the Graver filter. Yet before testing, the hydraulic resistance of a new 0.5-micron Mott filter was $0.3*10^{11} * m^{-1}$ while the resistance of a new Graver filter was $7.3 *10^{11} * m^{-1}$. Thus we see that the ratio of resistances increases from 1/24 before testing to about 2 after testing, which confirms the point made by Murkes and Carlsson (1988) that filter media with larger pores facilitate the penetration of small particles in the pores and, therefore, promote internal fouling.

4.2 Comparison of the Feeds

Tarleton and Wakeman (1993) state that fouling by particulates appears to be due to two apparently independent mechanisms which occur simultaneously. The first mechanism is subsurface fouling which is irreversible for all practical purposes (without chemical cleaning), and is caused by the rapid deposition and capture of the finer particles from the suspension and their subsequent penetration into the pores of the membrane. Subsurface fouling is a stochastic process, dependent on localized hydrodynamic conditions close to the pore entrances.

The second mechanism is largely reversible and causes further particulate layer(s) to form above the membrane surface in the form of a cake; this has also been referred to as the "dynamic membrane." The effects of the second mechanism on the filtrate flux are subdivided herein as follows: that which can be removed by back-pulsing the filter is defined as filter cake, that which cannot is defined surface fouling. (By definition, rinsing the system with water removes surface fouling from the membrane; if not, then it would be considered subsurface fouling.)

[1] The resistances measured here are not directly comparable with the fouling resistance from Table 4.2. The fouling resistances listed in Table 4.2 (column 3) are the total fouling which includes both surface and subsurface fouling. Table 4.1 resistances include the media resistance plus any subsurface fouling.

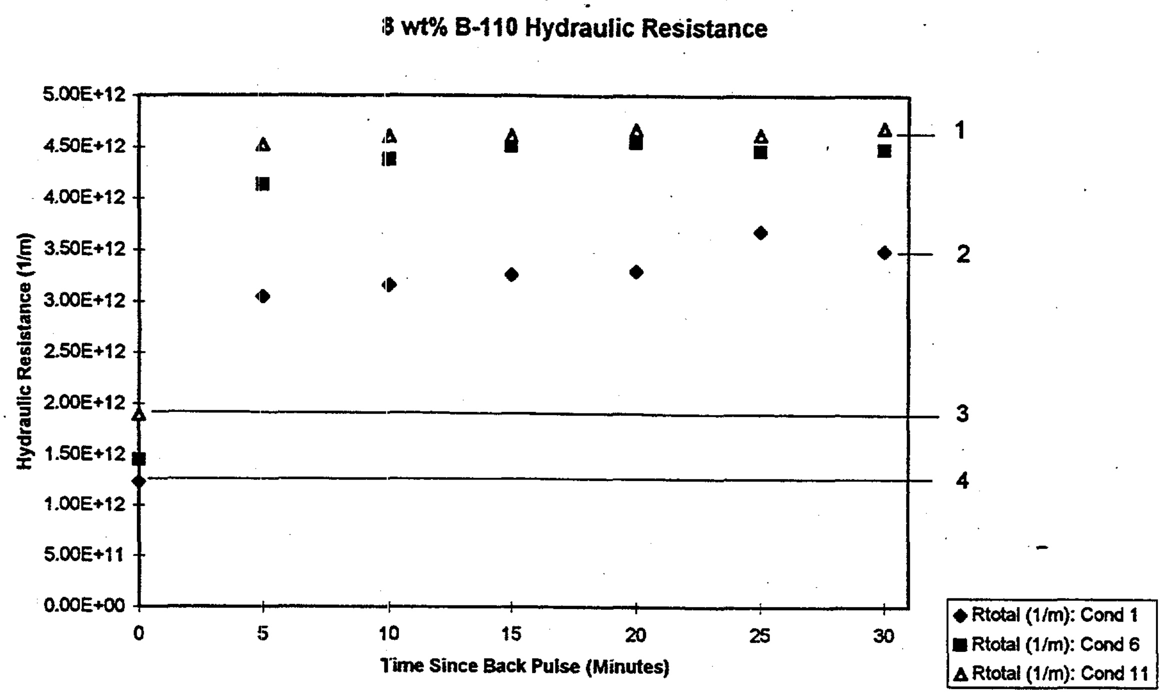

Figure 4.3. Hydraulic Resistance for 8 wt% B-110 Feed

Another cause of reducing the filtrate flux over time, not considered by Tartleton and Wakeman, is the result of the particle-size distribution change during the testing. If particles in the feed get smaller because of mechanical effects (deagglomeration) or chemical effects (peptization), then the resulting filter cake and fouling characteristics will change.

From an engineering standpoint, it is important to determine the causes of the flux decline so that efforts to improve the flux rate are focused correctly. If the bulk of the decline were caused by filter fouling, for example, then one may consider alternate filters to minimize such fouling. On the other hand, if deagglomeration were prevalent, then perhaps low shear pumps should be evaluated before scale-up. It is useful, therefore, to consider what fraction of the flux decline is caused by build up of the filter cake, changes in filter cake as a result of deagglomeration or peptization, and filter fouling. If the hydraulic resistances are calculated by application of Darcy's equation,[2] then an order-of-magnitude analysis of the causes of the filtrate-flux decline can be performed. The following definitions, visualized graphically in Figure 4.3, are used in the analysis:

- Filter Cake Resistance = $R_{t=30,\ Condition\ 1} - R_{t=0,\ Condition\ 1}$ (=2 - 4, as shown in Figure 4.3). The change in flux immediately after back-pulsing and 30 minutes after back-pulsing during condition 1 thus is attributed to the added resistance as a result of the build-up of filter cake. Some of the increase in resistance may also be attributable to fouling.

---

[2] Darcy's equation was applied to data of filtrate flux as a function of time (at constant axial velocity and transmembrane pressure) as shown in Figures 3.1, 3.4, 3.7, 3.10, 3.11, 3.12, 3.19, 3.20, 3.21, 3.28, 3.29, and 3.30 in this document.

deagglomeration is attributed to the change in filter-cake resistance measured between condition 11 and condition 1. If the back-pulse is ineffective at removing the filter cake or the effectiveness changes between conditions, then the credibility of this measurement declines. It is known that the effectiveness of back-pulsing is reduced with severe filter fouling. As a result, this measurement is considered least reliable when considering the feeds tested with the Mott filter where significant irreversible fouling was prevalent.

- Resistance Caused by Filter Fouling = $R_{t=0,\ Condition\ 11} - R_{t=0,\ Condition\ 1}$ (=3 - 4, as shown in Figure 4.3). The change in filtrate flux immediately after the back-pulse is attributed to filter fouling. In this instance, it should be recognized that the filter fouling does not necessarily mean the filter will require acid cleaning. In fact, for the Graver filter most of the fouling so defined is removable by rinsing the system.

Summing these three resistances, we end up with $R_{t=30,\ Condition\ 11} - R_{t=0,\ Condition\ 1}$ (=1 - 4, as shown in Figure 4.3), which is the total increase in hydraulic resistance during the experiment. The results are provided in Table 4.2.

4.2.1 Filter-Cake Resistance

Focusing attention on the filter-cake-resistance column, we see that this resistance generally increased with solids concentration in the feed. This was expected, as the filter-cake thickness, and hence resistance, should increase with increasing solids. Two exceptions to this trend were the B-110 and U-110 feeds, both of which had filter cakes of least resistance at the highest solids-concentration feed, despite the fact that the higher solids loadings produce thicker filter cakes. These feeds were also the only ones which had substantially less feed-deagglomeration resistance measured for the 8 wt% feed than for the 0.05 wt% feed. A possible explanation for this observation is that the lower salt content of the 0.05 wt% feeds resulted in peptization or rendered the feeds more susceptible to deagglomeration. Recall that the feeds were generated by diluting tank samples with inhibited water (0.01 M NaOH and 0.01 M $NaNO_2$); hence, feeds with lower solids content also had less-soluble salts than the higher solids feeds.

4.2.2 Deagglomeration Resistance

There was no effective change in the filter-cake resistance between the beginning and end of the test matrix for the simulants tested, indicating that deagglomeration of the simulants tested was not a problem. This was consistent with the observation that the filtrate flux did not decline as the testing progressed. Many of the actual tank wastes tested, in contrast, did exhibit significant change in the filter-cake resistance as the test progressed.

Examining the deagglomeration-resistance column, the S-107 feed exhibited significant deagglomeration for the 8 wt% feed and virtually none for the 1.5 and 0.05 wt% feeds. This makes sense because for this feed (only), the 8 wt% feed was run first and the remaining feeds were diluted for the original 8 wt% feed. Deagglomeration of S-107 during testing was reported in Geeting and Reynolds (1996). The C-106 feed did not exhibit any significant deagglomeration for any solids concentration tested, while the C-107, B-110, and the U-110 feeds did. For the C-107, the more concentrated feeds exhibited more resistance attributed to

Table 4.2. Comparison of Hydraulic Resistance Measured for Feeds Tested

Feed	Filter-Cake Resistance (10^{11} *m^{-1})	Deagglomeration Resistance (10^{11} *m^{-1})	Fouling Resistance (10^{11} *m^{-1})
Simulant S3, 0.05 wt%	2	1	-2
Simulant S3, 8 wt%	10	0	-1
Simulant S103, 0.05 wt%	4	0	2
Simulant S103, 8 wt%	13	4	-4
S-107, 0.05 wt%	15	2	43
S-107, 1.5 wt%	20	-7	64
S-107, 8 wt%	20	40	52
C-106, 0.05 wt%	24	-7	40
C-106, 1.5 wt%	27	4*	12*
C-106, 8 wt%	32	-2	11
C-107, 0.05 wt%	11	4	7
C-107, 1.5 wt%	32	37	15
C-107, 8 wt%	47	53	25
B-110, 0.05 wt%	26	43	8
B-110, 1.5 wt%	44	40	19
B-110, 8 wt%	23	5	7
U-110, 0.05 wt%	30	45	35
U-110, 1.5 wt%	18	13	2
U-110, 7.5 wt%	14	6	2

*These measurements used condition 6 instead of condition 11 as called for by the definitions.

deagglomeration, while as previously noted the B-110 and U-110 had the opposite trend. The C-107 feed thus was not susceptible to deagglomeration at low ionic strength (low solids loading), while the B-110 and U-110 feeds were susceptible.

The effectiveness of back-pulsing is reduced with severe filter fouling. As a result, the measurement of deagglomeration of the feed is least reliable when considering the feeds tested with the Mott filter where significant irreversible fouling was prevalent. This may explain the negative values measured for the feeds tested with the Mott filter. The physical significance of such a negative value is that the hydraulic resistance resulting from the filter cake building up between the back-pulse and steady state during condition 1 is greater than that measured for condition 11. Hence, if the effectiveness of back- pulsing significantly decreases, as may happen with fouling, then the measured filter-cake resistance during condition 11 would be reduced and a negative feed deagglomeration resistance is possible.

It is important to note that because of the small feed volumes used by the CUF and the rigorous testing required, the feed is subjected to significant shear. During the course of a run the feed makes approximately 12,500 cycles through the CUF pilot plant, which is significantly more than that envisioned for actual waste filtering. As a result, the effects of shear-induced deagglomeration on permeate flux rate may be magnified in the bench-scale testing reported herein compared with what might be expected in an actual plant.

4.2.2.1 Estimate of Change in Mean Particle Diameter Based on Change in Filter-Cake Resistance.

The change in particle diameter required to bring about the measured change in cake resistance (deagglomeration resistance, as shown in Table 4.2) can be calculated from the following relationship.

$$R_L=180(1-\epsilon)^2\,\delta_L/d_p^2\,\epsilon^3$$

Where R_L is hydraulic resistance of the filter cake; d_p is the particle diameter, ϵ is the cake porosity; and δ_L is the cake thickness. Assuming constant cake porosity and thickness, the ratio of the initial to final cake resistance is inversely proportional the square of the particle diameter; i.e., $R_{L,1}/R_{L,2}=d_{p,2}^2/d_{p,1}^2$, or $d_{p,2}=d_{p,1}(R_{L,1}/R_{L,2})^{½}$.

where
$d_{p,1}$ = particle diameter before testing
$d_{p,2}$ = particle diameter after testing
$R_{L,1}$ = initial resistance (filter-cake resistance from Table 4.2)
$R_{L,2}$ = final resistance (filter-cake resistance + deagglomeration resistance from Table 4.2).

The results are provided in Table 4.3. The data indicate that the particle size of the 8 wt% C-106 did not change significantly during testing (0.71 μm before and after testing). This result supports the analysis based on hydraulic resistance measurements that the 8 wt% C-106 did not deagglomerate. The calculated particle diameter after testing is 0.73 μm, which is very close to the measure value of 0.71 μm. Particle-size data for the 0.05 and 1.5 wt% feeds were lost during transport and preparation and unfortunately are not available.

Table 4.3. Calculated and Measured Median Particle Diameters

Feed	Measured Before Testing	Measured After Testing	Calculated After Testing
	Median Particle Diameter (μm)	Median Particle Diameter (μm)	Particle Diameter (μm)
C-106, 0.05 wt%	0.71	na	0.84
C-106, 1.5 wt%	0.71	na	0.56
C-106, 8 wt%	0.71	0.71	0.73
C-107, 0.05 wt%	0.74	0.87	0.63
C-107, 1.5 wt%	0.74	0.73	0.51
C-107, 8 wt%	0.74	0.74	0.51
B-110, 0.05 wt%	0.87	0.72	0.53
B-110, 1.5 wt%	0.87	0.73	0.63
B-110, 8 wt%	0.87	0.87	0.79
U-110, 0.05 wt%	0.93	0.76	0.59
U-110, 1.5 wt%	0.93	0.74	0.71
U-110, 7.5 wt%	0.93	0.82	0.78
S-107, 0.05 wt%	0.3	na	0.28
S-107, 1.5 wt%	0.3	0.3	0.36
S-107, 8 wt%	0.5	0.3	0.29

na: not available.

Particle-size data from C-107 also support the analysis based on the hydraulic resistance measurements summarized in Table 4.2. The measured particle size after testing is largest for the 0.05 wt% slurry and smaller for the 1.5 and 8 wt% slurries. These measurements are consistent with the analyses, which indicates significantly more deagglomeration at the higher wt% slurries. The calculated particle diameters are smaller than the measured values after testing, which may indicate a poor measurement/sample for the initial feed. It is interesting to note that if one calculates the particle diameter before testing based on the measured particle diameters after testing, then the results are 1.02, 1.09, and 1.08 microns from the 0.05, 1.5, and 8 wt% slurries, respectively. These numbers are surprisingly consistent and seem to support the hypothesis that the median particle diameter measured before testing is low.

Particle-size data in Table 4.3 support the hypothesis that the B-110 is susceptible to peptization at lower salt concentration, as the measured particle size (after testing) decreased with decreasing solids (and salt) content. Table 4.2 shows that the measured deagglomeration resistance is highest for the 0.05 wt% slurry and decreases at higher solids loadings.

A similar case can be made for U-110, which also displayed more deagglomeration resistance with decreasing solids content in the slurry. The particle-size data support the hypothesis that U-110 was more susceptible to deagglomeration at lower solids (and salt) content. The measured particle size after testing the 7.5 wt% slurry was 0.82 microns, while 0.74 and 0.76 microns were measured for the particle size after testing the 0.05 and 1.5 wt% slurries, respectively. The calculated particle size generally match the this trend, with the largest median particle size calculated for the 7.5 wt% slurry and smaller median particle sizes calculated for the more dilute slurries.

Finally, the S-107 data is included from Geeting and Reynolds (1996). The data indicate that the median particle diameter decreased from 0.5 microns before testing to 0.3 microns after testing at 8 wt% solids. All subsequent S-107 feeds were composed of dilutions from the 8 wt% feeds. After the initial deagglomeration, there was no measurable decrease in average particle diameter in subsequent testing. The calculated particle diameter (which is based on the initial particle diameter, and measured filter cake and deagglomeration resistances provided in Table 4.2) was remarkably consistent with the measured diameters and contributed significant credibility to the analysis.

It is recognized that obtaining representative analysis in a particle size distribution analyzer is difficult, because of, a) the lag time between sampling and actual analysis, b) the instrument shear required to keep the particles suspended, and c) the dilution required for most feed samples. All three of these factors can have an effect on the measured particle size distribution. Nevertheless, we see that the particle size analysis generally matched the results of the hydraulic resistance analysis, at least from a qualitative perspective.

4.2.3 Fouling Resistance

The Mott filter, when used for testing the simulants, exhibited little, if any, fouling, as indicated in Table 4.2. The fact that some of the measurements for fouling were negative provides an indication of the error associated with this analysis. Because these numbers are small, the data may indicate that the error in the analysis is low. Repeatability issues associated with this analysis are considered in Section 4.2.4.

Based only on the simulant testing, one would conclude that the Mott filter was appropriately sized for the simulants tested. The fact that the subsequent wastes tested with the Mott filter (S-107 and C-106) resulted in significant filter fouling illustrates the importance of actual waste testing.

The fouling resistance of S-107 and C-106 (which were tested with the 0.5-micron Mott filter) are not directly comparable because the filter was acid-cleaned between each run with the C-106 feed, but not for the S-107 feed. The S-107 had the most fouling of any feed tested. This feed also exhibited significant deagglomeration. The C-106 exhibited little or no feed deagglomeration; fouling of the 8 wt% feed was less than that of the 0.05 or 1.5 wt% feeds.

For the latter three feeds (C-107, B-110, U-110) which were tested with the Graver filter, the deagglomeration resistance increased when the filter-cake resistance and the fouling resistance increased. Hence, when a feed deagglomerates, the resulting filter cake has a greater hydraulic resistance and tends to foul the filter to a greater extent. As previously stated, it should be recognized that the fouling resistance, as measured, does not mean the filter required acid cleaning.

4.2.4 Repeatability

Because the filtrate flux is changing rapidly immediately after back-pulse (at time=0), repeatability of the preceding analysis is of concern. Measurements made immediately after back-pulse were taken in a very narrow time "window," and considered to be as repeatable as possible without using an automated data-acquisition system.

The initial filter media resistance measured by two different means is provided in Table 4.4. The first column provides the filter-media resistance as measured before testing when only clean water was in the system. These data provide a good reference for the second column which provides the media resistance at the very beginning of the test matrix at time=0 (shown graphically as point 4 of Figure 4.3). The agreement is very good and within $2 * 10^{11} * m^{-1}$, except when the filter was acid-cleaned before testing. Recall that for the Graver tests, acid cleaning was required just before the 8 wt% B-110 feed (or just after the 1.5 wt% B-110 feed as reported elsewhere in the report). In general, it is expected that the resistance measured at the beginning of the test would be higher than that measured with clean water, because solids in the feed will reduce the flux in the time necessary to initiate testing. This effect is more pronounced after acid cleaning. Note that filter- media resistance measured after acid cleaning (before testing 8 wt% B-110) is the same as that measured in the new filter (before testing 0.05 wt% C-107). The Graver filter exhibits some very minor fouling as the media resistance increased from $8*10^{11}*m^{-1}$. and leveled out at about $11*10^{11}*m^{-1}$.

The good agreement of the initial filter resistance measured with the clean-water flux and measured in the analysis has been established in Table 4.4 for the Graver filter. Similar data for the Mott filter are shown in Table 4.5. The comparison between the filter-media resistance measured with clean-water flux before testing with the resistance measured at the beginning of testing was not nearly as good. In all tests with the Mott filter, the clean-water flux measured before testing was conducted after acid cleaning the filter. As a result, the filter resistance significantly increased before taking the first measurement. This initial fouling may be the cause of the negative deagglomeration resistances seen in Table 4.2. The conclusion to be drawn is that if a filter has been acid-cleaned, then the correlation between the media resistance measured by the clean-water flux and the media resistance measured at the beginning of the test is poor.

Table 4.4. Comparison of Graver Filter-Media Resistance

Feed	Filter-media resistance, Rm, measured with clean-water flux before testing (10^{11} *m^{-1})	Filter-media resistance, Rm, measured with feed indicated at beginning of test (10^{11} *m^{-1})
C-107, 0.05 wt%	8	7
C-107, 1.5 wt%	12	13
C-107, 8 wt%	11	13
B-110, 0.05 wt%	12	14
B-110, 1.5 wt%	11	13
B-110, 8 wt%	8	12
U-110, 0.05 wt%	10	10
U-110, 1.5 wt%	11	11
U-110, 7.5 wt%	10	11

Table 4.5. Comparison of Mott Filter-Media Resistance

Feed	Filter-media resistance, Rm, measured with clean-water flux before testing (10^{11} *m^{-1})	Filter-media resistance, Rm, measured with feed indicated at beginning of test (10^{11} *m^{-1})
C-106, 0.05 wt%	5	20
C-106, 1.5 wt%	3	11
C-106, 8 wt%	2	21

4.4 Crossflow Filtration Feasibility for Use in Pretreatment of Hanford Tank Wastes

The Hanford Tank Waste Remediation System (TWRS) flowsheet[3] (Orme 1994) provides an estimate of the volumetric flowrates at various points in the pretreatment process assuming a 14-year processing time and a total on-line efficiency (TOE) of 60%.

The required filter area to meet each need based on volumetric flowrates provided in Orme (1994) is provided in Table 4.6. The nominal quasi steady-state (30 minutes after back-pulse) filtrate flux for the tanks tested herein was approximately 0.05 gpm/ft^2 with extremes of 0.015 and 0.15 gpm/ft^2. The nominal value was used in Table 4.6 to estimate the required filter area. It should be recognized that no testing was performed for Needs 2 or 3, and the actual processing rate is believed to be higher than assumed for two reasons: First, feeds from Needs 2 and 3 would have very low solids loadings, and crossflow-filtration flux rates generally increase with decreased solids loadings. Second, these feeds would have high ionic strength which, for some feeds, is believed to reduce their susceptibility to deagglomeration.

For comparison purposes, Savannah River Site (SRS) currently operates a crossflow filter with 432 ft^2 of filtration area. There are two modules in the plant; each module has 144 parallel tubes with a 10' active length/tube. The original bundles had an 0.575" ID, but the standard is now 0.625". The plant bundle area is 216 ft^2 (old) or 235 ft^2 (currently available). The bundles have separate pumps and back-pulse systems, but recirculate to the same tank (Tank 48H). Although both bundles may be operated simultaneously, normal operating mode is to operate one bundle at a time.

One can see from this comparison with the operating SRS crossflow filter that the filtration area estimated in Table 4.6 is not significantly greater than the system operated at SRS.

Table 4.6. Estimated Crossflow Filter Requirements for Various Hanford Pretreatment Needs

Need [4]	Description	Required Processing Rate (gpm)	Filtration Area (ft^2)
1a and 1b [5]	Initial retrieval and ESW separation	57	1140
2	Pre-ion exchange	29	580
3	Post-ion exchange	29	580

[3] The most recent Hanford flowsheet (i.e., Orme 1996) was not used because it is directed at the privatization-process baseline which assumes treatment of the waste in two phases. The older flowsheet thus provides more concise material balances and processing rates.

[4] Numbers correspond with those needs indicated in Figure 1.1.

[5] This analysis assumes that Needs 1a and 1b may be satisfied by one piece of equipment.

5.0 Conclusions and Recommendations

5.1 Conclusions

The permeate flux rates achieved (nominally 0.05 gpm/ft^2) during the testing of actual waste indicate that crossflow filtration is a feasible candidate technology for solid/liquid separations associated with the pretreatment of Hanford tank wastes. Based on throughput of all soluble waste and wash solutions estimated in the Hanford flowsheet, the nominal rate corresponds to a 1140-ft^2 filter requirement. For comparison, Savannah River Site currently is operating a crossflow filter with 432 ft^2.

Processing data indicate that the test matrix included sufficiently high axial velocity and transmembrane pressure to select operating conditions for 8 wt% slurries; however, the flux rates of the lower solids slurries (1.5 and 0.05 wt%) would improve with higher transmembrane pressure. The bench-scale apparatus used in testing cannot operate beyond the matrix selected in testing; to determine more optimal conditions for these lighter slurries, a different apparatus would have to be used.

Crossflow filtration was found to remove solids effectively, as judged by filtrate clarity and radiochemical analysis. If the filtrates from these tests were immobilized in a glass matrix, the resulting transuranic and ^{90}Sr activity would not breach low activity waste glass limits of 100 nCi/g (TRU) and 20 μCi/ml (^{90}Sr). Two exceptions were the transuranic activity in filtrates from processing 1.5 and 8 wt% C-106 tank waste. Subsequent analyses indicated that the source of the TRU activity in the filtrate was most likely due to soluble plutonium caused by complexation with carbonate. Re-testing of the C-106 supported these results. These data suggest the need to control carbonate and pH when processing tank wastes for immobilization.

Filtrate-flux rates declined during the course of testing the radioactive feeds. Data analysis indicates two causes for the decline: filter fouling and feed deagglomeration.

- Filter fouling was reduced by 60% after selecting a smaller pore-size filter (0.1 μm vs. 0.5 μm). In most instances, the smaller pore-sized filter was cleaned easily with water to restore the filtrate flux, while the larger pore-sized filter required acid cleaning.

- Feed deagglomeration was predicted based on analysis of hydraulic resistance measured during testing and confirmed by the particle-size distribution measurement. It is speculated that the observed effects of deagglomeration may be amplified because of the high shear apparatus used in testing.

Wastes from tanks B-110 and U-110 exhibited greater deagglomeration at lower solids concentration in the feed and lower ionic strength. Waste from tanks C-107 deagglomerated at all ionic strength solutions tested.

The 0.1-micron filter (Graver) is better sized for the purposes of filtering Hanford tank wastes than the 0.5-micron filter (Mott). It should be noted that this conclusion was based on a comparison of filtering different wastes, and fouling was found to be waste-dependent. To state that one filter is definitively better than another, a comparison should be made using the same feed.

The Hanford tank wastes tested exhibit different filtering characteristics, making bench- and pilot- scale testing a vital part of sizing equipment.

5.2 Recommendations

Additional work is recommended both to confirm the findings and extend the work presented. Specific recommendations follow.

(1) Filter the same waste type with both the Mott and Graver filters. A head-to-head comparison is needed to make a definitive recommendation for filter selection. Any comparisons made based on data taken to date are clouded by the fact that different wastes were tested with each of the filters and filter fouling has been found to be waste-dependent.

(2) Test additional waste types. Testing to date has accounted for 23% of the Hanford single-shell tank sludges, assuming the SORWT groups listed in Hill and Simpson (1994) have similar filtering characteristics. Additional sludge types are available for testing and would provide further valuable data. In addition to tank sludge, researchers have found that not all salt cake is soluble; in particular, approximately 17 wt% of the salt cake from U-108 was found to be insoluble. These insoluble salt-cake solids could be obtained for testing and would provide the first information on filtering solids, which heretofore have not been considered.

(3) Conduct additional testing on feeds found to be susceptible to deagglomeration at low ionic strength (e.g., B-110). Establish as a function of ionic strength where deagglomeration is and is not an issue. If a lower limit were established for ionic strength, then it may be possible to be applied during processing to prevent deagglomeration.

(4) Test crossflow filtration to establish its efficacy for other Hanford tank SLS needs; for example, crossflow filtration may be used before or after Cs ion exchange. These needs, which are clearly identified in the Hanford flowsheet, have not yet been considered for testing. The need just before ion exchange would be a "polishing" step and would involve a feed of high ionic strength and low solids loading. In some instances, the solids could be composed of precipitated solids. The need just after Cs ion exchange would also involve a feed of high ionic strength and would protect down-stream processes from any Cs-loaded resin fines.

(5) Before decommissioning, the CUF bench-scale pilot plant should be used to evaluate how concentrated crossflow filtration can make the retentate, and then to evaluate solids-washing efficiencies and compare with settle/decant. The solids concentration of the sludge is one of the most important parameters in the sizing and design of the pretreatment plant. A higher solids concentration gives a higher duty to the initial filtration circuit, but it reduces the quantities of sodium hydroxide and wash water. This work would involve testing with simulants to establish trends and upper limits for viscosity as a function of wt% solids and then verifying with actual tank waste.

6.0 References

Brooks, K.P., J.R. Philips, R.L. Meyers, K.G. Rappe, D.R. Rector, and P.A. Smith. 1996. *Sludge Pretreatment Studies Using Hanford Tank C-107.* Letter report to Westinghouse Hanford Company prepared by Pacific Northwest National Laboratory, Richland, Washington.

Geeting, J.G.H. and B.A. Reynolds. 1996. *Bench-Scale Cross Flow Filtration of Tank S-107 Sludge Slurries and Tank C-107 Supernatant.* PNNL-11376, Pacific Northwest National Laboratory, Richland, Washington.

Hill, J.G. and B.C. Simpson. 1994. *The Sort on Radioactive Waste Type Model: A Method to Sort Single-Shell Tanks Into Characteristic Groups.* PNL-9814. Pacific Northwest Laboratory, Richland, Washington.

Lumetta, G.J., B.M. Rapko, M.J. Wagner, C.D. Carlson, and R.J. Barrington. 1994a. *Sludge Treatment and Extraction Technology Development: Results of FY 1993 Studies.* PNL-9387, Pacific Northwest Laboratory, Richland, Washington.

Lumetta, G.J. and B.M. Rapko. 1994b. *Washing and Alkaline Leaching of Hanford Tank Sludges: A Status Report.* PNL-10078, Pacific Northwest Laboratory, Richland, Washington.

Lumetta, G.J., M.J. Wagner, F.V. Hoopes, and R.T. Steele. 1996a. *Washing and Caustic Leaching of Hanford Tank C-106 Sludge.* PNNL-11381, Pacific Northwest National Laboratory, Richland, Washington.

Lumetta, G.J., M.J. Wagner, F.V. Hoopes, and R.T. Steele. 1996b. *Washing and Caustic Leaching of Hanford Tank Sludges: Results of FY 1996 Studies.* PNNL-11278, Pacific Northwest National Laboratory, Richland, Washington.

Murkes, J. and C. Carlsson. 1988. *Crossflow Filtration.* John Wiley and Sons, New York.

Orme, R.M.. 1994. *Tank Waste Remediation System Process Flowsheet.* WHC-SD-WM-TI-613 Rev. 0, Westinghouse Hanford Company, Richland, Washington.

Orme, R.M., A.F. Manuel, L.W. Shelton, and E.J. Slaathaug. 1996. *Tank Waste Remediation System Privatization Process Technical Baseline.* WHC-SD-WM-TI-774 Rev. 0, Westinghouse Hanford Company, Richland, Washington.

Porter, M.C. 1972. "Concentration Polarization with Membrane Ultrafiltration." *Ind Eng Chem Prod Res Develop* **11**(3):234-248.

Tartleton, E.S. and R.J. Wakeman. 1993. "Understanding Flux Decline in Crossflow Microfiltration: Part I--Effects of Particle and Pore Size." *Trans IchemE* **71**:399-410.

Whyatt, G.A., R.J. Serne, S.V. Mattigod, Y. Onishi, M.R. Powell, J.H. Westsik, Jr., L.M. Liljergren, G.R. Golcar, K.P. Recknagle, P.M. Doctor, V.G. Zhirnov, J. Dixon. 1996. *Potential for Criticality in Hanford Tanks Resulting from Retrieval of Tank Waste.* PNL-11304. Pacific Northwest National Laboratory, Richland, Washington.

Yamaguchi, T., Y. Sakamoto and T. Ohnuki. 1994. Effect of the Complexation on Solubiltiy of Pu(IV) in Aqueous Carbonate Systems. *Radiochim. Acta*. 66/67:9-14.

Zydney, A.L. and C.K. Colton. 1986. "A Concentration Polarization Model for the Filtrate Flux in Crossflow Microfiltration of Particulate Suspensions." *Chem Eng Commun* **47**:1.

Appendix A

Data

Rows	Time Since Back Pulse	Flowrate (ft/s)	Pressure (psig)	Filtrate Flux (gpm/ft2)	Temp (C)
1	0	6	25	0.1401	33.5
2	5	6	25	0.0904	33.9
3	10	6	25	0.0772	33.9
4	15	5.9	25	0.075	34
5	20	6	25	0.066	34
6	25	6	24.5	0.0616	34.2
7	30	5.9	25	0.0596	34.1
8	0	6	25	0.1169	34.2
9	5	6.1	25	0.0716	34.3
10	10	6.1	25	0.0664	34.4
11	15	6.1	25	0.0625	34.4
12	20	6.1	25	0.0607	34.5
13	25	6.1	25	0.0579	34.4
14	30	6.1	25	0.0566	34.5
15	0	7.5	32.5	0.0647	36.7
16	10	7.5	32.5	0.049	38.2
17	20	7.6	32.5	0.0407	38.4
18	30	7.5	33	0.0454	38.8
19	0	7.5	32.5	0.0368	38.9
20	10	7.5	32	0.04	39.1
21	20	7.5	32.5	0.0353	39.3
22	30	7.4	33	0.0396	39.5
23	0	3	26.5	?	34.2
24	10	2.9	25	0.0527	33.2
25	20	3	25	0.059	32.8
26	30	2.9	25	0.0585	32.6
27	0	2.8	25	0.0449	32.3
28	10	3.1	25	0.0542	32.5
29	20	3.1	25.5	0.0574	32.5
30	30	2.9	25	0.0579	32.6
31	0	6	10	0.0172	32.8
32	10	6.1	10	0.0212	32.7
33	20	5.8	10	0.0243	32.5
34	30	5.8	10	0.0245	32.5
35	0	6	10.5	0.0403	33
36	10	5.9	10	0.0303	32.7
37	20	5.9	10	0.0322	33.3
38	30	6	10	0.0275	32.8
39	0	7.4	17.5	0.0392	35.5
40	10	7.4	17.5	0.0317	35.8
41	20	7.5	17.5	0.0335	35.8
42	30	7.6	17.5	0.0335	35.8
43	0	7.5	17	0.0309	36
44	10	7.6	17.5	0.0255	35.8
45	20	7.5	17.5	0.0268	35.8
46	30	7.5	18	0.0283	35.7
47	0	6.1	25	0.0455	36.2
48	5	6.1	25	0.0411	36.2
49	10	6.1	25	0.0366	36.7
50	15	6.1	25	0.0334	36.3
51	20	6.1	25	0.0344	36.3
52	25	6.1	25	0.033	36.5
53	30	6.1	25	0.0344	36.2
54	0	6.1	25	0.0443	36.2
55	5	6	25	0.0419	36.1
56	10	6	25	0.0431	36
57	15	6	25.5	0.0502	35.9
58	20	6.1	25	0.0522	35.9

Rows	Time Since Back Pulse	Flowrate (ft/s)	Pressure (psig)	Filtrate Flux (gpm/ft2)	Temp (C)
59	25	6	25	0.0559	35.7
60	30	6	25	0.0566	35.7
61	0	4.5	32.5	0.1012	35.8
62	10	4.5	32.5	0.085	35.5
63	20	4.5	32.5	0.0822	35.4
64	30	4.6	32.5	0.0772	35.5
65	0	4.5	32.5	0.1138	35.8
66	10	4.5	32.5	0.0792	35.8
67	20	4.5	32.5	0.0787	35.8
68	30	4.5	32.5	0.0763	35.8
69	0	6	40.5	0.0867	37.4
70	10	5.9	40	0.0657	39.4
71	20	6	40	0.0486	40
72	30	6	40.5	0.0514	40.4
73	0	5.9	40.5	0.0492	40.8
74	10	5.9	40	0.051	40.8
75	20	6	40	0.0479	40.8
76	30	6	40	0.0425	41
77	0	9	25.5	0.0202	40.6
78	10	8.9	25	0.0217	41
79	20	8.9	25.5	0.0227	41.7
80	30	8.9	25	0.0219	41.6
81	0	9	25	0.025	42.9
82	10	9.2	25	0.0228	4.34
83	20	9.1	25	0.0221	42.6
84	30	9	25	0.0222	42.2
85	0	4.5	17.5	0.02	34.6
86	10	4.5	17.5	0.0216	33.9
87	20	4.5	18	0.0267	33.7
88	30	4.5	17.5	0.0314	33.4
89	0	4.3	18	0.0472	33.5
90	10	4.4	18	0.0409	33.3
91	20	4.6	18	0.0431	33.2
92	30	4.5	17.5	0.0411	34
93	0	5.9	25	0.0486	34.7
94	5	6	25	0.0398	35.3
95	10	6	25	0.0386	35.6
96	15	5.9	25	0.0382	35.6
97	20	5.9	25	0.0375	35.7
98	25	5.9	25	0.0368	35.6
99	30	5.9	25	0.0364	35.7
100	0	5.9	25	0.036	36.2
101	5	5.9	25	0.0305	36.2
102	10	5.9	25	0.0298	36.1
103	15	5.9	25	0.0283	36
104	20	6.1	25	0.028	36.2
105	25	6.1	25	0.0271	36.4
106	30	6.1	25	0.0296	36.5

Rows	Time Since Back Pulse	Flowrate (ft/s)	Pressure (psig)	Filtrate Flux (gpm/ft2)	Temp (C)
1	0	6.1	25.5	0.2405	34.2
2	5	5.9	25	0.098	34.2
3	10	6	25.5	0.0844	34.4
4	15	6.1	25.5	0.0777	34.4
5	20	5.9	25	0.0728	34.4
6	25	6.1	25	0.0704	34.4
7	30	6	25	0.0693	34.6
8	0	6.1	25	0.2451	34.6
9	5	6	25	0.1004	34.7
10	10	6	25.5	0.0812	34.8
11	15	5.9	25.5	0.0787	34.9
12	20	6.1	25	0.0696	35
13	25	6	25	0.0693	35
14	30	6.1	25	0.0664	35
15	0	7.4	32	0.236	37
16	10	7.5	32.5	0.091	37.8
17	20	7.5	32.5	0.0792	38.2
18	30	7.5	32.5	0.0754	38.3
19	0	7.5	32.5	0.2601	38.7
20	10	7.5	32	0.0879	38.7
21	20	7.5	32.5	0.0763	38.4
22	30	7.5	32.5	0.0685	38.3
23	0	2.8	25	0.1795	33
24	10	3.1	25	0.0533	32.7
25	20	3.1	25	0.0469	32.5
26	30	3.1	25	0.0217	32.5
27	0	3	25	0.1961	32.7
28	10	3	25	0.0585	32.4
29	20	2.9	25	0.0455	32.4
30	30	3	25	0.0422	32.4
31	0	5.9	10	0.0476	32
32	10	6	10	0.0403	31.3
33	20	6	10	0.0375	31.2
34	30	6	10	0.036	31.3
35	0	6	10	0.059	31.5
36	10	6	10	0.0428	31.2
37	20	6	10	0.0386	31.2
38	30	6	10	0.0382	31.3
39	0	7.5	17.5	0.0988	33.3
40	10	7.5	17.5	0.0569	33.8
41	20	7.5	17.5	0.0527	33.9
42	30	7.5	17.5	0.0483	34
43	0	7.5	17.5	0.0924	34.4
44	10	7.6	17.5	0.0554	34.4
45	20	7.5	17.5	0.0522	34.5
46	30	7.5	18	0.0486	34.6
47	0	6	25	0.1138	35.4
48	5	6.1	24.5	0.0708	35.5
49	10	6	25	0.0607	35.6
50	15	6	25	0.0536	35.9
51	20	6	24.5	0.051	35.9
52	25	5.9	25	0.051	36.1
53	30	5.8	25	0.0476	36.1
54	0	6.1	25	0.108	36.7
55	5	6	25	0.0644	36.8
56	10	6	25	0.0579	36.8
57	15	6	25	0.0554	36.8
58	20	6.1	25	0.051	37

Rows	Time Since Back Pulse	Flowrate (ft/s)	Pressure (psig)	Filtrate Flux (gpm/ft2)	Temp (C)
59	25	6.1	25	0.0502	37.1
60	30	6	25	0.0472	37.2
61	0	4.7	32.5	0.1062	35.2
62	10	4.6	32.5	0.0554	36.4
63	20	4.6	33	0.0472	36.8
64	30	4.6	32.5	0.0449	36.9
65	0	4.4	32.5	0.1356	37.3
66	10	4.4	32.5	0.0549	37
67	20	4.5	32.5	0.0446	36.8
68	30	4.5	32.5	0.0428	36.8
69	0	5.9	40	0.1328	39.7
70	10	5.9	40.5	0.0613	40.3
71	20	5.9	40	0.0527	39.7
72	30	5.9	40	0.0494	40.3
73	0	5.9	40	0.0741	40.6
74	10	6.1	40	0.0613	40.7
75	20	6.1	39.5	0.0518	40.7
76	30	6	40	0.0506	41
77	0	8.5	25.5	0.0693	38.9
78	10	8.4	25	0.0422	39.8
79	20	8.1	25	0.0364	39.6
80	30	9	25	?	?
81	0	9	25	?	?
82	10	9	25	?	?
83	20	9	25	?	?
84	30	9	25	?	?
85	0	4.5	17.5	?	?
86	10	4.5	17.5	?	?
87	20	4.5	17.5	?	?
88	30	4.5	17.5	?	?
89	0	4.5	17.5	?	?
90	10	4.4	17.5	?	?
91	20	4.5	17.5	?	?
92	30	4.5	17.5	?	?
93	0	5.9	25	?	?
94	5	6	25	?	?
95	10	6	25	?	?
96	15	6	25	?	?
97	20	6	25	?	?
98	25	6	25	?	?
99	30	6	25	?	?
100	0	6	25	?	?
101	5	6	25	?	?
102	10	6	25	?	?
103	15	6	25	?	?
104	20	6	25	?	?
105	25	6	25	?	?
106	30	6	25	?	?

Rows	Time Since Back Pulse	Flowrate (ft/s)	Pressure (psig)	Filtrate Flux (gpm/ft2)	Temp (C)
1	0	5.9	21	0.102	31.3
2	5	6	20	0.0414	31.8
3	10	6.1	20	0.0393	31.8
4	15	6.1	20	0.0396	32.2
5	20	6.1	20	0.0401	32.7
6	25	6	20	0.0393	32.7
7	30	6	20	0.0401	32.3
8	0	6	20	0.0924	32.4
9	5	5.9	21	0.0411	32
10	10	6	20.5	0.0396	31.9
11	15	6	20	0.0366	31.9
12	20	6	20	0.0382	31.8
13	25	6.1	20	0.0375	31.8
14	30	6.1	20	0.0364	31.7
15	0	4.6	12.5	0.0494	30.8
16	10	4.4	12.5	0.029	29.5
17	20	4.5	12.5	0.0266	29.2
18	30	4.5	12.5	0.0264	29.2
19	0	4.5	12.5	0.0486	29.5
20	10	4.5	12.5	0.0283	29.3
21	20	4.6	12.5	0.026	29.3
22	30	4.5	12.5	0.0268	29.2
23	0	9	19.5	0.075	33.4
24	10	8.9	20	0.0637	34.4
25	20	8.9	21	0.0637	34.3
26	30	9	20	0.0449	35.1
27	0	9.1	20	0.0966	36.1
28	10	9.2	20.5	0.0352	35.8
29	20	9	20	0.0678	35.9
30	30	9	20	0.0644	35.4
31	0	5.9	35.5	0.0708	35.5
32	10	6	35	0.0319	36.1
33	20	6.2	35	0.0314	35.9
34	30	5.9	35.5	0.0334	35.8
35	0	6	35	0.085	36.4
36	10	6	35	0.038	36.6
37	20	6	35	0.0393	37.2
38	30	6.2	35	0.0391	36.7
39	0	4.6	27	0.0596	31.7
40	10	4.5	27	0.0296	31.9
41	20	4.5	27.5	0.0275	31.5
42	30	4.5	27.5	0.0269	31.1
43	0	4.4	27.5	0.0596	31.5
44	10	4.4	27.5	0.0287	31.3
45	20	4.4	28	0.0263	31.3
46	30	4.7	27.5	0.0254	31.3
47	0	5.9	20.5	0.0536	31.5
48	5	6	20	0.0371	31.3
49	10	6	21	0.0373	31.3
50	15	5.9	20	0.0352	31.3
51	20	5.7	20	0.0344	31.2
52	25	6.2	20	0.0332	31.3
53	30	6	20	0.0337	31.3
54	0	6.2	19.5	0.075	31.4
55	5	5.9	20.5	0.0417	31.3
56	10	6.1	20	0.0335	31.1
57	15	6	20	0.0343	31.1
58	20	6	20.5	0.0373	31.1

Rows	Time Since Back Pulse	Flowrate (ft/s)	Pressure (psig)	Filtrate Flux (gpm/ft2)	Temp (C)
59	25	6.1	20	0.0335	31.3
60	30	6	20	0.0332	31.3
61	0	7.6	12.5	0.054	30.8
62	10	7.4	12.5	0.0414	30.6
63	20	7.5	12.5	0.0422	31
64	30	7.5	12.5	0.0393	31
65	0	7.5	12.5	0.0569	31.6
66	10	7.5	12.5	0.0443	31.7
67	20	7.5	13	0.0446	31.8
68	30	7.6	12.5	0.0434	32
69	0	5.9	5.5	0.02	31.1
70	10	6.1	5	0.0206	29.9
71	20	6	5.5	0.0192	29.4
72	30	6	5.5	0.0196	29.1
73	0	6	5	0.0366	29.4
74	10	6	5.5	0.0328	29.2
75	20	6	5	0.0256	29.1
76	30	6	5	0.026	29.1
77	0	2.9	20	0.0354	29.6
78	10	3	20	0.0192	29.3
79	20	2.9	20	0.0171	29.3
80	30	2.9	20	0.0165	29.3
81	0	3.1	20	0.0607	29.6
82	10	3	20	0.0197	29.6
83	20	2.9	20	0.0211	29.3
84	30	3.1	20	0.0177	29.3
85	0	7.4	27.5	0.0937	34.5
86	10	7.3	27.5	0.0486	35.2
87	20	7.4	27.5	0.0494	35.3
88	30	7.1	27.5	0.0476	34.9
89	0	7.5	27.5	0.0637	35.4
90	10	7.5	27	0.0494	36.2
91	20	7.6	27.5	0.0425	36.3
92	30	7.7	27	0.0425	36.4
93	0	5.9	20.5	0.0527	35
94	5	5.9	20	0.0375	33.8
95	10	5.9	20	0.0358	33.2
96	15	6	20	0.0327	33.1
97	20	6	20	0.0309	33
98	25	6	20	0.0301	32.9
99	30	6	20	0.0317	32.9
100	0	6.1	20	0.075	33.2
101	5	5.9	20	0.0393	33
102	10	6	20	0.0356	33.1
103	15	6.1	20	0.0335	32.9
104	20	5.8	21	0.036	32.8
105	25	6	20	0.0339	33.4
106	30	6.2	20	0.0344	33.3

Rows	Time Since Back Pulse	Flowrate (ft/s)	Pressure (psig)	Filtrate Flux (gpm/ft2)	Temp (C)
1	0	6	25	0.4014	27.9
2	5	5.9	26	0.236	28.1
3	10	6.2	25	0.177	28.4
4	15	6.2	25	0.1655	28.5
5	20	6	25	0.1517	28.5
6	25	6	25	0.1482	28.5
7	30	5.9	24.5	0.1356	28.5
8	0	5.9	24.5	0.3186	28.6
9	5	6	25	0.236	28.8
10	10	6	25	0.1992	28.7
11	15	6	25	0.1874	28.8
12	20	6	25	0.1699	28.9
13	25	6.2	25	0.15	29.2
14	30	6	25	0.1448	29.4
15	0	7.3	32	0.4112	31.7
16	10	7.5	32.5	0.1847	32.1
17	20	7.4	33	0.1536	32.4
18	30	7.4	32.5	0.1342	32.9
19	0	7.8	31	0.2499	32.8
20	10	7.3	33	0.1746	33
21	20	7.3	33	0.1416	33.1
22	30	7.5	32	0.1159	32.8
23	0	2.9	25.5	0.1931	29.5
24	10	3.1	25.5	?	27.7
25	20	3.1	25	0.1159	27
26	30	3.1	25	0.1028	26.9
27	0	3	25	0.2405	26.8
28	10	3	25	0.15	26.8
29	20	3.2	25	0.125	27
30	30	2.9	25	0.1202	26.7
31	0	6	10	0.102	26.7
32	10	6.1	10	0.0763	26.5
33	20	6	10	0.0671	26.4
34	30	6	10	0.0628	26.3
35	0	5.9	10.5	0.1053	26.3
36	10	5.9	10	0.075	26.3
37	20	5.9	10	0.0693	26.2
38	30	6	10	0.0637	26.1
39	0	7.7	17.5	0.1847	28.1
40	10	7.3	17.5	0.1314	28.7
41	20	7.5	17.5	0.1191	28.8
42	30	7.5	18	0.1062	28.9
43	0	7.3	18	0.1821	29.1
44	10	7.4	18	0.1262	29.4
45	20	7.6	18	0.1062	29.6
46	30	7.5	18	0.1017	29.6
47	0	6.1	25	0.2549	29.2
48	5	5.9	25	0.1795	29.2
49	10	6	25.5	0.1593	29.3
50	15	6	25.5	0.1432	29.3
51	20	5.9	25.5	0.1328	29.3
52	25	6	25	0.1262	29.4
53	30	6	25	0.1138	29.4
54	0	6.1	25	0.2549	29.5
55	5	6	25	0.1655	29.6
56	10	6	25	0.1448	29.6
57	15	5.9	25	0.1314	29.5
58	20	6	25	0.1237	29.5

Rows	Time Since Back Pulse	Flowrate (ft/s)	Pressure (psig)	Filtrate Flux (gpm/ft2)	Temp (C)
59	25	6	25	0.1058	29.4
60	30	6	24.5	0.1128	29.3
61	0	4.6	32.5	0.3227	29.7
62	10	4.6	32.5	0.1634	30
63	20	4.6	32.5	0.1401	30
64	30	4.5	32.5	0.1287	29.8
65	0	4.4	33.5	0.3642	29.8
66	10	4.6	32.5	0.1692	29.6
67	20	4.6	33	0.1371	29.7
68	30	4.5	32.5	0.1275	29.5
69	0	5.9	41	0.4249	31.1
70	10	5.9	40	0.1722	32.2
71	20	6	40	0.1517	32.6
72	30	5.9	41	0.1401	33.1
73	0	5.8	40	0.3134	33.1
74	10	5.9	405	0.15	33.3
75	20	6	40	0.1342	33.3
76	30	6	40	0.1169	33.3
77	0	9	25.5	0.1593	33.7
78	10	9	25	0.102	33.7
79	20	9	25	0.0891	33.6
80	30	9	25.5	0.0658	33.8
81	0	9.2	25	0.1053	34.7
82	10	9.1	25.5	0.0926	35.3
83	20	9	25	0.0867	34.7
84	30	9.1	25	0.0782	34.5
85	0	4.4	17.5	0.0937	27.4
86	10	4.5	17.5	0.0674	27.9
87	20	4.5	17.5	0.0689	27.5
88	30	4.4	18	0.07	27.2
89	0	4.5	18	0.1287	27.2
90	10	4.6	17.5	0.0812	27.1
91	20	4.5	17.5	0.075	27.2
92	30	4.5	17.5	0.0708	27.1
93	0	6	26	0.1722	28.4
94	5	6	25.5	0.0917	29.3
95	10	6.1	25	0.0844	29.5
96	15	6.1	25	0.0833	29.7
97	20	6.2	25	0.0839	29.8
98	25	6.1	25	0.0855	29.8
99	30	6	25	0.085	29.8
100	0	6.1	25	0.1847	29.8
101	5	6	25	0.1301	29.9
102	10	6	25	0.1108	29.9
103	15	6	25.5	0.1045	29.9
104	20	6	25	0.0958	29.9
105	25	6.1	25	0.0917	29.9
106	30	6.1	25	0.0885	29.9
107	45	6	25	0.0812	29.8
108	60	6	25	0.0777	29.8
109	75	6	25	0.0741	29.6
110	90	6	25	0.0708	29.6
111	105	5.9	25	0.0712	30.2
112	120	5.9	25	0.0674	30.3

Rows	Time Since Back Pulse	Flowrate (ft/s)	Pressure (psig)	Filtrate Flux (gpm/ft2)	Temp (C)
1	0	6.1	25	0.2056	26.7
2	5	6	25	0.1152	26.8
3	10	6	25.5	0.102	26.9
4	15	5.8	25	0.0833	26.9
5	20	5.9	25.5	0.0759	26.9
6	25	6	25	0.07	27
7	30	5.9	25	0.0637	26.9
8	0	5.9	25	0.1746	27.3
9	5	5.9	25	0.0817	27.6
10	10	5.9	25	0.0657	27.7
11	15	5.8	25.5	0.0579	27.9
12	20	6	25	0.0538	27.9
13	25	5.9	25	0.049	28
14	30	5.9	25	0.0483	28
15	0	7.4	33	0.1482	30.7
16	10	7.5	32.5	0.0657	31.7
17	20	7.4	32.5	0.0554	31.6
18	30	7.5	32	0.0488	31.6
19	0	7.4	33	0.1677	32
20	10	7.5	32.5	0.0569	32
21	20	7.3	33.5	0.0486	32.1
22	30	7.5	32.5	0.0446	32.5
23	0	3	22.5	0.1128	27
24	10	3.1	24.5	0.0352	26.6
25	20	2.6	26.5	0.029	26.3
26	30	2.6	27	0.0223	26.2
27	0	2.9	25	0.098	26.3
28	10	2.9	27	0.0346	26.3
29	20	2.8	28	0.0288	26.3
30	30	3.1	27	0.0235	26.2
31	0	6.1	10	0.054	26
32	10	6.1	10	0.0285	25.9
33	20	6	10	0.0243	25.9
34	30	6	10.5	0.0225	26.3
35	0	5.7	9.5	0.0431	25.9
36	10	5.9	9.5	0.0275	25.9
37	20	5.9	10	0.0245	25.8
38	30	6	10	0.0224	25.8
39	0	7.5	17.5	0.1089	30.7
40	10	7.6	18	0.0418	30.8
41	20	7.5	18	0.0366	30.7
42	30	7.3	17.5	0.0344	30.5
43	0	7.5	18	0.1118	30.4
44	10	7.4	17.5	0.0366	29.9
45	20	7.5	18	0.0327	29.7
46	30	7.5	18	0.0323	29.7
47	0	6	25	0.1517	29.9
48	5	5.9	26	0.0502	30
49	10	6	25	0.0358	29.9
50	15	5.9	25	0.0348	29.8
51	20	5.9	26	0.0311	29.8
52	25	5.9	25	0.0292	29.7
53	30	5.9	25	0.0292	29.7
54	0	6	25	0.1159	29.9
55	5	5.9	25	0.0411	29.8
56	10	6	25	0.0368	29.8
57	15	6	25	0.0335	29.8
58	20	5.9	25	0.0291	29.8

Rows	Time Since Back Pulse	Flowrate (ft/s)	Pressure (psig)	Filtrate Flux (gpm/ft2)	Temp (C)
59	25	6	25	0.0296	29.7
60	30	6	24.5	0.0292	29.7
61	0	4.2	32.5	0.1012	29.4
62	10	4.3	32.5	0.0396	29.5
63	20	4.5	33	0.0292	29.6
64	30	4.5	33	0.025	29.6
65	0	4.4	32.5	0.1356	29.7
66	10	4.3	32	0.0335	29.7
67	20	4.3	32	0.0267	29.7
68	30	4.4	32.5	0.0257	29.8
69	0	5.9	40	0.1401	32.7
70	10	5.8	39.5	0.0411	33.2
71	20	5.8	40	0.0334	33.4
72	30	5.9	40	0.0311	33.5
73	0	5.9	39.5	0.1416	33.5
74	10	5.8	40	0.0409	33.4
75	20	5.8	40.5	0.0328	33.4
76	30	5.8	40	0.0309	33.9
77	0	8.6	27	0.0637	33.6
78	10	8.9	24	0.0366	33.4
79	20	8.8	26	0.0348	34.7
80	30	9.3	25	0.032	35.4
81	0	9	25	0.118	35.9
82	10	9.1	25	0.0049	35.9
83	20	9.3	25	0.0391	36.3
84	30	9.1	25.5	0.0377	36
85	0	4.6	18.5	0.0807	28.3
86	10	4.5	17.5	0.0238	27.3
87	20	4.5	17.5	0.0192	27.2
88	30	4.5	17.5	0.0178	27.1
89	0	4.5	18	0.0855	27.4
90	10	4.5	17.5	0.0227	27.1
91	20	4.5	17.5	0.02	26.9
92	30	4.5	17.5	0.0171	26.9
93	0	6	26	0.085	29.3
94	5	5.9	25	0.0356	29.4
95	10	6	25	0.0305	29.5
96	15	5.9	25	0.0271	29.5
97	20	6	25	0.0255	29.4
98	25	5.9	25	0.0214	29.4
99	30	6	25	0.0243	29.4
100	0	5.9	26	0.0973	29.6
101	5	6.1	25.5	0.0352	29.7
102	10	6	26	0.0311	29.9
103	15	5.9	25	0.0276	29.8
104	20	5.9	25	0.0253	29.8
105	25	6	26	0.0233	29.9
106	30	5.9	25	0.0281	29.9
107	45	5.9	25.5	0.0242	29.6
108	60	6.1	26	0.0217	29.5
109	75	6.1	25	0.0208	29.7
110	90	6.1	25	0.0215	29.6
111	105	6	25	0.0226	29.6
112	120	5.9	25	0.0202	29.3

Rows	Time Since Back Pulse	Flowrate (ft/s)	Pressure (psig)	Filtrate Flux (gpm/ft2)	Temp (C)
1	0	6.1	20	0.1634	26.4
2	5	6	20	0.0619	26.6
3	10	6	20	0.0536	26.8
4	15	6	20	0.0483	26.9
5	20	6	20	0.0444	27
6	25	6.1	20.5	0.0472	27.1
7	30	6.1	20	0.0398	27.1
8	0	6.2	20.5	0.1401	27.5
9	5	6	20	0.0494	27.6
10	10	6.1	20	0.0462	27.6
11	15	6.1	20.5	0.0428	27.8
12	20	6.1	20	0.0386	27.7
13	25	6	20	0.0278	27.7
14	30	5.9	19	0.0275	27.6
15	0	7.7	27.5	0.0973	29.7
16	10	7.5	27.5	0.0494	30.4
17	20	7.5	28	0.0455	30.9
18	30	7.6	27.5	0.0403	31.7
19	0	7.5	27.5	0.1401	32.2
20	10	7.5	26.5	0.0431	31.6
21	20	7.4	27	0.0384	31.5
22	30	7.5	27.5	0.0377	31.8
23	0	2.9	19	0.1275	27.9
24	10	3	20.5	0.0237	26.9
25	20	2.9	20.5	0.0198	26.5
26	30	3.1	21	0.0176	26.2
27	0	3.3	20	0.1226	25.2
28	10	3.3	21	0.0232	25.5
29	20	3.5	20	0.0183	25.7
30	30	3.4	20	0.0165	25.8
31	0	6	5	0.024	25.5
32	10	5.9	5	0.0217	25.6
33	20	6	5	0.0228	25.5
34	30	6.2	5	0.0208	25.6
35	0	6	5	0.0358	25.5
36	10	6	5	0.0227	25.1
37	20	6	5	0.0194	25
38	30	6	5	0.019	25
39	0	7.5	12.5	0.0708	27
40	10	7.6	12.5	0.0319	27.6
41	20	7.5	12.5	0.0282	27.8
42	30	7.4	12.5	0.0282	28
43	0	7.4	12.5	0.0574	28.2
44	10	7.4	13	0.0294	28.2
45	20	7.5	12.5	0.0277	28.3
46	30	7.4	12.5	0.0267	28
47	0	6	19.5	0.1028	28.9
48	5	6.1	20	0.0341	29
49	10	5.9	20.5	0.0277	29.1
50	15	6	20	0.0246	29
51	20	6	20	0.0232	29
52	25	6	20	0.0227	29.1
53	30	6.1	20.5	0.0225	29.2
54	0	6	20	0.0951	29.3
55	5	6	20.5	0.0317	29.3
56	10	6	20	0.0264	29.2
57	15	6.1	21.5	0.0261	29.3
58	20	6	20.5	0.0235	29.1

Rows	Time Since Back Pulse	Flowrate (ft/s)	Pressure (psig)	Filtrate Flux (gpm/ft2)	Temp (C)
59	25	5.9	20	0.0203	28.9
60	30	6	19.5	0.0209	28.9
61	0	4.7	27	0.108	29.1
62	10	4.4	27	0.0218	29.1
63	20	4.5	27.5	0.0194	28.8
64	30	4.5	28	0.0175	28.7
65	0	4.5	27.5	0.0898	28.9
66	10	4.5	28	0.0221	28.7
67	20	4.5	28.5	0.0189	28.7
68	30	4.4	28	0.0158	28.6
69	0	5.9	35	0.1099	33.7
70	10	5.9	35	0.0258	33.7
71	20	5.9	35	0.0237	33.6
72	30	6	35	0.0215	33.7
73	0	5.8	35	0.01045	33.9
74	10	5.9	35	0.0287	34
75	20	6.1	35	0.0227	34
76	30	6.1	35	0.0199	33.8
77	0	9	20	0.0885	33.6
78	10	8.9	20	0.0294	33.3
79	20	9	21	0.0276	33.5
80	30	9	20.5	0.0271	33.6
81	0	8.9	20	0.091	33.6
82	10	9	20	0.0285	33
83	20	9	21	0.0283	33.1
84	30	9.1	20	0.023	33.4
85	0	4.4	12.5	0.0483	31.4
86	10	4.7	12.5	0.0154	27.9
87	20	4.4	12.5	0.0111	27.1
88	30	4.4	12.5	0.0105	26.5
89	0	4.6	12.5	0.0549	26.7
90	10	4.6	12.5	0.0155	26.5
91	20	4.5	12.5	0.0127	26.5
92	30	4.5	12.5	0.0112	26.4
93	0	6	20.5	0.075	28.7
94	5	6	20	0.0233	28.7
95	10	5.6	20	0.0191	28.5
96	15	6	20	0.0165	28.6
97	20	6	20	0.0153	28.6
98	25	5.9	19.5	0.0151	28.6
99	30	5.9	20.5	0.0148	29
100	0	5.6	20	0.0531	27.9
101	5	6	20	0.0227	28.2
102	10	6.1	21	0.0194	28.5
103	15	6.1	21	0.0172	28.7
104	20	6	20.5	0.016	28.9
105	25	6	20.5	0.0149	29
106	30	5.9	20	0.0146	29.1
107	45	6	21	0.013	29.3
108	60	6	20.5	0.0136	29.4
109	75	5.9	20	0.013	29.4
110	90	5.9	20	0.013	29.4
111	105	5.9	20	0.0126	29.4
112	120	5.8	20.5	0.0129	30.2

Rows	Time Since Back Pulse	Flowrate (ft/s)	Pressure (psig)	Filtrate Flux (gpm/ft2)	Temp (C)
1	0	6.1	25	0.2023	30
2	5	6.1	25	0.1328	30.5
3	10	6.1	25	0.1071	30.5
4	15	6.1	26	0.0973	30.7
5	20	6	25	0.085	30.7
6	25	6	25	0.0763	30.6
7	30	6.1	25	0.07	30.6
8	0	6	25	0.1573	30.8
9	5	6.1	25	0.0966	29.4
10	10	6.1	26	0.085	29.1
11	15	6.1	26	0.0724	28.9
12	20	6	26	0.0693	28.7
13	25	6	25	0.0585	28.5
14	30	6	25	0.0564	28.4
15	0	7.5	32.5	0.1613	30.5
16	10	7.5	32.5	0.0828	31.2
17	20	7.3	32.5	0.0671	31.5
18	30	7.5	32.5	0.0625	31.7
19	0	7.5	33	0.1902	31.9
20	10	7.6	33	0.0787	32.2
21	20	7.5	32.5	0.065	32.1
22	30	7.5	32.5	0.0579	32.2
23	0	2.9	25.5	0.125	28.9
24	10	3	25	0.0545	27.7
25	20	3	26	0.0414	27.2
26	30	2.9	25.5	0.0375	26.9
27	0	2.9	26	0.1138	26.9
28	10	3	25	0.0476	26.6
29	20	2.8	23.5	0.0303	26.5
30	30	2.9	24	0.0301	26.4
31	0	6	10	0.0391	26.6
32	10	6	10	0.0312	26.5
33	20	6.1	10	0.0273	26.5
34	30	6	10	0.0279	26.5
35	0	6	10	0.0439	26.7
36	10	6	10	0.0302	26.6
37	20	6	10	0.0268	26.6
38	30	6	10	0.027	26.5
39	0	7.5	17.5	0.0787	28.5
40	10	7.4	17.5	0.0443	28.7
41	20	7.3	17	0.0373	28.8
42	30	7.5	17.5	0.0348	28.8
43	0	7.4	17.5	0.0879	28.9
44	10	7.5	18	0.0443	29
45	20	7.5	17.5	0.0384	28.9
46	30	7.6	18	0.0375	29.2
47	0	5.9	25	0.0708	29.4
48	5	5.9	25	0.0462	29.5
49	10	6.1	26	0.0431	29.7
50	15	6	25	0.0391	29.6
51	20	6	25	0.036	29.6
52	25	5.9	24.5	0.0334	29.5
53	30	5.9	24	0.0322	29.3
54	0	6	25.5	0.108	29.4
55	5	6.1	25	0.054	29.3
56	10	6.1	25	0.0443	29.3
57	15	6.1	25	0.0393	29.3
58	20	6.1	25	0.036	29.3

Rows	Time Since Back Pulse	Flowrate (ft/s)	Pressure (psig)	Filtrate Flux (gpm/ft2)	Temp (C)
59	25	6.1	25	0.0346	29.3
60	30	6.1	25	0.0327	29.3
61	0	4.5	32.5	0.1554	28.3
62	10	4.5	33	0.0458	28.7
63	20	4.5	32.5	0.0364	28.6
64	30	4.4	33	0.032	28.7
65	0	4.4	32.5	0.1722	29.1
66	10	4.4	32.5	0.0465	28.9
67	20	4.4	33	0.0364	28.8
68	30	4.5	32.5	0.0315	28.7
69	0	6	40	0.2317	31.7
70	10	6	40.5	0.0564	32.6
71	20	6	40	0.0472	33
72	30	6.1	40	0.0393	33.3
73	0	6	40	0.2276	33.3
74	10	6	41	0.0569	33.3
75	20	6	40	0.0446	33.3
76	30	5.9	40	0.0393	33.3
77	0	9	25	0.0271	34.8
78	10	8.9	24.5	0.0276	34.9
79	20	9	25	0.0267	34.9
80	30	9	25	0.0271	34.8
81	0	9	25	0.0518	34.8
82	10	9	24.5	0.0417	34.6
83	20	9	25	0.0408	34.6
84	30	9	25	0.0401	34.6
85	0	4.5	17	0.0741	27.8
86	10	4.5	17.5	0.0281	27.5
87	20	4.4	17	0.022	27.1
88	30	4.5	17	0.0175	27
89	0	4.5	18	0.0549	27
90	10	4.6	17.5	0.0284	27
91	20	4.3	17.5	0.0235	26.8
92	30	4.6	17.5	0.0206	26.9
93	0	6	25.5	0.0966	28.6
94	5	6	25.5	0.0494	28.8
95	10	5.9	25	0.0382	28.8
96	15	6	25	0.0303	28.9
97	20	6	25	0.0295	28.9
98	25	6	25	0.0278	28.9
99	30	6	25	0.0273	28.9
100	0	6.1	25.5	0.1287	29.3
101	5	6.1	25	0.0476	29.3
102	10	6.1	25	0.0364	29.7
103	15	6.1	25	0.0317	29.5
104	20	6	25	0.0303	29.5
105	25	6.1	25	0.0288	29.5
106	30	6	25	0.0281	29.4
107	45	5.9	25	0.025	29.2
108	60	5.9	24	0.024	29
109	75	5.9	24.5	0.024	29.3
110	90	6	25	0.0241	29.4
111	105	6.1	25	0.0241	29.6
112	120	6.1	25	0.0246	30.4

Rows	Time Since Back Pulse	Flowrate (ft/s)	Pressure (psig)	Filtrate Flux (gpm/ft2)	Temp (C)
1	0	5.8	26	0.2056	27
2	5	6	25	0.0828	27.2
3	10	6	25	0.0631	27.2
4	15	5.9	25	0.0569	27.3
5	20	6.1	25	0.0522	27.4
6	25	5.9	25	0.0506	27.4
7	30	5.9	25.5	0.0469	27.4
8	0	5.9	25	0.1913	27.5
9	5	5.8	25	0.085	27.4
10	10	5.9	25.5	0.0631	27.6
11	15	6	25.5	0.0536	27.6
12	20	6	25.5	0.0505	27.6
13	25	5.9	25.5	0.0449	27.7
14	30	6.1	25	0.0422	27.7
15	0	7.6	32.5	0.2089	30.1
16	10	7.5	32.5	0.0685	30.8
17	20	7.4	33	0.054	31.3
18	30	7.5	32.5	0.049	31.4
19	0	7.6	32	0.1931	31.5
20	10	7.4	32.5	0.059	31.5
21	20	7.5	32.5	0.049	31.6
22	30	7.5	32.5	0.0434	31.7
23	0	3.2	24.5	0.1554	27.3
24	10	3	25.5	0.0425	26.7
25	20	3	26	0.0341	26.4
26	30	3	25.5	0.0266	26.1
27	0	2.9	25	0.1385	26.1
28	10	3	25	0.0411	26
29	20	3	25	0.0308	26.1
30	30	3.1	25	0.0256	25.9
31	0	6	10	0.0569	25.7
32	10	6	10	0.0298	25.5
33	20	6	10	0.0259	25.4
34	30	5.9	10	0.0232	25.3
35	0	5.9	10	0.0506	25.5
36	10	6	10	0.0305	25.5
37	20	6	10	0.026	25.5
38	30	6	10	0.0234	25.4
39	0	7.5	17.5	0.0944	30.9
40	10	7.5	17.5	0.0419	30.5
41	20	7.4	17.5	0.036	30.2
42	30	7.4	17.5	0.0325	29.7
43	0	7.5	17.5	0.0879	29.4
44	10	7.5	17.5	0.0377	28.6
45	20	7.5	17.5	0.0323	28.3
46	30	7.4	17.5	0.0302	28.1
47	0	5.9	25	0.1169	27.9
48	5	5.9	25.5	0.0502	27.7
49	10	6.1	24.5	0.0384	27.7
50	15	6	25	0.0356	27.7
51	20	6.1	25	0.0319	27.7
52	25	6	25	0.0308	27.6
53	30	6	25	0.0291	27.6
54	0	6.1	25	0.1108	27.7
55	5	6	24.5	0.0462	27.6
56	10	6.1	26	0.0403	27.6
57	15	5.9	24.5	0.0335	27.6
58	20	6	25	0.0312	27.6

Rows	Time Since Back Pulse	Flowrate (ft/s)	Pressure (psig)	Filtrate Flux (gpm/ft2)	Temp (C)
59	25	6	25.5	0.0298	27.6
60	30	6.1	25.5	0.0286	27.7
61	0	4.3	33	0.1275	27.9
62	10	4.7	32	0.0379	27.8
63	20	4.3	32.5	0.0298	27.9
64	30	4.4	32.5	0.0253	27.6
65	0	4.4	32.5	0.1225	27.7
66	10	4.4	32.5	0.0368	27.7
67	20	4.4	33	0.0288	27.7
68	30	4.5	32.5	0.0249	27.8
69	0	5.9	40	0.1416	30.4
70	10	6	40	0.0425	30.9
71	20	5.9	40.5	0.0354	31
72	30	6.1	40	0.0305	31.1
73	0	5.9	40	0.1287	31.4
74	10	6.1	39.5	0.0386	31.4
75	20	6.1	40	0.0315	31.5
76	30	6.1	40	0.0276	31.5
77	0	8.9	25	0.0944	31.7
78	10	9.1	25	0.036	31.5
79	20	9	25	0.032	31.4
80	30	9	25	0.0296	31.3
81	0	8.9	25.5	0.1062	31.6
82	10	9	25	0.0389	31.3
83	20	9	25	0.0325	31.2
84	30	9	25	0.0299	31.2
85	0	4.5	17.5	0.0637	27.3
86	10	4.5	17.5	0.0251	26.4
87	20	4.5	17.5	0.0193	25.9
88	30	4.5	17.5	0.0182	25.6
89	0	4.5	17.5	0.0657	25.5
90	10	4.5	17.5	0.0255	25.4
91	20	4.4	17.5	0.0186	25.3
92	30	4.4	17.5	0.0181	25.3
93	0	5.7	25	0.0797	27.1
94	5	5.9	25	0.0382	27.3
95	10	6	25	0.0295	27.6
96	15	6.1	25	0.0267	27.8
97	20	6.1	25.5	0.0243	28
98	25	6	25	0.0236	28
99	30	6	25	0.0219	27.9
100	0	6	25	0.0787	28
101	5	6	25	0.0373	27.9
102	10	6	25	0.029	28
103	15	6	25.5	0.0263	28
104	20	6	25	0.0255	28
105	25	6	25	0.0232	28
106	30	6	25	0.0219	28
107	45	6	25	0.02	28
108	60	6.1	25	0.0197	28
109	75	6.1	25	0.0192	28.1
110	90	6.1	25	0.0183	28.1
111	105	6.1	25	0.0176	28.1
112	120	6.1	25	0.0178	28.1

Rows	Time Since Back Pulse	Flowrate (ft/s)	Pressure (psig)	Filtrate Flux (gpm/ft2)	Temp (C)
1	0	6.1	20	0.1634	35.4
2	5	6.1	20	0.0741	34.2
3	10	6	20	0.07	32.8
4	15	6	20	0.0693	32
5	20	6	20	0.065	31.5
6	25	6	20	0.0613	31
7	30	6	20	0.0619	30.5
8	0	6	20	0.1722	30.4
9	5	6	20	0.0619	30.1
10	10	6	20	0.0613	29.9
11	15	6	20	0.0579	29.9
12	20	5.9	21	0.0607	30.3
13	25	6	20	0.0514	29.9
14	30	6.1	21	0.0569	29.8
15	0	7.4	27.5	0.1961	31.9
16	10	7.4	27	0.0716	32.9
17	20	7.4	27.5	0.0716	33.2
18	30	7.4	28	0.0724	33.6
19	0	7.4	28	0.1931	33.8
20	10	7.5	27.5	0.0787	34.7
21	20	7.6	28.5	0.0797	35.2
22	30	7.5	27.5	0.075	34
23	0	2.8	20.5	0.0966	31.9
24	10	3	20.5	0.0302	29.2
25	20	3	20	0.027	28
26	30	3	20	0.0253	27.6
27	0	3	20	0.1385	27.5
28	10	3	20	0.0286	27.2
29	20	3	20	0.0257	27.1
30	30	3	20	0.0259	27.1
31	0	6.1	6	0.0554	27.2
32	10	6.1	5.5	0.0384	26.9
33	20	6.1	5	0.0298	26.7
34	30	6	5	0.0279	26.5
35	0	6	5	0.0425	26.6
36	10	6	5	0.0352	26.5
37	20	6	5	0.0354	26.4
38	30	6	5	0.0356	26.3
39	0	7.4	12.5	0.1099	28.1
40	10	7.5	12.5	0.0569	28.8
41	20	7.6	13	0.0625	29.1
42	30	7.5	12.5	0.0579	29.1
43	0	7.5	12.5	0.1062	29.2
44	10	7.5	12.5	0.0619	29.3
45	20	7.5	13	0.059	29.3
46	30	7.5	12.5	0.0607	29.3
47	0	6	20.5	0.1448	29.7
48	5	6	20	0.0502	29.7
49	10	5.9	20	0.0458	29.8
50	15	6	20	0.0452	29.9
51	20	6	20	0.0455	29.9
52	25	6	20	0.0458	29.9
53	30	6	20	0.0469	29.9
54	0	6	20	0.1416	30
55	5	6	20	0.0502	30
56	10	6	20	0.049	30
57	15	6	20	0.0469	30
58	20	6	20	0.0458	30

Rows	Time Since Back Pulse	Flowrate (ft/s)	Pressure (psig)	Filtrate Flux (gpm/ft2)	Temp (C)
59	25	6	20	0.0472	30
60	30	6	20	0.0458	30.1
61	0	4.5	27.5	0.1634	31.7
62	10	4.5	27.5	0.0398	31.9
63	20	4.4	27	0.0382	32
64	30	4.6	27.5	0.0379	31.9
65	0	4.5	27.5	0.1613	31.4
66	10	4.4	27.5	0.0382	31.2
67	20	4.5	27.5	0.037	31.3
68	30	4.5	27.5	0.036	31.4
69	0	6	34.5	0.1821	34
70	10	6.2	35	0.0545	34.5
71	20	6.1	35	0.0531	34.9
72	30	5.9	34.5	0.0506	34.9
73	0	6	35	0.1746	35.3
74	10	6	35	0.0549	35.4
75	20	6	35	0.0545	35.5
76	30	6	34.5	0.0536	35.5
77	0	9	20	0.1314	35.2
78	10	9	20	0.0797	34.7
79	20	9	20	0.075	34.4
80	30	8.9	20	0.0768	34.3
81	0	8.9	20	0.1385	34.6
82	10	9	20	0.0741	34.5
83	20	9	20.5	0.075	34.6
84	30	9	20	0.075	34.6
85	0	4.5	13	0.1045	33
86	10	4.5	13	0.0296	30.4
87	20	4.5	13	0.0288	29.1
88	30	4.5	12.5	0.0262	28.4
89	0	4.4	12.5	0.0904	28.2
90	10	4.5	12.5	0.0278	27.6
91	20	4.5	12.5	0.0267	27.5
92	30	4.5	12.5	0.271	27.4
93	0	6	20	0.1138	29.3
94	5	6.1	20	0.0452	29.8
95	10	6	20	0.0443	30
96	15	6	20	0.0439	30.2
97	20	6	20	0.0439	30.3
98	25	6	20	0.0446	30.5
99	30	6	20.5	0.0449	30.6
100	0	6	20	0.1053	30.8
101	5	6	20	0.0465	30.8
102	10	6	20	0.0458	30.7
103	15	6	20.5	0.0449	30.7
104	20	6	20	0.0449	30.7
105	25	6	20	0.0452	30.7
106	30	6	20	0.0436	30.8
107	45	6	20	0.0431	30.7
108	60	5.9	20	0.0428	30.6
109	75	6	20	0.0428	30.8
110	90	6	20	0.0431	30.9
111	105	6	20	0.0436	30.9
112	120	6	20	0.0436	30.9

Rows	Time Since Back Pulse	Flowrate (ft/s)	Pressure (psig)	Filtrate Flux (gpm/ft2)	Temp (C)
1	0	6.1	25	0.2897	30.8
2	5	6	25	0.1593	31.5
3	10	5.9	25.5	0.1138	31.7
4	15	6	25	0.1028	31.3
5	20	6.1	25	0.0861	31
6	25	6.1	25	0.0851	30.9
7	30	6.1	24.5	0.0732	30.7
8	0	6	24.5	0.1991	30.6
9	5	6	24.5	0.1028	30.4
10	10	6	25	0.0817	30.4
11	15	6	25	0.0678	30.5
12	20	6	25	0.0619	30.4
13	25	6	25	0.0564	30.3
14	30	5.9	25	0.0527	30.4
15	0	7.5	32	0.1931	32.1
16	10	7.5	32	0.0657	33.6
17	20	7.4	32.5	0.0579	34.3
18	30	7.4	32.5	0.0527	34.7
19	0	7.3	32.5	0.1465	32.5
20	10	7.5	32	0.0549	32
21	20	7.4	32.5	0.0502	32.5
22	30	7.4	32.5	0.0465	35.4
23	0	3	25	0.0335	32.4
24	10	3	25	0.0246	30
25	20	2.8	24	0.0199	28.9
26	30	3.1	25	0.0184	28.6
27	0	3	25	0.1385	28.2
28	10	3	25.5	0.0306	27.9
29	20	3.1	25.5	0.0216	27.8
30	30	3	25.5	0.0189	27.7
31	0	6	10	0.0708	29.2
32	10	6	10	0.0246	28.1
33	20	6	10	0.0233	27.5
34	30	6	10	0.0212	27.1
35	0	6	10	0.0724	27.1
36	10	5.9	10	0.0226	26.8
37	20	6	10	0.0203	26.7
38	30	6	10	0.0201	26.6
39	0	7.6	17.5	0.0898	28.8
40	10	7.4	18	0.0311	28.9
41	20	7.5	17.5	0.0299	29.3
42	30	7.5	18	0.0288	29.4
43	0	7.3	17.5	0.098	29.4
44	10	7.4	18	0.0302	29.5
45	20	7.5	17.5	0.0281	29.5
46	30	7.4	17.5	0.0272	29.3
47	0	6	24.5	0.108	29.9
48	5	6	24.5	0.0335	29.7
49	10	6	25	0.0272	29.7
50	15	6	25	0.0255	29.7
51	20	5.9	24	0.0226	29.6
52	25	6	25.5	0.0229	29.7
53	30	6.1	25	0.0224	29.8
54	0	6	25	0.118	29.8
55	5	6	25	0.0314	29.8
56	10	6	25	0.0257	29.7
57	15	6	25	0.0263	29.7
58	20	6	24.5	0.0196	29.8

Rows	Time Since Back Pulse	Flowrate (ft/s)	Pressure (psig)	Filtrate Flux (gpm/ft2)	Temp (C)
59	25	6	25	0.0198	29.7
60	30	6	25	0.0188	29.8
61	0	4.6	32	0.1159	29.3
62	10	4.6	32	0.0232	29.6
63	20	4.6	32.5	0.0197	30
64	30	4.6	32.5	0.0182	30
65	0	4.6	32.5	0.0924	30.4
66	10	4.6	32.5	0.0233	30.2
67	20	4.5	32.5	0.0187	30.3
68	30	4.5	32.5	0.017	30.2
69	0	6	40	0.0777	33.9
70	10	5.9	40	0.0291	34.4
71	20	5.9	40	0.026	34.7
72	30	5.9	40	0.0244	34.9
73	0	5.9	40	0.065	35.1
74	10	6	40	0.0272	35.1
75	20	5.9	40.5	0.026	35.1
76	30	5.9	40	0.0249	35.1
77	0	9.1	25	0.0716	35.2
78	10	9.2	25.5	0.0425	35.4
79	20	9	25.5	0.0384	34
80	30	9.1	25	0.0377	33.8
81	0	9	25	0.0732	34.4
82	10	9	25	0.0382	33.6
83	20	9	25	0.0366	33.7
84	30	9	25.5	0.0379	33.7
85	0	4.4	17.5	0.0419	31.2
86	10	4.4	17.5	0.0165	28.3
87	20	4.6	18	0.0148	27.5
88	30	4.5	17.5	0.0147	27.2
89	0	4.5	18	0.0431	26.9
90	10	4.5	17.5	0.0162	26.6
91	20	4.4	17.5	0.014	26.5
92	30	4.7	17.5	0.0136	26.2
93	0	6	25	0.0574	31.2
94	5	5.9	25.5	0.0263	31
95	10	6.1	25	0.0221	30.8
96	15	6	25.5	0.0224	30.5
97	20	6	25	0.0208	30.2
98	25	6.1	25	0.0228	30.1
99	30	6.1	25	0.0218	30
100	0	6	25	0.0536	30.1
101	5	6	25.5	0.0254	30
102	10	6	25	0.022	30
103	15	6	25	0.0182	30
104	20	6	25	0.023	29.9
105	25	6	25	0.0207	29.8
106	30	6	25	0.0203	29.8
107	45	6	25.5	0.0203	29.9
108	60	6	25	0.0197	29.8
109	75	6	25	0.0196	29.8
110	90	6	25.5	0.0193	29.8
111	105	6	25	0.0183	29.7
112	120	6	25	0.0184	29.8

Rows	Time Since Back Pulse	Flowrate (ft/s)	Pressure (psig)	Filtrate Flux (gpm/ft2)	Temp (C)
1	0	6	25	0.2583	26.9
2	5	6	26.5	0.1482	26.8
3	10	6.1	25	0.1202	26.9
4	15	6	25	0.1118	26.8
5	20	6.1	25	0.0996	26.7
6	25	6.1	25	0.0933	26.8
7	30	5.9	24.5	0.0898	26.6
8	0	6	24.5	0.2276	26.4
9	5	6.1	25	0.1356	26.4
10	10	6	25	0.1118	26.8
11	15	5.9	24.5	0.098	26.7
12	20	5.8	24	0.0924	26.7
13	25	6.1	24.5	0.0885	27.1
14	30	6	24.5	0.0861	27.3
15	0	7.3	34	0.2549	29.5
16	10	7.5	33	0.1385	30.3
17	20	7.5	32.5	0.118	30.9
18	30	7.6	32.5	0.1012	31.1
19	0	7.6	32	0.2941	31.2
20	10	7.3	32	0.137	31.1
21	20	7.5	32.5	0.108	31
22	30	7.3	33.5	0.1062	31
23	0	3	24.5	0.2197	29.6
24	10	2.9	25	0.0898	27.5
25	20	3	25	0.0664	27
26	30	3	25.5	0.0644	26.6
27	0	3.2	25	0.1991	26.6
28	10	3	25	0.0885	26.2
29	20	3	25	0.0708	25.9
30	30	3	25	0.0631	25.7
31	0	6	10	0.0924	25.4
32	10	6.1	10	0.0637	25.1
33	20	6	10	0.059	25.1
34	30	6	10	0.0536	25.1
35	0	6	10	0.0891	25
36	10	6	10	0.0644	25
37	20	6	10	0.0559	25
38	30	6	10	0.0531	24.7
39	0	7.5	18	0.177	30.3
40	10	7.5	17.5	0.0925	29.7
41	20	7.5	17.5	0.0797	29.2
42	30	7.5	17.5	0.0741	28.7
43	0	7.4	17.5	0.1655	28.6
44	10	7.5	17.5	0.0797	28.1
45	20	7.5	17.5	0.0732	28
46	30	7.5	17.5	0.0716	27.7
47	0	6	26	0.236	27.9
48	5	5.9	24	0.1138	27.7
49	10	6.1	25.5	0.0951	28.1
50	15	5.9	25	0.0807	27.8
51	20	5.8	25	0.0724	27.7
52	25	5.9	25.5	0.0732	27.7
53	30	6	24.5	0.0657	27.6
54	0	6.1	25	0.2197	27.6
55	5	5.9	24.5	0.0996	27.3
56	10	6	24.5	0.0828	27.2
57	15	5.9	25	0.075	27.1
58	20	6.1	25	0.0732	27.3

Rows	Time Since Back Pulse	Flowrate (ft/s)	Pressure (psig)	Filtrate Flux (gpm/ft2)	Temp (C)
59	25	6.1	25.5	0.0741	27.4
60	30	5.9	24.5	0.0625	27.2
61	0	4.5	32.5	0.2771	27.4
62	10	4.5	32	0.091	27.3
63	20	4.5	32.5	0.0716	27.3
64	30	4.5	32.5	0.0637	27.3
65	0	4.5	32.5	0.2712	27.5
66	10	4.6	32.5	0.091	27.4
67	20	4.6	32.5	0.0741	27.5
68	30	4.6	32.5	0.0625	27.5
69	0	6	40	0.3414	29
70	10	6	40	0.1108	30.3
71	20	6	40	0.0937	30.8
72	30	5.9	40.5	0.0787	31.1
73	0	5.9	40	0.4111	31.2
74	10	6.1	40	0.4032	31.2
75	20	6.1	40	0.085	31.2
76	30	6.1	40	0.0807	31.3
77	0	9	26	0.2549	31.8
78	10	8.9	25.5	0.0996	32
79	20	9	24.5	0.085	31.9
80	30	9	24.5	0.0861	32
81	0	9.1	25	0.236	32.1
82	10	9.1	24.5	0.0937	32.3
83	20	9.1	24.5	0.085	32.2
84	30	9	25.5	0.091	32.3
85	0	4.5	17.5	0.1573	28.2
86	10	4.5	17.5	0.0671	26.6
87	20	4.5	17.5	0.0522	26.2
88	30	4.5	17.5	0.0479	25.8
89	0	4.5	17.5	0.1554	25.7
90	10	4.5	17.5	0.0657	25.5
91	20	4.5	17.5	0.0527	25.4
92	30	4.5	17.5	0.0476	25.2
93	0	6	25	0.1991	27
94	5	6	25	0.0898	27.2
95	10	5.9	25	0.0777	27.1
96	15	5.9	25	0.0685	27.2
97	20	5.9	25	0.0657	27.3
98	25	6.1	24	0.0631	27.4
99	30	6.1	25	0.0585	27.5
100	0	6.1	25	0.2089	27.7
101	5	6	25	0.098	27.7
102	10	6	25	0.0797	27.7
103	15	6	25	0.07	27.8
104	20	6	25	0.0644	27.7
105	25	6	25	0.0607	27.7
106	30	5.9	25	0.0574	27.7
107	45	6	25	0.0554	27.8
108	60	5.9	25	0.054	27.8
109	75	6	24	0.0522	27.7
110	90	5.9	25	0.0514	27.7
111	105	5.9	25	0.0527	27.8
112	120	5.9	25	0.0522	27.7

Rows	Time Since Back Pulse	Flowrate (ft/s)	Pressure (psig)	Filtrate Flux (gpm/ft2)	Temp (C)
1	0	5.9	19	0.2124	27.8
2	5	6.2	20	0.1138	28.1
3	10	5.8	20	0.1028	28.7
4	15	5.9	21	0.1159	29.2
5	20	6	20	0.1062	29.5
6	25	6.1	20	0.1028	29.9
7	30	6	20	0.075	30
8	0	6	20	0.1677	30
9	5	6	20	0.0996	30
10	10	6.1	20	0.0924	30.3
11	15	6.2	20	0.0951	30.2
12	20	6.1	20	0.0944	30
13	25	6.2	20	0.091	30
14	30	6.2	20	0.091	30
15	0	6.4	28	0.2549	33.5
16	10	6.4	27	0.1385	34.6
17	20	6.8	27.5	0.1275	35.2
18	30	6.8	27	0.1159	35.6
19	0	6.7	27.5	0.2771	35.4
20	10	6.5	27.5	0.1138	34.7
21	20	6.5	27.5	0.108	34.4
22	30	6.5	27	0.1028	34.2
23	0	3.2	18	0.125	32.5
24	10	2.9	20	0.0479	29.7
25	20	3	20	0.0411	28.3
26	30	3	20.5	0.0393	27.7
27	0	3	20	0.177	27.4
28	10	3	20	0.0434	27
29	20	3.2	20	0.0384	26.9
30	30	3.1	20	0.0379	26.7
31	0	6	5	0.0574	27
32	10	5.9	5.5	0.0671	27.6
33	20	5.8	5	0.0479	26.5
34	30	5.9	5	0.0527	26.4
35	0	5.8	5	0.0579	26.4
36	10	6	5.5	0.0527	26.1
37	20	6.1	5.5	0.054	26.2
38	30	6	5	0.051	26.1
39	0	7.4	13	0.1118	28.2
40	10	7.6	12.5	0.0873	29.9
41	20	7.6	12.5	0.0924	30.1
42	30	7.6	12.5	0.0828	30.3
43	0	7.5	12.5	0.1385	30.4
44	10	7.4	13	0.091	30.4
45	20	7.4	12	0.0787	30.6
46	30	7.5	12.5	0.0828	30.9
47	0	6	20	0.1655	30.7
48	5	5.9	20	0.0807	30.5
49	10	6	20	0.0708	30.9
50	15	5.9	20	0.0724	30.8
51	20	6	20	0.0678	30.7
52	25	6.2	20	0.0664	30.8
53	30	6	20.5	0.07	30.9
54	0	6	20	0.1328	30.6
55	5	6	20	0.0759	30.4
56	10	6	20.5	0.0716	30.6
57	15	6.1	20	0.0716	30.4
58	20	6	20	0.0724	30.3

Rows	Time Since Back Pulse	Flowrate (ft/s)	Pressure (psig)	Filtrate Flux (gpm/ft2)	Temp (C)
59	25	6.1	19.5	0.0678	30.3
60	30	6	20	0.0685	30.2
61	0	4.5	27.5	0.177	32.1
62	10	4.5	27.5	0.059	33.2
63	20	4.5	27.5	0.0564	33.1
64	30	4.4	28	0.0564	32.8
65	0	4.6	28	0.1554	32.7
66	10	4.6	27	0.0549	32.9
67	20	4.7	27	0.0518	32.7
68	30	4.6	27.5	0.0527	32.3
69	0	6	32.5	0.1613	35.8
70	10	6	32	0.0787	37.8
71	20	6.1	32	0.0797	38.7
72	30	6	32.5	0.0817	39.1
73	0	6	32.5	0.2317	38.9
74	10	6	32	0.0828	38.6
75	20	5.9	32	0.085	38.7
76	30	5.9	32.5	0.075	38.1
77	0	7.4	20	0.1902	37.4
78	10	7.6	20	0.0873	37.1
79	20	7.5	20	0.091	36.4
80	30	7.6	20	0.091	35.9
81	0	7.4	20	0.1634	35.9
82	10	7.5	20	0.091	35.7
83	20	7.5	20	0.0898	35.8
84	30	7.5	20	0.0797	36
85	0	4.6	12.5	0.2056	28.9
86	10	4.5	12.5	0.0436	28.3
87	20	4.5	12.5	0.0375	28.1
88	30	4.6	12.5	0.0389	27.6
89	0	4.5	12.5	0.118	27.9
90	10	4.5	12.5	0.0417	27.7
91	20	4.6	12.5	0.0401	27.8
92	30	4.6	12.5	0.0403	27.9
93	0	6.1	20	0.1677	31.2
94	5	6.1	20	0.0619	31.7
95	10	6.1	20	0.0637	32.3
96	15	6	20	0.0631	32.3
97	20	6	20	0.0631	32.8
98	25	6.1	20	0.0631	32.9
99	30	6	20	0.0637	33
100	0	6	20	0.1554	33.3
101	5	6.1	20	0.0678	33.4
102	10	6	21	0.0678	33.3
103	15	6.1	20.5	0.065	33.2
104	20	6.1	20	0.0644	33
105	25	5.9	20	0.0644	33.1
106	30	5.9	20	0.0619	33
107	45	6	20	0.0601	33.3
108	60	6	19.5	0.0585	33.2
109	75	6	20	0.0613	33.3
110	90	5.9	20.5	0.0631	33.2
111	105	6	20	0.0607	33.3
112	120	6	20	0.0625	33.2

Appendix B

Table B.1. Tc Analysis for C-106

Feed Sample Identification	Feed Sample (µCi/ml)	Filtrate Sample (µCi/ml)	Condition Number Filtrate Sample Taken[1]
C-106, 0.05 wt%	2.5	3.3	1
		2.7	3
		2.6	4
		26.4	8
		2.5	9
C-106, 1.5 wt%	76	77.8	1
		73.3	3
		73.4	4
		4.8	8
		6.66	9
C-106, 8 wt%	304	273	1
		254	3
		12.2	4
		277	8
		264	9

[1] For processing conditions listed, refer to Table 3.1 for corresponding transmembrane pressure and axial velocity.

Table B.2. Tc Analysis for C-107, B-110, and U-110

Feed Sample	Feed (µCi/ml)	Filtrate (µCi/ml)
C-107, 0.05 wt%	<10, 14 +/-9	2.2
C-107, 1.5 wt%	10 +/-8	1.6
C-107, 8 wt%	<10	1.5
B-110, 0.05 wt%	<10	3.0
B-110, 1.5 wt%	46 +/-7	27.2
B-110, 8 wt%	150	170
U-110, 0.05 wt%	25 +/-13, <10	2.3
U-110, 1.5 wt%	33 +/-18	3.0
U-110, 8 wt%	22, 17+/-11	9.9

Table B.3. ^{137}Cs Analysis

Feed Sample Identification	Feed Sample (µCi/ml)	Filtrate Sample (µCi/ml)	Condition Number Filtrate Sample Taken [2]
C-106, 0.05 wt%	0.22	0.10	1
		0.18	3
		0.16	4
		0.17	8
		0.21	9
C-106, 1.5 wt%	6.6	6.3	1
		6.0	3
		5.9	4
		6.3	8
		11	9
C-106, 8 wt%	35	24	1
		24	3
		22	4
		24	8
		23	9

[2] For processing conditions listed, refer to Table 3.1 for corresponding transmembrane pressure and axial velocity.

Distribution

No. of
Copies

OFFSITE

Phil McGinnis
ORNL
P.O. Box 2008
Oak Ridge, TN 37831-6273

Charles Nash, 676-15T
Westinghouse Savannah River Company
P.O. Box 616
Aiken, SC 29802

Dan McCabe, 773-43A
Westinghouse Savannah River Company
P.O. Box 616
Aiken, SC 29802

Reid Peterson, 676-T
Westinghouse Savannah River Company
P.O. Box 616
Aiken, SC 29802

Tim Kent
ORNL
P.O. Box 2008, Bldg 3017
Oak Ridge, TN 37831

Arlen Olsen
Lockhead Martin Idaho Technologies Co.
P. O. Box 1625
Idaho Falls, ID 83415-5218

No. of
Copies

ONSITE

No. of Copies	Name	Mail Stop
3	DOE Richland Operations Office	
	N. R. Brown	K6-51
	R. Carreon	K6-51
	R. A. Gilbert	K6-51
3	J. N. Appel	G3-21
	W. B. Barton	R2-11
	K. A. Gasper	G3-21
2	Numatec Hanford Corp.	
	R. A. Kirkbride	H5-27
	R. M. Orme	H5-27
2	SGN Eurisys Services Corp.	
	G. T. MacLean	H5-61
	D. E. Place	H5-27
27	Pacific Northwest National Laboratory	
	W. F. Bonner	K9-14
	K. P. Brooks	P7-43
	B. C. Bunker	K8-93
	J.G.H. Geeting (5)	P7-28
	J. H. Holbrook	K9-81
	L. K. Holton	K6-51
	D. E. Kurath	P7-20
	G. J. Lumetta	P7-25
	E. V. Morrey	P7-28
	D. R. Rector	K7-15
	B. A. Reynolds (6)	K6-51
	Inforamtion Release (7)	